# PREPARATION AND PROPERTIES OF LAYER STRUCTURED CRYSTAL β-ZIRCONIUM CHLORIDE NITRIDE

MASAO OHASHI

1989

CONTENTS

# 1 BACKGROUND AND PURPOSES OF THIS STUDY

Inorganic layer structured crystals have two-dimensional character in the arrangements of atoms and bonds. In contrast to the strong intralayer lateral bonds, interlayer bonds which stack the layers with each other are relatively weak. They are van der Waals interaction, hydrogen bonds or weak electrostatic bonds. Some layer structured crystals take up molecules, atoms or ions into their interlayer spaces.[1-7] This type of reactions are called intercalation, and the resulting products are called intercalation compounds. Much attention has been paid to intercalation compounds by physicists as well as chemists. Physicists are interested in the properties of low dimensional crystals and the dramatic changes in the properties before and after the intercalations.[8-10] Chemists are more interested in the intercalation mechanism, the interaction between host layers and guest species, and the industrial applications of the intercalation compounds. In table 1-I, typical inorganic layered crystals which are known to form intercalation compounds are listed together with guest species. Among the layered crystals listed in the table, graphite, silicate layered minerals and transition metal chalcogenides have been most extensively studied on their intercalation compounds.

Graphite and its intercalation compounds have been studied for a long time and a large number of experimental results have

Table 1-I Layer structured crystals that form intercalation compounds.

| | Example | Guests |
|---|---|---|
| Element | C (graphite)[9,10] | Alkali metals, Alkali earth metals, Rare earth metals, Halogen, Metal halides, Metal oxides, Acid ($HNO_3$, $H_2SO_4$, etc.) |
| Oxide | $MoO_3$,[11,12], $V_2O_3$,[13] $Li_xCoO_2$[14] | Hydrogen, Alkali metals |
| Chalcogenide | Transition metal dichalcogenides[3,5,6] ($TiS_2$, $TaS_2$, $MoS_2$, $NbSe_2$, etc.), Metal phosphorus trichalcogenides[15-18] ($FePS_3$, $MnPSe_3$, etc.), $Ta_2CS_2$[19,20] | Alkali metals, Alkali earth metals, Amines, Amides, Phosphines, Organometallic compounds, etc. |
| Mixed anion compound | FeOCl,[21-23] $WO_2Cl_2$,[24] $FeMoO_4Cl$,[25] ZrClN, etc. | Alkali metals, Amines, Organometallic compounds |

Table 1-I (Continued)

| | Examples | Guests |
|---|---|---|
| Oxoacid salt | $Zr(HPO_4)_2 \cdot nH_2O$,[26-28] Clay minerals[1] (montmorillonite, kaolinite, etc.), $K_4Nb_6O_{17}$,[29] $KTiNbO_5$,[30] etc. | $H_2O$, $NH_3$, Alcohols, Acetone, Amines, Amides, Aldehydes, Aromatics, Hydrazine, Organometallic compounds, etc. |
| Miscellaneous | $Ag_2C_2O$,[31] $Ni(CN)_2$,[32] etc. | |

been accumulated. An important characteristic of graphite is that it is amphoteric, i. e., it can accommodate both electron donors and acceptors. No other layer structured crystals are intercalated by electron acceptors. Another characteristic feature of graphite is the formation of stage compounds in which intercalated species are separated by single or multiple graphite layers in regular manners. There have been a number of theoretical as well as experimental approaches to the graphite intercalation compounds because perhaps graphite has the simplest layer structure.[33,34)]

Clay minerals, layered silicates, have also been studied for a long time like graphite.[1)] In particular, montmorillonite has been most extensively studied. Inorganic compounds of clays with organic and inorganic guests are called clay-organic and clay-inorganic compounds, respectively. Clay-organic compounds with higher alkylammonium ions which are introduced by ion-exchange are used as excellent gelling and swelling agents in organic solvents. The interlayer spaces of clays are also solvated with a variety of neutral molecules forming intercalation compounds. Recently, clay-inorganic compounds with metal oxide pillars have been synthesized. They have zeolitic micropores in the interlayer spaces and are expected to be potential heterogeneous catalysts and catalytic supports.[35,36)]

Layer structured transition metal dichalcogenides can intercalate alkali metals and organic bases. On intercalation

of these electron donors into transition metal dichalcogenides, the electronic properties are drastically changed. For instance, semiconductor for $MoS_2$ with a band gap of 1 eV changes into a metal with a critical temperature for superconductor at 0.4 K after intercalation of potassium.[37] Such changes are interpreted in terms of charge transfers from guest species to host layers.

The number of layered crystals which are known to form intercalation compounds is not so large as seen in Table 1-I. However, the combinations of the host layered crystals and guest species are almost limitless, and this fact makes intercalation compounds attractive to chemists, solid state physicists and materials scientist.

In this thesis, I have developed a new type of layered host β-zirconium chloride nitride, β-ZrClN. As described in more detail in the next chapter(Chapter 2), the layer structure of β-ZrClN has close-packed chlorine interlayers which sandwich Zr-N double layers. Unlike usual metal chlorides, β-ZrClN is not hygroscopic, and insoluble in water. Moreover, it is thermally stable up to 1120 K and 720 K, in a vacuum and in air, respectively. Although there are pretty large number of layered crystals with chalcogenide and oxide interlayers, few stable layered crystals with chloride interlayers have been reported as intercalation hosts.

β-ZrClN was first prepared by Juza and Heners in 1964[38] and the crystal structure was analyzed on the basis of the X-ray powder diffraction data.[39] Regardless of its attractive structure and stability, very few studies have been done on β-ZrClN since they analyzed the structure. This is probably due to the difficulty in the preparation of β-ZrClN of high purity and high crystallinity. Juza and Heners used $ZrCl_4$ and $NH_3$ at elevated temperature. In this thesis, I have re-examined their preparation procedures and clarified the problems which give rise to the difficulties in the preparation of β-ZrClN (Chapter 3), and then a new preparation method is developed, which uses $ZrH_2$ or Zr instead of $ZrCl_4$ as a zirconium source and gives us β-ZrClN in high yield (Chapter 4).

Highly crystalline sample can be obtained by chemical transport of the as-prepared sample and its transport mechanism is elucidated. Similar preparation procedures are also applied to layered crystals ZrXN (X= Br and I) (Chapter 4). It has been found that β-ZrClN can intercalate lithium chemically and electrochemically, and nonaqueous solvent molecules are co-intercalated with the lithium. Some structural models for the interlayer arrangements of the molecules are discussed (Chapter 5). The electrochemical properties and the possible use of β-ZrClN as a cathode electrode for a rechargeable lithium battery are studied (Chapter 6). It has also been found that β-ZrClN can uptake hydrogen as well as lithium. The electric

conductivities of the hydrogenated samples are measured and the structure is discussed (Chapter 7). β-ZrClN seems to be a promising candidate for the electrode of electrochromic device because the color of the crystal changes electrochemically from yellow green to black on intercalation. Preparation of β-ZrClN films on glass substrate is attempted from the view point of the application to such electrode (Chapter 8).

## 2 STRUCTURE OF β-ZrClN AND RELATED CRYSTALS

The structure of β-ZrClN is shown in Fig. 2-1, and the structural data according to Juza and Friedrichsen are summarized in Table 2-I.[39] As seen from the figure, each unit layer of β-ZrClN consists of double corrugated ZrN layers sandwiched by two close-packed chlorine layers. Such ZrClN layers sequenced Cl-Zr-N-N-Zr-Cl are stacked by van der Waals interactions. The XRD pattern of β-ZrClN was indexed on the basis of a hexagonal cell with a = 0.2081 and c = 0.9234 nm, which contains only 2/3 ZrClN formula unit. Juza and Friedrichsen explained this by the random stacking of the ZrClN layers as that found in $CdBr_2$ where the unit layers are stacked as an irregular mixture of the $CdI_2$ and the $CdCl_2$ type structures. The partial unit cell used by Juza and Friedrichsen is depicted in Fig. 2-2. Each zirconium atom is coordinated to three chlorine and three nitrogen atoms. Each nitrogen and chlorine atoms are in turn octahedrally coordinated: three zirconium and three nitrogen atoms, and three zirconium and three chlorine atoms, respectively. The distance between two adjacent chlorine atoms in the intralayer (0.374 nm) is slightly larger than that in the interlayer (0.360 nm). This suggests that the structure of β-ZrClN is layered.

Another polymorph called α-ZrClN was synthesized and its structure was analyzed by Juza and Heners.[38] The structure and lattice parameters are shown in Fig.2-3 and table 2-II,

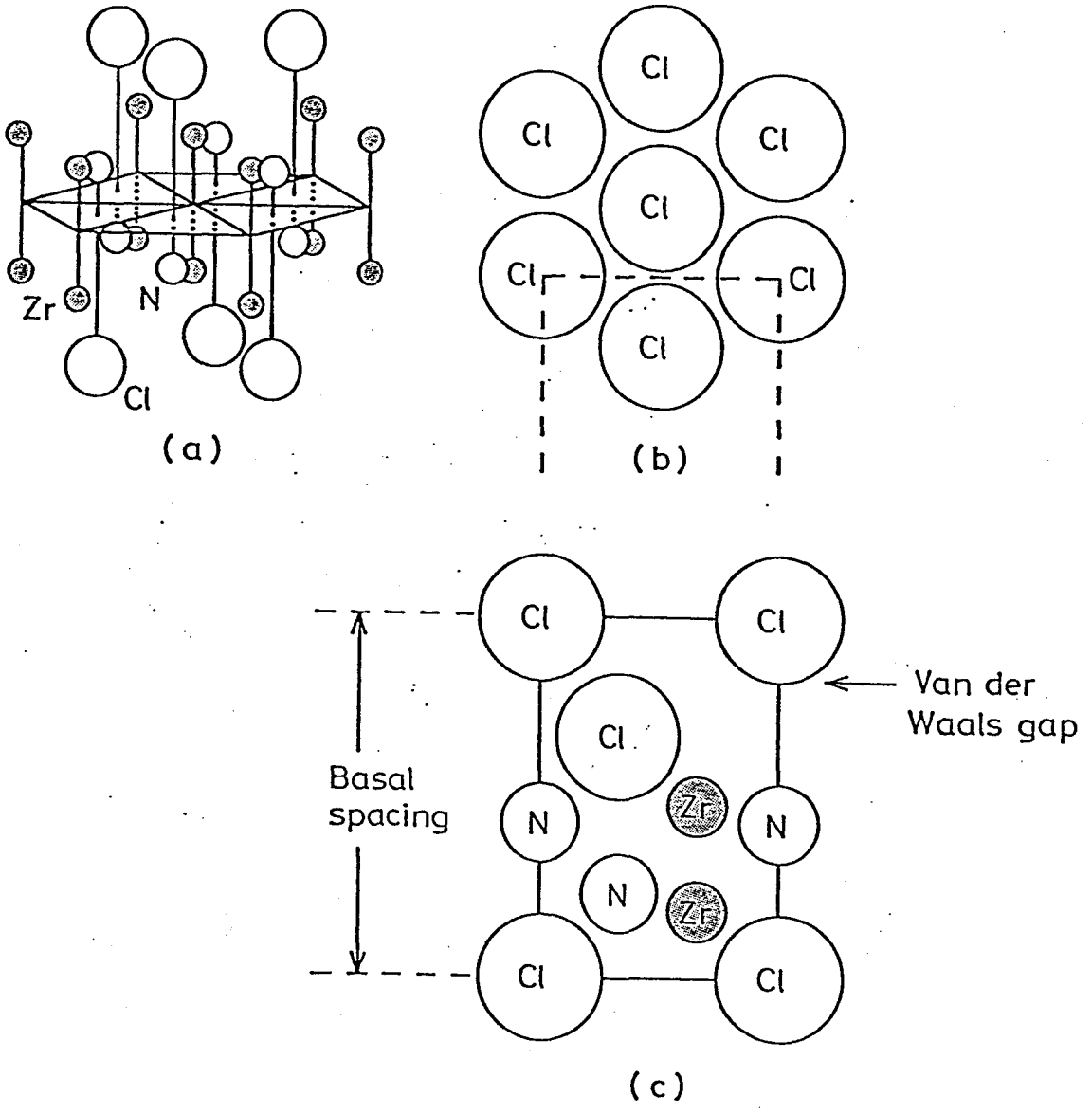


Fig. 2-1 Schematic structure model of β-ZrClN. (a) perspective view, (b) viewed perpendicular to the close-packed chlorine layer, (c) viewed parallel to the layers.

Table 2-I Crystallographic data and interatomic distances of β-ZrClN.

hexagonal, a = 0.2081 nm, c = 0.9234 nm, Z = 2/3

Atom parameter

| | x | y | z |
|---|---|---|---|
| Zr(1) | 0 | 0 | 0.147 |
| Zr(2) | 0 | 0 | -0.147 |
| Cl(1) | 2/3 | 1/3 | 0.332 |
| Cl(2) | 1/3 | 2/3 | -0.332 |
| N(1) | 1/3 | 2/3 | 0.10 |
| N(2) | 2/3 | 1/3 | -0.10 |

Distances /nm

| | | |
|---|---|---|
| Zr(1) - Zr(1) | 0.360 | parallel to the layer |
| Zr(1) - Zr(2) | 0.271 | vertical to the layer (interlayer) |
| Zr(1) - Cl(1) | 0.269 | nearest |
| Zr(1) - N(1) | 0.213 | nearest |
| Cl(1) - Cl(1) | 0.360 | interlayer (parallel to the layer) |
| Cl(1) - Cl(2) | 0.374 | intralayer |

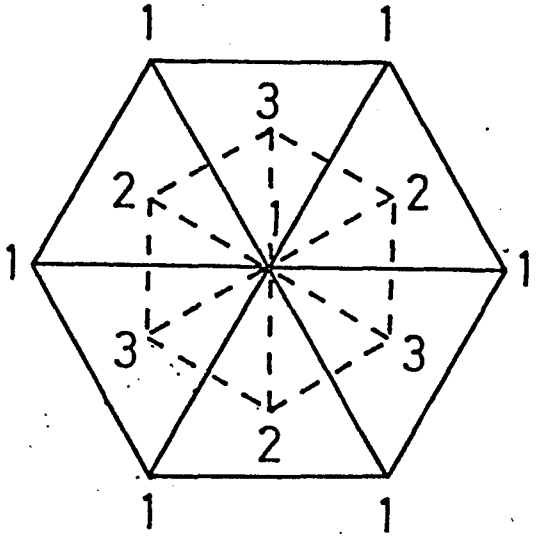


Fig. 2-2 (001) projection of hexagonal cell. 1; Zr site, 2; N site, 3; Cl site.

Table 2-II Lattice parameters of α-ZrClN in comparison with those of FeOCl.

| | a / nm | b / nm | c / nm |
|---|---|---|---|
| α-ZrClN | 0.408 | 0.352 | 0.857 |
| FeOCl | 0.3780 | 0.3302 | 0.7917 |

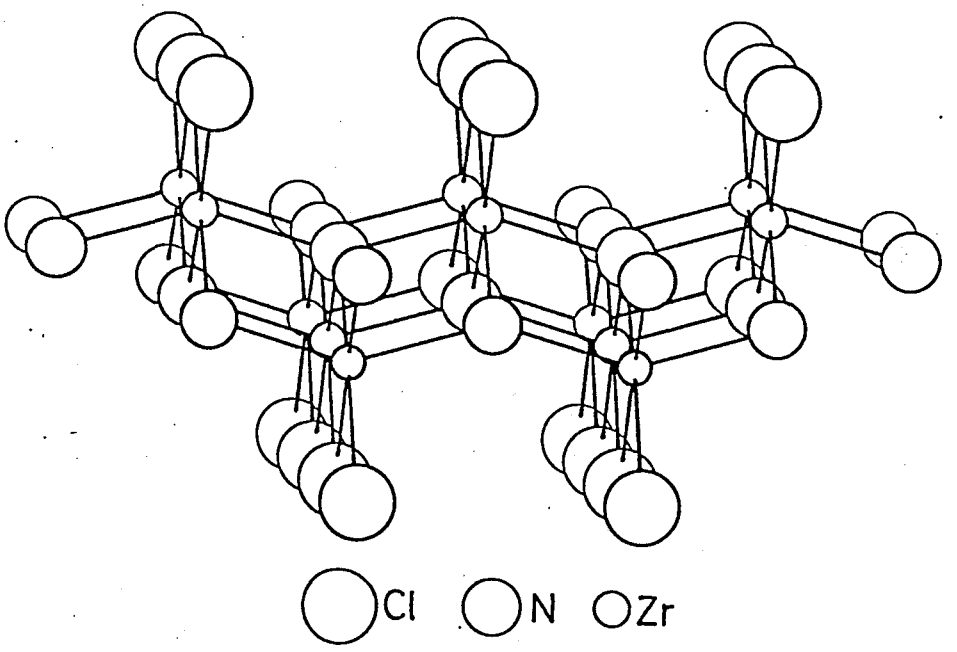


Fig. 2-3 Structure of α-ZrClN, showing part of one layer viewed almost parallel to the layer.

respectively. As seen from Fig.2-3, each unit layer of α-ZrClN consists of double corrugated ZrN layers sandwiched between two chlorine layers in a manner similar to β-ZrClN, but α-ZrClN has the FeOCl type structure. It is well known that FeOCl forms intercalation compounds with a wide variety of electron donors, and thus α-ZrClN is also attractive crystal for intercalation host layer. However, α-ZrClN is very unstable to moisture in air in contrast to β-ZrClN. In the present thesis, β-ZrClN was mainly studied. There are a series of layer structured crystals $M^{IV}XN$ ($M^{IV}$=Zr,Ti, X=Cl,Br,I) which are isostructural with α or β-ZrClN.[38,39] These crystals are classified in Table 2-III by the structures. Although I have mainly focused on β-ZrClN in this thesis, α-ZrBrN, β-ZrBrN, and ZrIN are synthesized by the new method developed for β-ZrClN (Chapter 4).

Table 2-III Layer structured metal halide nitride $M^{IV}XN$ ($M^{IV}$ = Zr, Ti; X = Cl, Br, I). (Colors of crystals are shown in the parentheses.)

| α - form | β - form |
|---|---|
| α-ZrClN (yellow) | β-ZrClN (yellow green) |
| α-ZrBrN (yellow) | β-ZrBrN (yellow green) |
| ZrIN (orange) | |
| TiClN (black) | |
| TiBrN (black) | |
| TiIN (black) | |

# 3 PREPARATIONS OF β-ZrClN BY THE REACTION OF $ZrCl_4$ WITH $NH_3$

β-ZrClN was first prepared by Juza and Heners on 1967 through the reaction of zirconium tetrachloride with ammonia.[38] I have also tried to prepare β-ZrClN after their method, but found that the yield on the basis of the amount of $ZrCl_4$ loaded is as low as 20-30%. In order to improve the yield and to understand the formation mechanism, the reaction of $ZrCl_4$ with $NH_3$ was re-examined and it has been found that the low yield is mainly due to the formation of a volatile compound $(NH_4)_2ZrCl_6$, which is physically transported to a cooler part outside the reaction zone before being decomposed to β-ZrClN. In this chapter, $(NH_4)_2ZrCl_6$ is prepared and its thermal behavior in an ammonia atmosphere is studied by using a quartz spring balance. Similar study is performed on $ZrCl_4$ in an ammonia atmosphere. Synthesis of β-ZrClN by thermal decomposition of zirconium amide trichloride is also investigated.

## 3.1 Preparation of β-ZrClN by the Method of Juza and Heners

Figure 3-1 shows a schematic drawing of the apparatus used for the reaction of $ZrCl_4$ with $NH_3$ at elevated temperatures. It consists of a fused silica tube with ground-glass joints at the ends for gas inlet and outlet. The dimensions of the tube are about 1 m in length and 35 mm in diameter. $ZrCl_4$ was purified

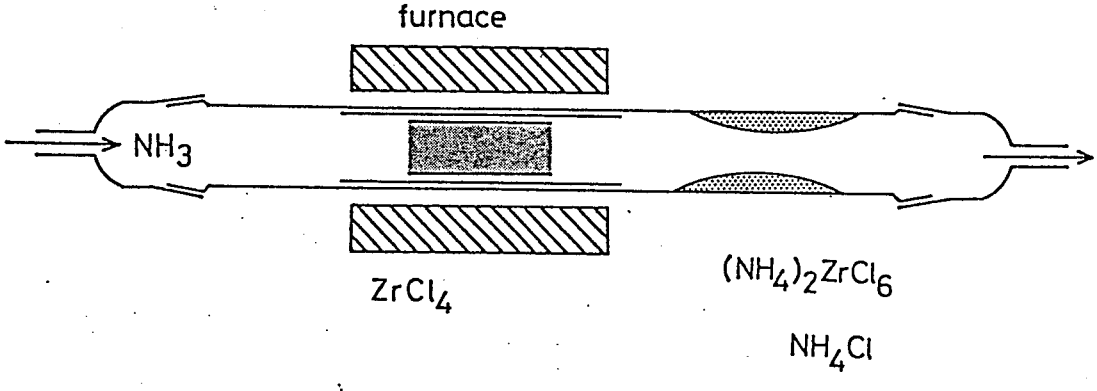


Fig. 3-1 Apparatus for the reaction of $ZrCl_4$ with $NH_3$.

by sublimation in vacuum at 573 K. About 10 g of the purified $ZrCl_4$ was loaded in the reactor under a flowing dry nitrogen. After evacuation, a stream of gaseous ammonia was passed through the reactor at a rate of about 200 $cm^3$ $min^{-1}$ during the reaction. After the $ZrCl_4$ was allowed to stand for 1 h in the stream of ammonia at room temperature, the temperature was raised up to 873 K at the rate of 3 K $min^{-1}$, and kept at this temperature for 5 h.

The $ZrCl_4$ loaded was changed into powders with yellow green color, which was identified to be β-ZrClN by XRD analysis. The yield of β-ZrClN on the basis of the amount of $ZrCl_4$ loaded was determined to be about 20-30%. On the cooler part of the reactor, designated by C in Fig. 3-1, a pretty large amount of white powder was deposited after the reaction. It consisted of $(NH_4)_2ZrCl_6$ and $NH_4Cl$. The low yield of β-ZrClN from $ZrCl_4$ is probably due to the formation of $(NH_4)_2ZrCl_6$, which was removed from the reaction system by vaporization during the heating step before decomposing to β-ZrClN.

## 3.2 Preparation and Properties of $(NH_4)_2ZrCl_6$

As seen in the following chapters, $(NH_4)_2ZrCl_6$ is a key compound for the synthesis of β-ZrClN. I have prepared $(NH_4)_2ZrCl_6$ and studied on the thermal behavior in ammonia in comparison with that of $ZrCl_4$.

### 3.2.1 Experimental

**Preparation of $(NH_4)_2ZrCl_6$** Ammonium hexachlorozirconate(IV) $(NH_4)_2ZrCl_6$ was prepared by the dry method similar to that reported by Rister and Flengas[40] for $K_2ZrCl_6$ in the following procedure: zirconium tetrachloride was purified by sublimation and mixed with ammonium chloride dried at 453 K under vacuum in the molar ratio of 1:2 in a dry box. The mixture was placed in a Pyrex boat and heated to 673 K in a stream of dry nitrogen. After the mixture was kept at the temperature for 5 h, the resulting residue in the Pyrex boat was taken out and vacuum sealed in a Pyrex tube, which was then placed in a two-zone furnace. The temperature of the residue was regulated at 673 K, the other end of the sealed tube being at 373 K. After standing for 5 h, white crystals of $(NH_4)_2ZrCl_6$ were transported to the lower temperature zone. Found: Zr, 27.4; N, 8.23; Cl, 62.6%. Calcd. for $(NH_4)_2ZrCl_6$: Zr, 26.8; N, 8.24; Cl, 62.6%.

**Analyses** Since most of the products treated in the present section are sensitive to the humidity in air, those were manipulated in a dry box unless otherwise noted. XRD patterns were measured under a dry argon atmosphere by using a cylindrical cover having thin polyethylene windows; nickel-filtered Cu-$K_\alpha$ radiation was used.

Elemental analyses for zirconium, chlorine and nitrogen were carried out after the sample was dissolved in 2 mol $dm^{-3}$ sulfuric

acid. The nitrogen content was determined by Kjeldahl method; zirconium and chlorine were determined gravimetrically as $ZrO_2$ and AgCl, respectively. The density of $(NH_4)_2ZrCl_6$ was measured pycnometrically with toluene at 298 K.

**Thermogravimetric Study in Ammonia** The amount of ammonia taken up by $(NH_4)_2ZrCl_6$ was measured gravimetrically by using a quartz spring balance as a function of pressure of ammonia at 298 K. The sample was heated in an ammonia stream (flow rate of 50 $cm^3$ $min^{-1}$) to 923 K for a heating rate of 3 K $min^{-1}$. Similar experiment was performed on $ZrCl_4$.

### 3.2.2 Characterization of $(NH_4)_2ZrCl_6$

**X-ray Diffraction Study** The XRD data of $(NH_4)_2ZrCl_6$ is shown in Table 3-I. The XRD pattern is very similar to that of $K_2ZrCl_6$ reported by Rister and Flengas[40] and all the diffraction peaks can be indexed on the basis of a cubic lattice with a = 1.0127(2) nm. Moreover, the lattice type of $(NH_4)_2ZrCl_6$ is face-centered cubic because the diffraction peaks are only present when h,k,l are all even or all odd. Engel[41] showed that a series of hexachloro complexes with the general formula $A_2MCl_6$ (A = K, $NH_4$, Rb, Cs, Tl; M = Ti, Se, Zr, Sn, Te, Pt, Pb) had the $K_2PtCl_6$ structure and that for the complexes with an A ion in common, the lattice constants can be related with those of the corresponding Rb- salts by a linear relation as shown in Fig. 3-2. Although $(NH_4)_2ZrCl_6$ is not included in his plot, the

Table 3-I X-ray diffraction data of $(NH_4)_2ZrCl_6$

| $d_{obs}$/nm | $d_{calc}$/nm | hkl | $I/I_0$ |
|---|---|---|---|
| 0.5844 | 0.5847 | 111 | 100 |
| 0.5068 | 0.5064 | 200 | 65 |
| 0.3577 | 0.3580 | 220 | 15 |
| 0.3050 | 0.3053 | 311 | 50 |
| 0.2923 | 0.2923 | 222 | 60 |
| 0.2534 | 0.2532 | 400 | 100 |
| 0.2320 | 0.2323 | 331 | 20 |
| 0.2263 | 0.2264 | 420 | 50 |
| 0.2070 | 0.2067 | 422 | 5 |
| 0.1947 | 0.1949 | 333 | 25 |
| 0.1791 | 0.1790 | 440 | 60 |
| 0.1712 | 0.1712 | 531 | 20 |
| 0.1687 | 0.1688 | 600,442 | 25 |
| 0.1462 | 0.1462 | 444 | 10 |

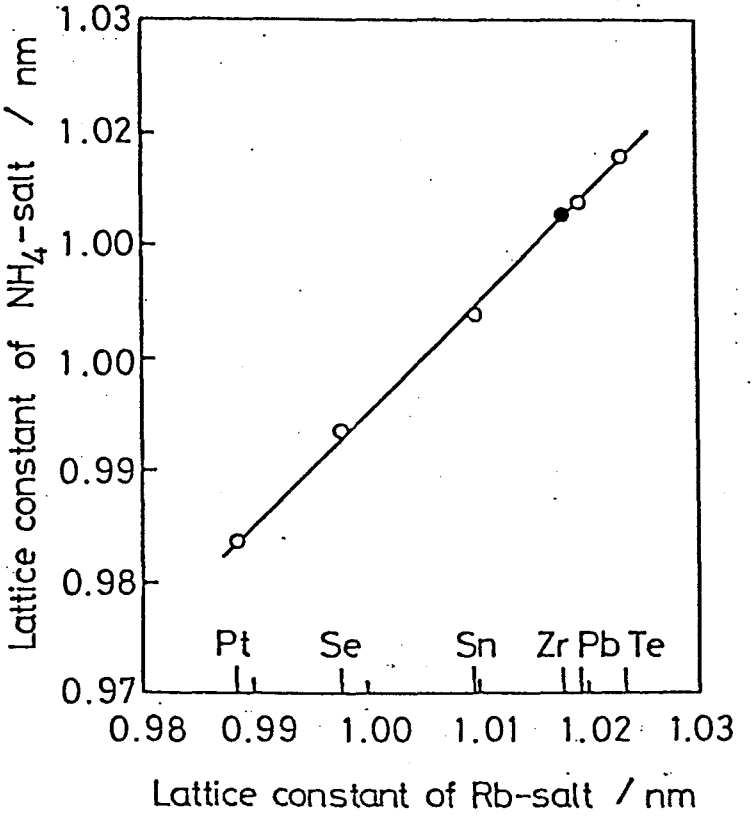


Fig. 3-2 Linear relationship between the lattice constants of $NH_3$-salt and those of Rb-salt. (●): This work, (o): results done by Engel.[41)]

value obtained above fits well on the line for the ammonium series. This fact indicates that $(NH_4)_2ZrCl_6$ has the $K_2PtCl_6$ structure. The density determined for the $(NH_4)_2ZrCl_6$ prepared by the direct method in this study is 2.14 g $cm^{-3}$, which is in good agreement with the value of 2.17 g $cm^{-3}$ calculated on the basis of the $K_2PtCl_6$ structure with a = 1.0127 nm.

Ammonium hexachlorozirconate can be also prepared by the wet method from hot aqueous solutions of zirconium dichloride oxide and ammonium chloride.[42,43] If the solution is saturated with hydrogen chloride and gradually cooled, the crystals of $(NH_4)_2ZrCl_6$ precipitate. It is found that the crystals thus prepared exhibit the XRD pattern identical to that of the crystals obtained by the direct method. Toptygina and Barskaya[42] prepared $(NH_4)_2ZrCl_6$ by the wet method and reported its XRD data, which however, do not coincide with ours. Since their chemical analysis data are in agreement with ours for $(NH_4)_2ZrCl_6$, they probably used the sample hydrolyzed in air for the measurement of the XRD pattern. Yajima et al.[44] investigated the reaction of gaseous $ZrCl_4$ with ammonia at elevated temperatures, and reported that in the temperature range 573 - 673 K, white crystals with composition $ZrCl_4 \cdot 2NH_3$ were formed. Strangely, the XRD pattern reported by them for the crystal is identical to that of $(NH_4)_2ZrCl_6$. Although the detailed procedures are not reported, it is likely that Yajima et al. analyzed the as-deposited sample without purification: the sample was probably a mixture of $(NH_4)_2ZrCl_6$ and non-crystalline

zirconium amide trichloride $ZrCl_3(NH_2)\cdot xNH_3$ and the overall ratio of Zr : N : Cl of the mixture is 1 : 2 : 4. The formation of the zirconium amide trichloride will be discussed later in more details.

**Uptake of ammonia by $(NH_4)_2ZrCl_6$** Fig. 3-3 shows the amounts of ammonia taken up by $(NH_4)_2ZrCl_6$ at 298 K as a function of increasing-decreasing pressure of ammonia. The amount was recorded after standing for 2 d at each pressure although the rate of uptake or release of ammonia is so slow that it takes more than 2 d to attain complete equilibrium. As seen in the figure, the amount of uptake gradually increases with the pressure and approaches 9 moles per mole of $(NH_4)_2ZrCl_6$ at the pressure of about 1 atm. On reducing the pressure to $1.4\times10^3$ Pa, only 2 moles of ammonia are removed. By prolonged evacuation at the pressure of $10^{-1}$ Pa for 4 d, additional 5 moles of ammonia are removed, but 2 moles of ammonia are tenaciously retained.

Separate samples of $(NH_4)_2ZrCl_6$ were also treated similarly and taken out to see the crystalline phases present at the different stages of uptake of ammonia. The XRD pattern of the sample equilibrated with 1 atm of ammonia exhibited the intense diffraction peaks due to $NH_4Cl$ with the disappearance of the peaks due to $(NH_4)_2ZrCl_6$. The sample evacuated after the uptake of ammonia still exhibited only the peaks due to $NH_4Cl$.

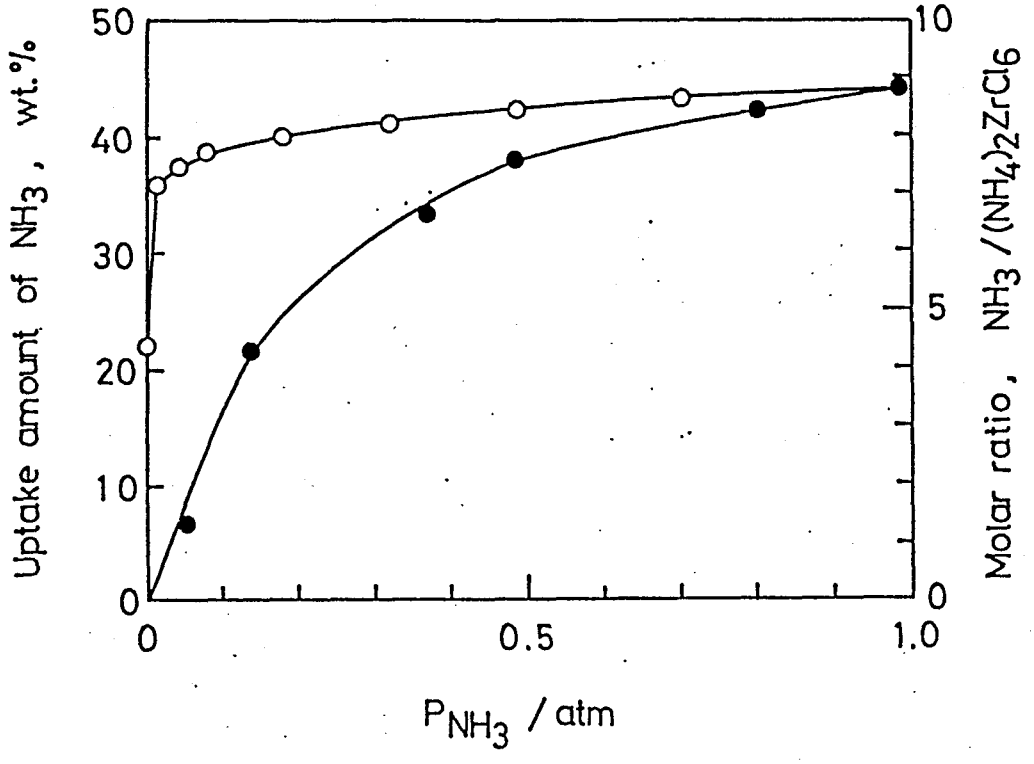


Fig. 3-3 Amount of ammonia taken up by $(NH_4)_2ZrCl_6$ at 298 K as a function of ammonia. (●): increasing pressure, (○): decreasing pressure.

### 3.2.3 Thermogravimetric Analyses of $(NH_4)_2ZrCl_6$ and $ZrCl_4$ in Ammonia

The thermogravimetric analysis of $(NH_4)_2ZrCl_6$ was carried out in a stream of ammonia after about 9 moles of ammonia were taken up. As shown in Fig. 3-4, the ammonia is gradually removed with an increase in the temperature, and at 520 K the sample reverts to the initial state in weight. The XRD pattern of the sample measured at this state indicated that the diffraction peaks of $NH_4Cl$ extremely decreased in the intensity and, on the contrary, those of $(NH_4)_2ZrCl_6$ were almost completely recovered. The sample vaporized at about 720 K and only 15% of the initial weight was left in the thermogravimetric analysis cell. The residue was found to be a mixture of α- and β-ZrClN.

Similar analysis was performed on $ZrCl_4$ in a stream of ammonia. During standing in ammonia of the pressure of 1 atm for 8 h, one mole of $ZrCl_4$ took up ammonia as much as 8 moles. Then, the temperature of the sample was raised in the manner similar to that of the analysis of $(NH_4)_2ZrCl_6$. Figure 3-5 shows the thermogravimetric curve observed. The curve is very similar to that observed for $(NH_4)_2ZrCl_6$ except that the weight does not revert to the initial state; as seen from the figure, about 1 mole of ammonia is retained up to 670 K at which the vaporization of the sample begins. On heating to 923 K, about 60% of the initial weight was lost and the residue was β-ZrClN.

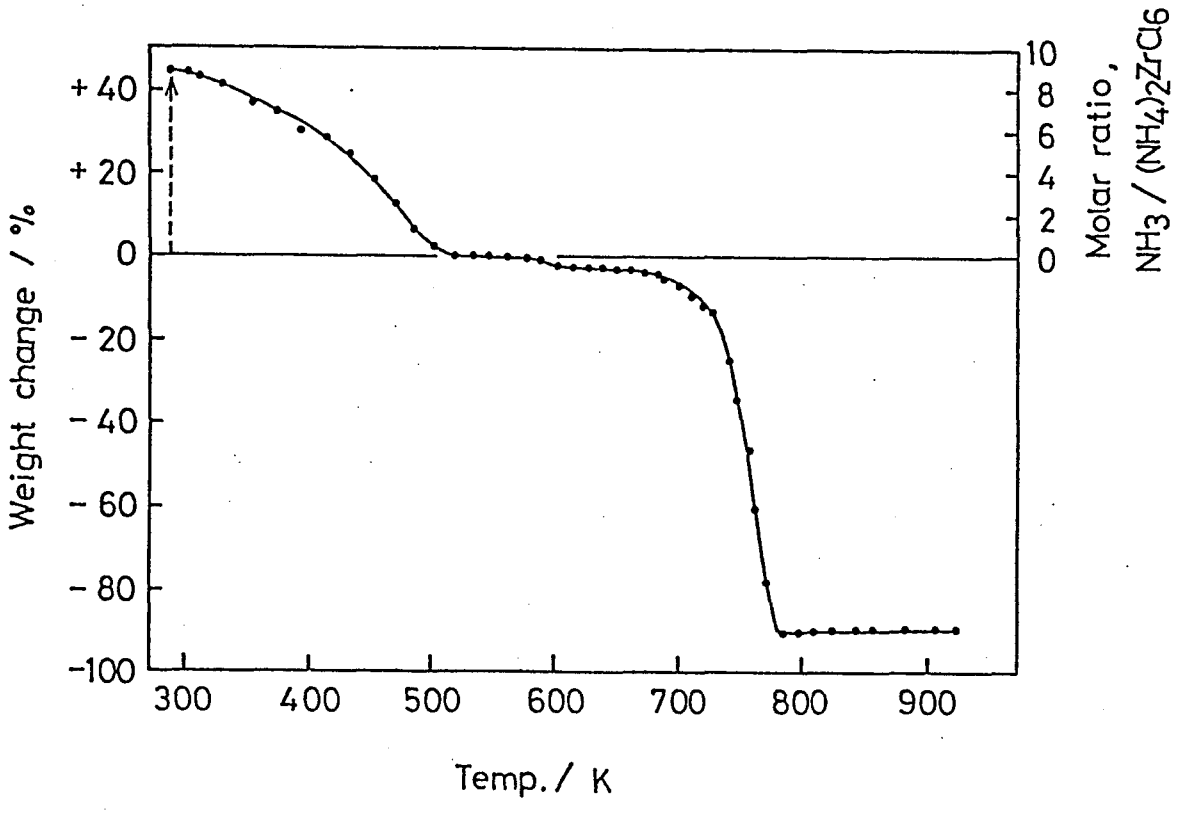


Fig. 3-4 Thermogravimetric curve for $(NH_4)_2ZrCl_6$ in an ammonia stream.

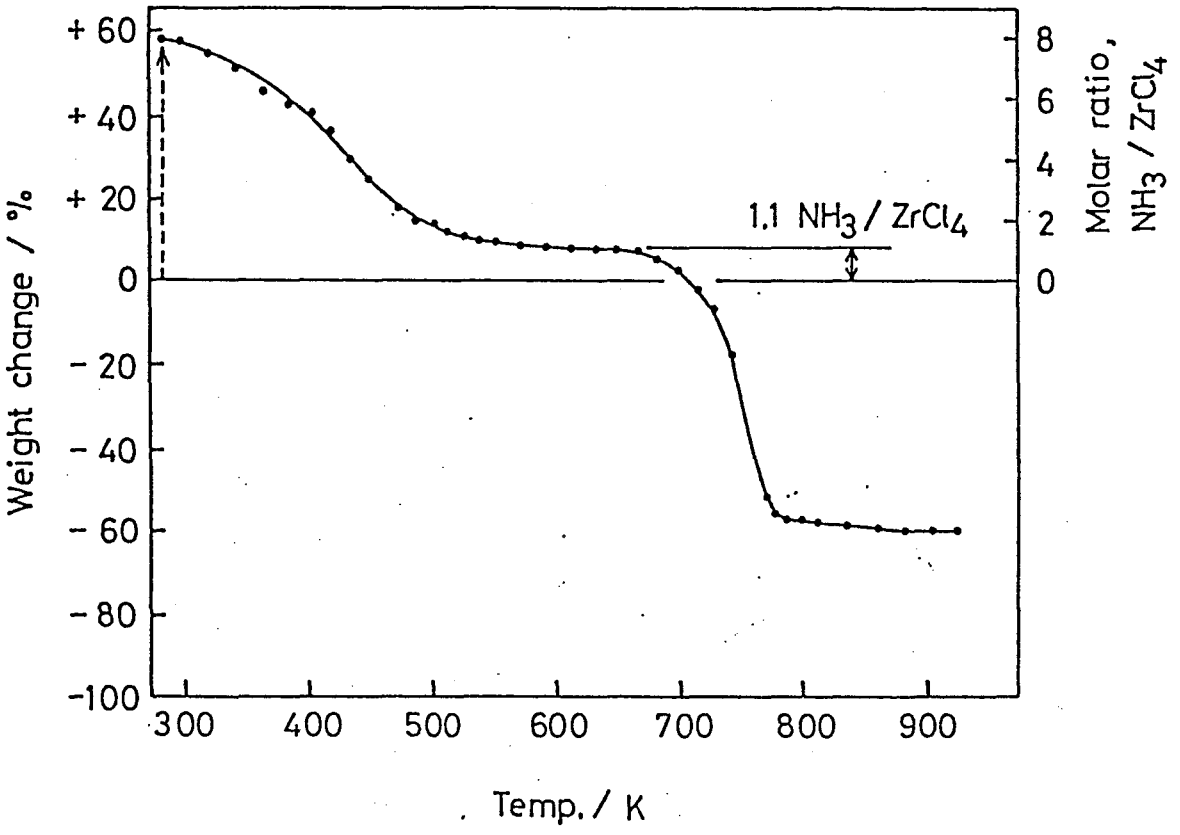


Fig. 3-5 Thermogravimetric curve for $ZrCl_4$ in an ammonia stream.

### 3.2.4 Thermal Behavior of $(NH_4)_2ZrCl_6$ and $ZrCl_4$ in Ammonia

Drake and Fowles[43] studied the ammonolysis of $(NH_4)_2ZrCl_6$ with liquid ammonia. They showed that $(NH_4)_2ZrCl_6$ behaved essentially like $ZrCl_4$. $ZrCl_4$ is subjected to ammonolysis to only one Zr-Cl bond in liquid ammonia, giving the zirconium amide chloride[45]:

$$ZrCl_4 \xrightarrow{NH_3} ZrCl_3(NH_2)\cdot xNH_3 + NH_4Cl$$

Similarly $(NH_4)_2ZrCl_6$ undergoes ammonolysis to one Zr-Cl bond

$$(NH_4)_2ZrCl_6 \xrightarrow{NH_3} (NH_4)_2[ZrCl_5(NH_2)]\cdot xNH_3 + NH_4Cl$$

On washing with liquid ammonia, the complex decomposes into ammonium chloride and zirconium amide trichloride:

$$(NH_4)_2[ZrCl_5(NH_2)]\cdot xNH_3 \longrightarrow 2\ NH_4Cl + ZrCl_3(NH_2)\cdot xNH_3$$

The tensimetric study of $ZrCl_4$ by Fowles and Pollard[46], and our study of zirconium amide trichloride which is described in later section show that x is about 6-7 in the above equations.

The results of thermogravimetric analyses seem to suggest that $(NH_4)_2ZrCl_6$ and $ZrCl_4$ are subjected to ammonolysis with gaseous ammonia in a similar manner:

$$(NH_4)_2ZrCl_6 + 9\ NH_3 \longrightarrow 3\ NH_4Cl + ZrCl_3(NH_2)\cdot 7NH_3 \qquad (3.1)$$

$$ZrCl_4 + 8\ NH_3 \longrightarrow NH_4Cl + ZrCl_3(NH_2)\cdot 6NH_3 \qquad (3.2)$$

In the reaction with gaseous ammonia, however the resulting $NH_4Cl$ is not washed out, but remains in the product. The XRD pattern of the product indicates the formation of $NH_4Cl$ with the disappearance of $(NH_4)_2ZrCl_6$ . The zirconium amide trichloride $ZrCl_3(NH_2)\cdot xNH_3$ is likely a non-crystalline polymeric solid as suggested by Allbutt and Fowles[45]. The XRD results tell us that on heating, the reaction of eq. (3.1) is reversed, and $NH_4Cl$ reacts with $ZrCl_3(NH_2)$ and reforms $(NH_4)_2ZrCl_6$. A very small drop in weight is observed at 600 K in the thermogravimetric curve of Fig. 3-4. This drop can be attributed to the sublimation of $NH_4Cl$ remaining unreacted in the system.

In the case of $ZrCl_4$, one mole of ammonia remains in the system above 520 K until the vaporization of the sample begins at 670 K. This difference in the behavior of the ammonolysis products of $(NH_4)_2ZrCl_6$ and $ZrCl_4$ can be interpreted in terms of the insufficient $NH_4Cl$ in the latter ammonolysis product. Since only one mole of $NH_4Cl$ is present in the product (eq. (3.2)), only one third of $ZrCl_3(NH_2)$ is converted into $(NH_4)_2ZrCl_6$ according to the following reaction:

$$ZrCl_3(NH_2)\cdot 6NH_3 + NH_4Cl \longrightarrow \frac{1}{3}(NH_4)_2ZrCl_6 + \frac{2}{3}ZrCl_3(NH_2) + \frac{26}{3}NH_3$$

It is interesting to note that the abrupt decreases in weight occur at the same temperature irrespective of the kinds of

starting samples. It is apparent that the temperature of 720 K corresponds to the vaporization of $(NH_4)_2ZrCl_6$, although the decomposition of $ZrCl_3(NH_2)$ to β-ZrClN is also accompanied around this temperature as shown in section 3.3.

In the preparation procedure of β-ZrClN from $ZrCl_4$ and $NH_3$, the formation of $(NH_4)_2ZrCl_6$ as a by-product is unavoidable, which is removed from the reaction system by vaporization above 670 K. This should be responsible for the low yield of β-ZrClN.

## 3.3 Preparation of β-ZrClN by Thermal Decomposition of $ZrCl_3(NH_2)\cdot xNH_3$

As shown in the previous section, $ZrCl_4$ are subjected to ammonolysis with gaseous as well as liquid ammonia and form the amide $ZrCl_3(NH_2)\cdot xNH_3$ and $NH_4Cl$. One third of the amide reverts to $(NH_4)_2ZrCl_6$ in the present of $NH_4Cl$ at elevated temperature. In the preparation of β-ZrClN, if the amide is isolated from $NH_4Cl$, it is expected that the formation of $(NH_4)_2ZrCl_6$ as by-product is avoidable. In the present section, thermal decomposition processes of the isolated amide in an ammonia stream and under vacuum are studied.

### 3.3.1 Experimental

**Preparation of Zirconium Amide Trichloride.** Drake and

Fowles[47] revealed that $ZrCl_4$ was subjected to ammonolysis to only one Zr-Cl bond in liquid ammonia, giving the zirconium amide chloride:

$$ZrCl_4 + (x + 2)NH_3 \longrightarrow ZrCl_3(NH_2)\cdot xNH_3 + NH_4Cl$$

They removed the resulting ammonium chloride by washing the separated solid with liquid ammonia repeatedly. In the present study, a glass apparatus was used, which was so designed that the ammonium chloride could be continuously leached out with liquid ammonia, as shown in Fig. 3-6. The apparatus works essentially as a Soxhlet extraction unit. Under a dry nitrogen atmosphere, about 4 g of zirconium tetrachloride purified by sublimation was placed on the glass filter E in the reaction tube D, the upper end of which is connected to a Dry Ice-methanol condenser B by a ground joint. Dry ammonia gas (99.999%) was introduced into the apparatus through the valve A and liquified by the condenser. The liquified ammonia comes down and reacts with the $ZrCl_4$ on the glass filter. The ammonium chloride formed by the reaction was dissolved in the liquid ammonia and leached out into the flask F connected below by a ground joint. The ammonia gas rising from the flask through the bypass C can also be liquified by the condenser. After refluxing for 3 h, the liquid ammonia was removed and the apparatus was purged with dry nitrogen. The amide was left on the glass filter in the form of white flocculent.

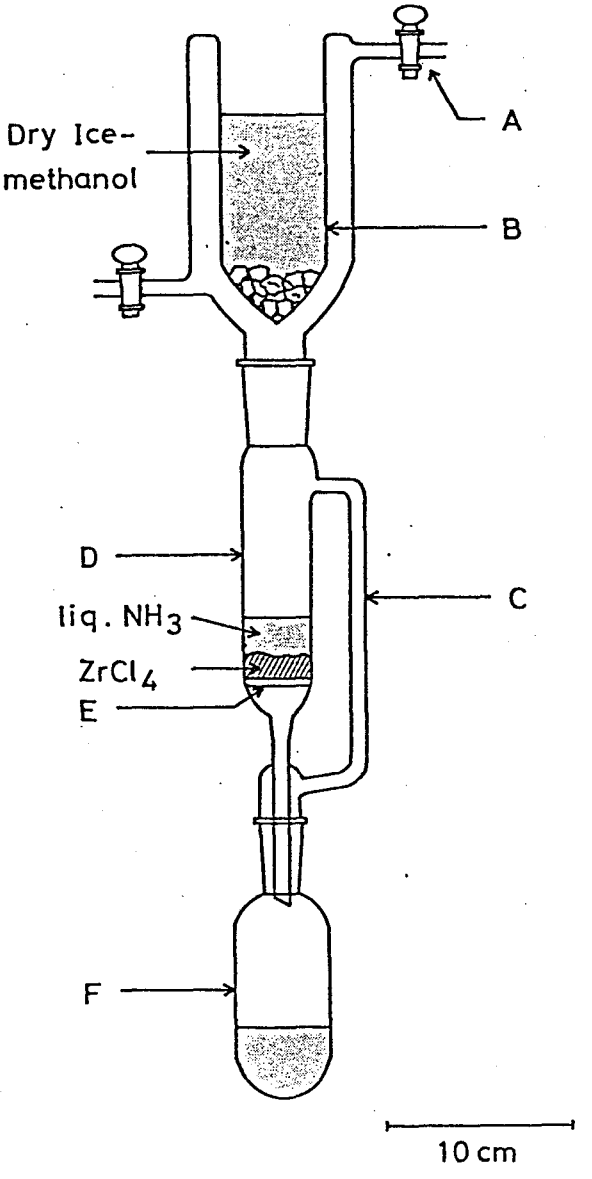


Fig. 3-6 Soxhlet type glass apparatus used for the preparation of zirconium amide trichloride.

**Analyses.** Elemental analyses for zirconium and nitrogen were carried out according to the procedures described in section 3.2 Chlorine content was analyzed by Fajans' method. The thermogravimetric analysis of the zirconium amide chloride was carried out by using a quartz spring balance in a vacuum and in an ammonia stream for a heating rate of 3 K $min^{-1}$. The flow rate of the ammonia was 50 $cm^3$ $min^{-1}$.

### 3.3.2 Results and Discussion

The chemical analysis of the product showed that the contents of Zr, N and Cl were 28.1, 33.6 and 31.5%, respectively. This analytical result corresponds to the atomic ratio Zr : N : Cl = 1.00 : 7.8 : 2.9, indicating that only one of the Zr-Cl bonds was subjected to ammonolysis and that the zirconium amide chloride with an approximately stoichiometric composition $ZrCl_3(NH_2)\cdot 7NH_3$ was obtained.

The thermogravimetric analysis curves of the zirconium amide chloride are shown in Fig. 3-7. On evacuation at room temperature for 3 h, the amide lost about 4 moles of ammonia, and then 3 moles of ammonia are gradually removed up to 510 K.

$$ZrCl_3(NH_2)\cdot 7NH_3 \longrightarrow ZrCl_3(NH_2)\cdot 3NH_3 + 4\ NH_3$$

$$ZrCl_3(NH_2)\cdot 3NH_3 \longrightarrow ZrCl_3(NH_2) + 3\ NH_3$$

In the second decomposition stage accompanied by a steep weight loss beginning from 550 K, white sublimate consisting of $ZrCl_4$

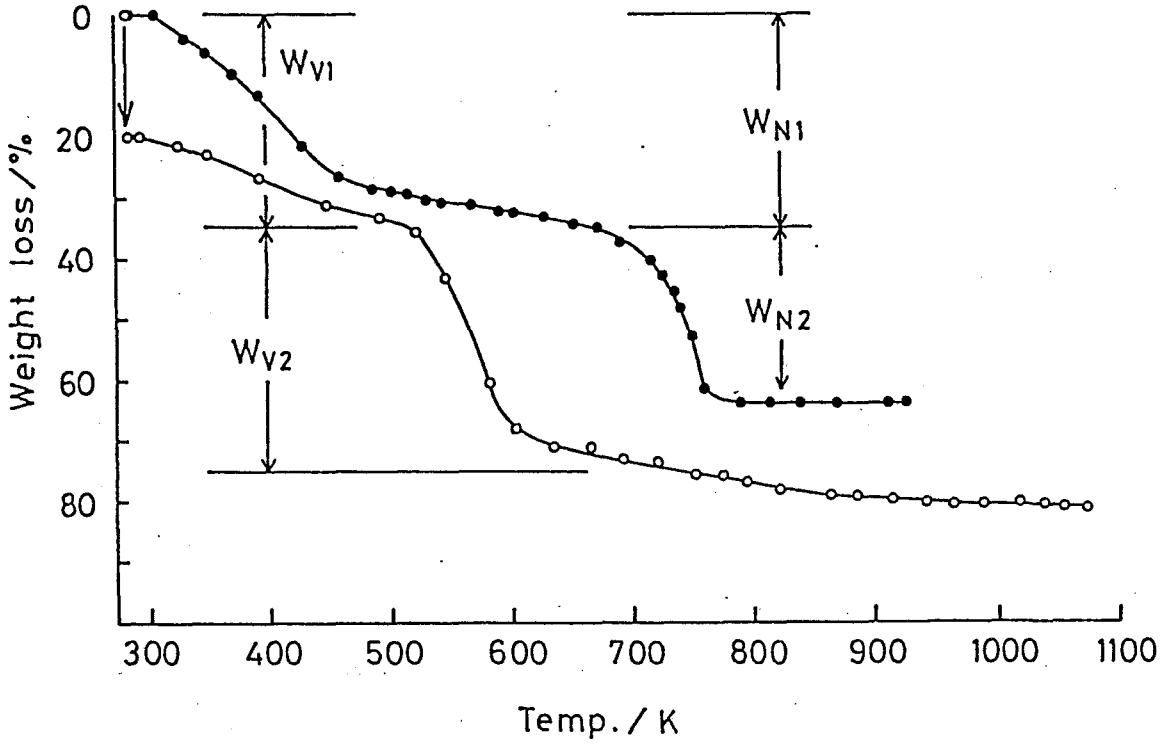


Fig. 3-7 Thermogravimetric curves for zirconium amide trichloride $ZrCl_3(NH_2)\cdot 7NH_3$ measured in a vacuum (o) and in an ammonia stream (●).

and $NH_4Cl$ appeared on the cooler parts of the glass walls. Probably, the following decomposition occurs in this heating stage:

$$2\ ZrCl_3(NH_2) \longrightarrow ZrClN + ZrCl_4 + NH_4Cl$$

The amount of the weight loss for this reaction was calculated to be 67%. On the ammoniate formula ($ZrCl_3(NH_2)\cdot 7NH_3$) basis, this amount is reduced to 43%, which is in good agreement with the amount of the loss $W_{V2}$ (40%). Yellow solid having the atomic ratio $Zr_{1.0}Cl_{1.0}N_{0.8}$ was obtained when the decomposition was interrupted at 720 K. The solid was very reactive and took fire when dropped into water. Irrespective of the similarity of the atomic ratio, it is apparent that the solid is different from our desired β-ZrClN which is stable in water. Similar unknown yellow solid was also found by Fowles and Pollard[46] in the course of the preliminary study of the decomposition of the zirconium amide trichloride. On further heating up to 1073 K, the sample lost the weight gradually and gave black powder, which was found to be ZrN by XRD analysis.

Even in an ammonia stream, the amount of the first weight loss ($W_{N1}$) corresponded almost to the first weight loss ($W_{V1}$) observed in a vacuum. However, the second weight loss began at the temperature higher by about 420 K than that of the decomposition in a vacuum. The residue obtained after the decomposition at 923 K was identified to be β-ZrClN by XRD analysis. The amount of the weight loss (ammoniate formula

basis) calculated on the basis of the following reaction was 22%:

$$ZrCl_3(NH_2) + 2\ NH_3 \longrightarrow ZrClN + 2\ NH_4Cl$$

Although the amount of the weight loss $W_{N2}$ (29%) was a little larger than the calculated amount, it is apparent that the zirconium amide trichloride could be efficiently converted into β-ZrClN. It should be noted that in the ammonia stream, the decomposition temperature of $ZrCl_3(NH_2)$ is much higher than the temperature in a vacuum. It seems likely that the ammonia suppresses the decomposition of the amide, and that no sooner the $ZrCl_4$ is evolved at the higher decomposition temperature than it reacts with ammonia, forming β-ZrClN.

# 4 NEW PREPARATION ROUTE FOR β-ZrClN AND ITS CHEMICAL VAPOR TRANSPORT

In the preparation of β-ZrClN from the reaction of $ZrCl_4$ with $NH_3$, volatile compound $(NH_4)_2\ ZrCl_6$ is easily formed, resulting in the low yield of β-ZrClN. The thermal decomposition of the amide $ZrCl_3(NH_2)$ in an ammonia atmosphere gives β-ZrClN in high yield, as shown in the foregoing chapter, however, the starting amide was also prepared by the ammonolysis of hydrolyzable $ZrCl_4$ with liquid ammonia. In this chapter, a new and simple synthesis route for β-ZrClN has been developed, and a similar procedure is applied to the preparation of ZrXN ( X = Br and I ).

It will be shown that β-ZrClN can be chemically transported to a higher temperature zone. The mechanism of the transport is discussed.

## 4.1 Novel Preparation Method of β-ZrClN

A new preparation route of β-ZrClN is developed. β-ZrClN can be synthesized in a high yield by the direct reaction of zirconium metal or zirconium hydride with the vapor of ammonium chloride. The advantages of this method are in the use of $ZrH_2$ or Zr, which are not sensitive to moisture, simplicity in the procedure, and high yield.

### 4.1.1 Experimental

**Materials** Zirconium metal and zirconium hydride used were powder forms with the particle size of about 40 μm (Mitsuwa Pure Chemicals). The purity of gaseous ammonia was 99.999%. Ammonium chloride was dried by evacuation for 8 h at 420 K prior to use.

**Preparation** Figure 4-1 shows the schematic diagram of a fused silica tube reactor with ground-glass joints at the ends for gas inlet and outlet. The dimensions of the tube are about 1 m in length and 35 mm in diameter. Two electric heaters, H1 and H2, were installed to surround the reactor. About 5 g of the dried ammonium chloride was loaded in a Pyrex glass tube with one end closed and placed in the reactor on the side of the heater H1; about 0.5 g of zirconium metal or zirconium hydride was weighed in a fused silica boat and placed in the reactor on the side of the heater H2. After evacuation, a stream of gaseous ammonia was passed through the reactor at a rate of about 50 $cm^3$ $min^{-1}$ during the reaction. The zirconium metal or zirconium hydride was heated by using the heater H2 to a desired preset temperature in the range of 673 to 1173 K, and then ammonium chloride was vaporized at about 630 K by using the heater H1. The average vaporization rate of the ammonium chloride was measured to be about 100 mg $min^{-1}$. After standing for 30 min, the heater H1 was detached to stop the vaporization of ammonium chloride; the reactor was purged with dry nitrogen

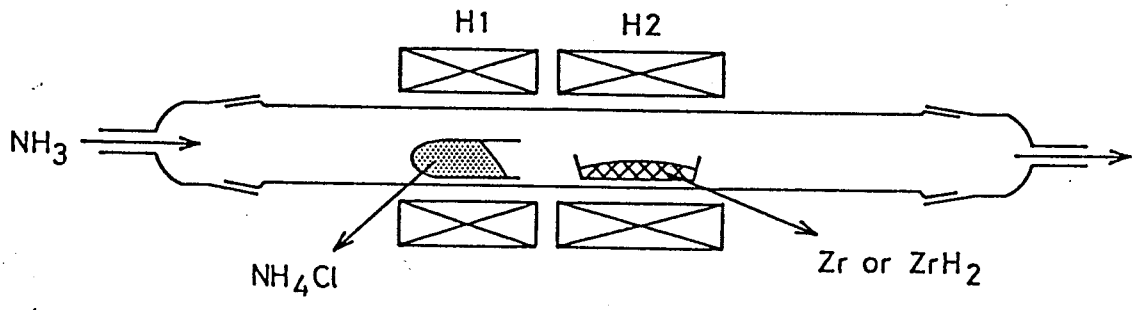


Fig. 4-1 Apparatus for the reaction of Zr or $ZrH_2$ with gaseous $NH_4Cl$.

and cooled to room temperature. The resulting product in the boat was weighed and the phases present were identified by the measurement of the XRD patterns by using Ni filtered Cu $K_\alpha$ radiation.

**Chemical analyses** A weighed amount of the product (about 100 mg) was dissolved in 10 $cm^3$ of 2 mol $dm^{-3}$ sulfuric acid containing 2 $cm^3$ of concentrated hydrofluoric acid. The zirconium and chlorine contents were determined gravimetrically as $ZrO_2$ and AgCl, respectively. Before filtration of the AgCl precipitate, 50 $cm^3$ of 5% boric acid solution was added to the solution to prevent the glass filter from erosion by hydrofluoric acid. Nitrogen was analyzed by the Kjeldahl method. The oxygen content was determined by the chlorination method: the product was heated in a stream of chlorine gas at 873 K for 1 h. The oxygen contained in the product remained in the boat as zirconium oxide.

### 4.1.2 Results

**Formation region** The reactivities of zirconium metal and zirconium hydride were found to be very similar in the reactions with ammonium chloride. In most cases, the hydride was used as reactant. The phases identified in the reaction products of zirconium hydride at different temperatures are listed in Table 4-I. As seen from the table, β-ZrClN was obtained as a single phase at the temperatures ranging from 773 K to 973 K. At

Table 4-I Reaction products of $ZrH_2$ with gaseous $NH_4Cl$ and the yields of β-ZrClN at various temperatures.

| Temp./ K | Products | Yield / % |
|---|---|---|
| 673 | $(NH_4)_2ZrCl_6$, α-ZrClN | |
| 773 | β-ZrClN | 30 |
| 823 | β-ZrClN | 76 |
| 873 | β-ZrClN | 66 |
| 923 | β-ZrClN | 74 |
| 973 | β-ZrClN | 80 |
| 1073 | β-ZrClN, $ZrNH_{0.6}$ | |
| 1173 | β-ZrClN, ZrN, $ZrNH_{0.6}$ | |

higher temperatures, the phases without containing chlorine such as $ZrNH_{0.6}$[48] and ZrN were accompanied. These phases seem to result from the thermal decomposition of β-ZrClN. At a lower reaction temperature of 673 K, $(NH_4)_2ZrCl_6$ and β-ZrClN were formed. As for the products containing β-ZrClN as a single phase, apparent conversion of zirconium hydride to β-ZrClN or yield was calculated on the basis of the weight changes observed before and after the reactions. The calculated values are shown in Table 4-I. The conversion as high as 75% was attained in the temperature range from 823 to 923 K.

**Analyses.** The chemical analysis data for the product obtained from zirconium hydride at 923 K are shown in Table 4-II. The data are in good agreement with the values calculated for β-ZrClN. The product is contaminated with about 2% of oxygen. It is reasonable to assume that the oxygen is bound to zirconium in the form of $ZrO_2$. The contamination of oxygen probably comes from zirconium hydride powder which may be covered with thin oxidized surfaces.

Figure 4-2 shows the XRD pattern of the product obtained at 923 K. Although the pattern is broad, almost all the reflections can be indexed on the basis of a hexagonal cell of a = 0.208 and c = 0.935 nm, the dimensions of which are in good agreement with those for β-ZrClN reported by Juza and Friedrichsen (a = 0.208 and c = 0.923 nm). The remaining unindexed peaks appearing at the diffraction angles ranging from 28 to 32 can be attributed to a mixture of monoclinic and

Table 4-II Chemical analysis data of β-ZrClN obtained at 923 K.

| | Calcd. / % | Found / % | Atomic ratio* |
|---|---|---|---|
| Zr | 64.8 | 64.8 | 1.07 |
| N | 9.96 | 9.30 | 1 |
| Cl | 25.2 | 23.7 | 1.01 |
| O | | 2.07 | 0.19 |
| total | 100.0 | 99.9 | |

* with reference to nitrogen.

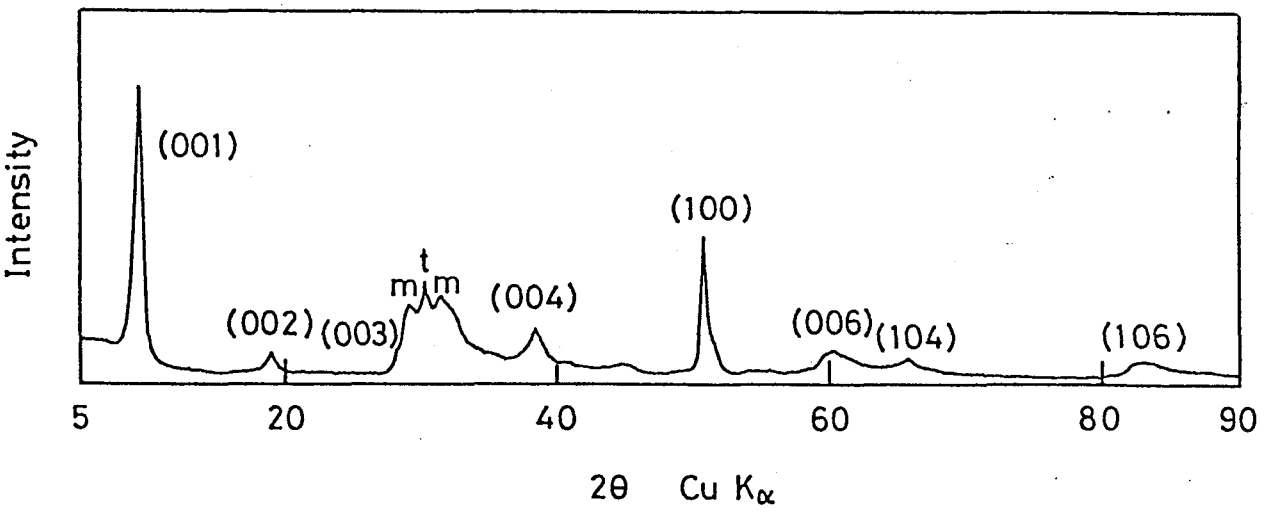


Fig. 4-2 X-ray powder diffraction pattern of β-ZrClN prepared at 923 K.

tetragonal zirconia, which are designated by m and t in the XRD pattern, respectively. The product obtained from zirconium metal also showed a very similar XRD pattern. It appears that the β-ZrClN from zirconium metal is also contaminated with $ZrO_2$ to the same extent.

### 4.1.3 Discussion

In most reactions, ammonia was used as a flowing gas. However, even by using argon or nitrogen gas, β-ZrClN was obtained in a similar manner, although the yield was about 20% lower. Evidently, ammonia is not essential for the formation of β-ZrClN from zirconium metal or zirconium hydride. The fundamental reactions can be written by the following equations:

$$Zr + NH_4Cl \longrightarrow ZrClN + 2\,H_2$$

$$ZrH_2 + NH_4Cl \longrightarrow ZrClN + 3\,H_2$$

In previous sections, it was shown that $(NH_4)_2ZrCl_6$ was an easily formed phase in the reaction systems $ZrCl_4$-$NH_3$, $ZrCl_4$-$NH_4Cl$ and $ZrCl_3(NH_2)\cdot xNH_3$-$NH_4Cl$, and began to vaporize at about 670 K by raising the temperature. As mentioned in section 3.1, in the preparation of β-ZrClN by the method of Juza and Heners[38], the vaporization of $(NH_4)_2ZrCl_6$ does occur during the course of the heating step and results in very low yield of β-ZrClN. Even in the present reaction systems of zirconium metal or zirconium hydride with ammonium chloride, $(NH_4)_2ZrCl_6$ also appears at a low

reaction temperature of 673 K. The reactions may be written as

$$Zr + 6\,NH_4Cl \longrightarrow (NH_4)_2ZrCl_6 + 4\,NH_3 + 2\,H_2$$

$$ZrH_2 + 6\,NH_4Cl \longrightarrow (NH_4)_2ZrCl_6 + 4\,NH_3 + 3\,H_2$$

It seems reasonable to consider that similar reactions occur even at higher reaction temperatures. However, if the temperature of zirconium metal or zirconium hydride is high enough, it is likely that the $(NH_4)_2ZrCl_6$ is decomposed to β-ZrClN as soon as it is formed on the surface of the zirconium metal or zirconium hydride.

$$(NH_4)_2ZrCl_6 \longrightarrow \beta\text{-ZrClN} + NH_4Cl + 4\,HCl$$

As shown in Table 4-I, the yield for β-ZrClN is only 30 % at 773 K, which is remarkably low compared with the yields for the reaction above 823 K. It seems reasonable to conclude that the rate of the above decomposition is not fast enough at 773 K, and large portions of $(NH_4)_2ZrCl_6$ are carried away with the flowing ammonia before converting to β-ZrClN.

Savranskii et al[49] investigated the reactions of zirconium metal and zirconium nitride with ammonium chloride under a high pressure of 3-4 GPa and at a high temperature of 1273-1773 K. They found that ZrN and β-ZrClN were obtained from the systems Zr-$NH_4Cl$ and ZrN-$NH_4Cl$, respectively. We have also examined the reactions of ZrN with the vapor of $NH_4Cl$ at atmospheric pressure in the temperature range of 773 to 1073 K. Although β-ZrClN was also obtained, ZrN was less reactive than zirconium and zirconium

hydride, and part of the ZrN remained unreacted. It should be emphasized that in the method developed in this study, no high pressure nor high temperature was necessary.

## 4.2 Preparation of ZrXN (X = Br, I)

Layer structured crystals ZrXN (X = Br, I) were also prepared by Juza and Heners[38] by the reaction of anhydrous solid $ZrX_4$ with dry ammonia in a manner similar to that of ZrClN. However, $ZrBr_4$ and $ZrI_4$ are more hydrolyzable than $ZrCl_4$. Special precautions must be taken to minimize the contamination from oxide in the products. β-ZrClN could be synthesized in high yield by the direct reaction of zirconium metal or zirconium hydride with the vapor of ammonium chloride. Similar method seems applicable even to the preparation of above zirconium halide nitrides (α-ZrBrN, β-ZrBrN, and ZrIN). In the present section, the reactions of zirconium metal or zirconium hydride with the vapors of ammonium bromide and iodide are studied.

### 4.2.1 Experimental

For the preparation of β-ZrClN (section 4.1, Fig. 4-1), two electric heater were used, one for the vaporization of $NH_4Cl$ and the other for the heating of zirconium metal or zirconium

hydride. For the preparations of bromide and iodide derivatives, only one electric heater was used, so that the apparatus and the procedure were simpler. About 0.5 g of zirconium hydride was weighed in a fused silica boat and placed in the reactor at the center of the heater. Ammonium halide of about 5 times of the molar quantity of the zirconium hydride was loaded in a Pyrex glass tube with one end closed. This tube was placed beside the silica boat with the open end facing to the boat. After evacuation, a stream of gaseous ammonia was passed through the reactor at a rate of about 50 $cm^3$ $min^{-1}$ during the reaction. The zirconium metal or zirconium hydride and ammonium halide were heated to a desired preset temperature for a heating rate of 25 K $min^{-1}$. During raising the temperature, the ammonium halide was vaporized and carried to the silica boat with the flowing ammonia. After standing for 30 min, the reactor was purged with dry nitrogen and cooled to room temperature. The resulting product in the boat was weighed to estimate the apparent conversion rate of $ZrH_2$ and the phases present were identified by the measurement of the XRD patterns. Since the forms were unstable to moisture in air, the XRD patterns were measured under an argon atmosphere in a cylindrical cover having thin polyethylene windows.

### 4.2.2 Results and Discussion

The reactivities of zirconium metal and zirconium hydride

were found to be very similar for the reactions with ammonium bromide or iodide. In most cases, unless otherwise specified the hydride was used as reactant. The phases identified in the products at different reaction temperatures are listed in Table 4-III.

As seen from the table, α-ZrBrN was obtained as a single phase at the temperatures ranging from 923 to 1023 K. At higher temperatures, phases such as $ZrNH_{0.6}$[48] and $Zr_3N_4$[50,44] were formed. These phases seem to result from the thermal decomposition of α-ZrBrN. As for the products containing α-ZrBrN as a single phase, apparent conversion of zirconium hydride to α-ZrBrN or yield was calculated on the basis of the weight changes observed before and after the reactions. The calculated values are shown in parentheses in Table 4-III. The conversion as high as 75% was attained as found in the case of β-ZrClN.

ZrIN was obtained as a single phase at the temperatures ranging from 823 to 973 K. At higher temperatures, the phases such as $ZrNH_{0.6}$ and ZrN were formed. These phases also seem to result from the thermal decomposition of ZrIN. The conversion as high as 85% was attained. This conversion was higher than those of β-ZrClN and α-ZrBrN.

As seen from Table 4-III, β-ZrBrN was not obtained by the direct reaction of zirconium metal or zirconium hydride with $NH_4Br$. However, it was found that the α-ZrBrN could be converted to the β form when it was vacuum sealed in a fused silica

Table 4-III Reaction products of $ZrH_2$ with gaseous $NH_4Br$ and and $NH_4I$ at various temperatures. The yields of α-ZrBrN and ZrIN are indicated in parentheses.

| Temp./ K | Reactant | |
|---|---|---|
| | $NH_4Br$ | $NH_4I$ |
| 823 | α-ZrBrN (73%) | ZrIN (81%) |
| 923 | α-ZrBrN (71%) | ZrIN (84%) |
| 1023 | α-ZrBrN, $ZrNH_{0.6}$ | ZrIN (85%) |
| 1073 | α-ZrBrN, $ZrNH_{0.6}$ | ZrIN, $ZrNH_{0.6}$, ZrN |
| 1173 | $ZrNH_{0.6}$, $Zr_3N_4$ | $ZrNH_{0.6}$, ZrN |

tube, and annealed at 1073 K for 15 h. In the case of ZrIN, the α form is not known. Similar annealing in the temperature range of 1073-1223 K did not convert ZrIN into the β form, although the as-prepared α form changed into highly crystalline α form.

As described in chapter 2, α-ZrBrN and ZrIN are of the FeOCl type structure and α-ZrBrN is isostructural with α-ZrClN. Figure 4-3 shows the XRD patterns of α-ZrBrN and ZrIN obtained at 923 and 1023 K, respectively. Although the patterns are broad, all the reflections of each pattern can be indexed on the basis of orthorhombic cells (Table 4-IV). Figure 4-4 shows the XRD patterns of the products after the annealing. All the reflections of β-ZrBrN and ZrIN can be also indexed on the basis of hexagonal and orthorhombic cells, respectively (Table 4-IV).

Although the c dimensions of α-ZrBrN and ZrIN prepared at 923 and 1023 K were relatively larger than those reported by Juza and Heners, other lattice parameters were in good agreement with the reported values. It is interesting to note that the β-ZrBrN obtained after annealing the α form at 923 K has random layer structure, whereas the highly crystalline β-ZrClN has 3R structure. The chemical analysis data of β-ZrBrN and ZrIN are shown in Table 4-V.

In most reactions, ammonia was used as a flowing gas. However, even by using argon or nitrogen gas, α-ZrBrN and ZrIN were obtained in a similar manner. The fundamental reaction can be written by the following equation.

$$ZrH_2 + NH_4X \longrightarrow ZrXN + 3\ H_2 \qquad (X = Br,\ I)$$

It should be noted that by the direct reactions of zirconium hydride with the vapor of $NH_4Br$ and $NH_4I$, α-ZrBrN and ZrIN can also prepared in a manner similar to that for β-ZrClN.

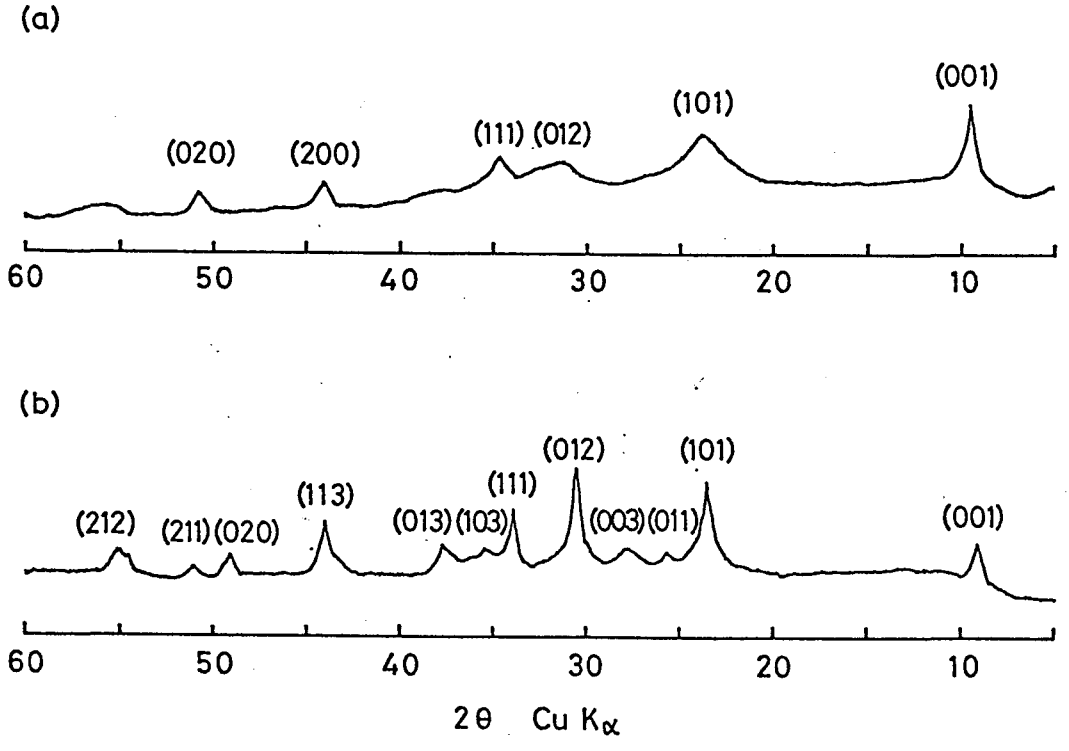


Fig. 4-3 XRD patterns of (a) α-ZrBrN obtained at 923 K and (b) ZrIN obtained at 1023 K.

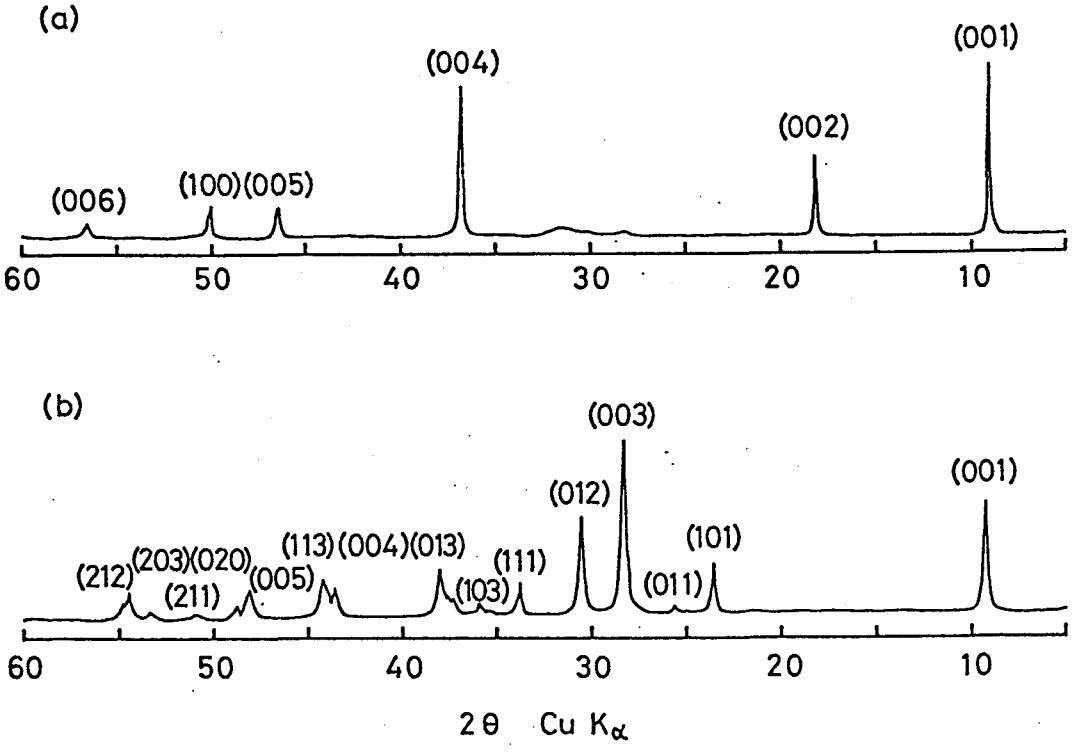


Fig. 4-4 XRD patterns of the products after the heat treatment at 1073 in evacuated tube: (a) β-ZrClN and (b) ZrIN

Table 4-IV Lattice parameters of the products.

| | orthorhombic | | |
|---|---|---|---|
| | a / nm | b / nm | c / nm |
| α-ZrBrN | 0.411 | 0.356 | 0.912 |
| | (0.4116)* | (0.3581) | (0.8701) |
| ZrIN(as-prepared) | 0.411 | 0.371 | 0.952 |
| ZrIN(annealed) | 0.4112(2) | 0.3730(1) | 0.9440(3) |
| | (0.4114) | (0.3724) | (0.9431) |

| | hexagonal | |
|---|---|---|
| β-ZrBrN | 0.2101(1) | 0.9761(2) |
| | (0.2100) | (0.9751) |

* The lattice parameters reported Juza and Heners[38] are indicated in the parentheses.

Table 4-V Chemical analysis data of β-ZrBrN and ZrIN.

β-ZrBrN

| | Calcd/% | Found/% | Atomic ratio* |
|---|---|---|---|
| Zr | 49.3 | 50.3 | 1.12 |
| N | 7.5 | 6.9 | 1 |
| Br | 43.2 | 40.9 | 1.03 |
| O | | 2.1 | 0.27 |
| Total | 100 | 100.2 | |

ZrIN (as-prepared)

| | Calcd/% | Found/% | Atomic ratio* |
|---|---|---|---|
| Zr | 39.3 | 44.0 | 1.11 |
| N | 6.0 | 6.1 | 1 |
| I | 54.7 | 47.2 | 0.85 |
| O | | 2.2 | 0.32 |
| Total | 100 | 99.5 | |

* with reference to nitrogen

## 4.3 Chemical Vapor Transport of β-ZrClN and Its Mechanism

β-ZrClN can be obtained by the direct reaction of zirconium metal or zirconium hydride with the vapor of ammonium chloride in high yield ( > 70 %). However, the as-prepared sample is contaminated with about 2% of oxygen, and not highly crystalline. In the present chapter, the β-ZrClN is purified by chemical vapor transport, and the mechanism of the transport is studied by identifying the gaseous species involved in the reactions. Some thermodynamic properties have also been determined by the measurement of the vapor pressures.

### 4.3.1 Experimental

**Materials** β-ZrClN was prepared from $ZrH_2$ and $NH_4Cl$ by the procedure described in section 4.1. $ZrH_2$ was subjected to reaction with gaseous $NH_4Cl$ in a stream of $NH_3$ at 923 K, and directly converted to β-ZrClN in high yields (>70%) via the reaction:

$$ZrH_2 + NH_4Cl \longrightarrow \beta\text{-}ZrClN + 3\ H_2$$

Ammonium hexachlorozirconate $(NH_4)_2ZrCl_6$ was synthesized by the direct reaction of $ZrCl_4$ and $NH_4Cl$ in a sealed glass tube, and purified by sublimation according to the method described in section 3.2. Found: Zr,27.3; N,8.22; Cl,62.6 %. Calcd. for $(NH_4)_2ZrCl_6$: Zr, 26.8; N, 8.24; Cl,62.6 %.

**Vapor pressure measurement** The sublimation vapor pressure of $(NH_4)_2ZrCl_6$ was measured up to 773 K. A Pyrex glass Bourdon gauge with a spoon-shaped membrane was used, which was designed after the gauge used by Saeki.[51] A quartz Bourdon gauge was also used, but the Pyrex one was found to be satisfactory for the measurements in the temperature range below 773 K. A schematic drawing of the gauge is shown in Fig. 4-5. Under a dry argon atmosphere, a weighed amount of $(NH_4)_2ZrCl_6$ (about 20 mg) was loaded into the gauge (about 40 $cm^3$), and then the entire system was evacuated to a pressure of about $10^{-1}$ Pa, and sealed off at the point A. The sealed apparatus was heated in a vertical furnace at a heating rate of 1 K $min^{-1}$. In the course of raising the temperature, the gauge was intermittently kept at constant temperatures at several measurement points in order to check the equilibrium of the system. The vapor pressure in the spoon was balanced with the same pressure of air introduced to the chamber C through the valve D. The balancing air pressure was measured by a digital pressure transducer (Tokyo Kokukeiki, Model DG-630) within an accuracy of $1.3 \times 10^2$ Pa. The imbalance of the pressures was detected from the deflections of a fiber B attached to the top end of the spoon using a cathetometer.

**Mass spectra** The mass spectrometer used was a double-focusing type with a sample holder heatable up to 873 K (Denshi-Kagaku, Model EMD-05SH). $(NH_4)_2ZrCl_6$ was heated at a heating rate of 20 K $min^{-1}$, and the volatile species were analyzed as a function of temperature in the sweep range of 1-500 m/z for the

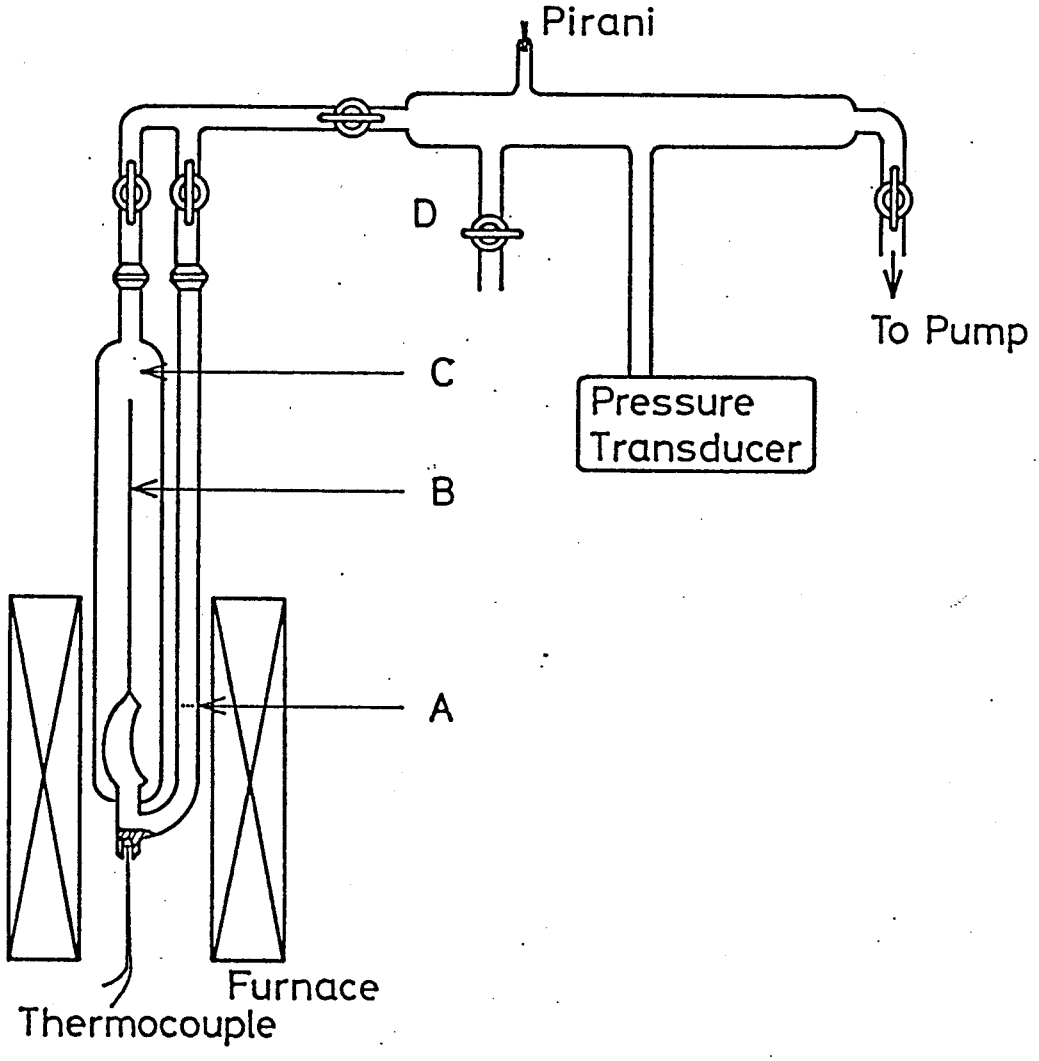


Fig. 4-5 Bourdon gauge for the measurement of vapor pressures of $(NH_4)_2ZrCl_6$.

ionization energy of 70 eV.

### 4.3.2 Chemical Vapor Transport

The as-prepared β-ZrClN powder sample was vacuum-sealed in a quartz tube and placed in a furnace with a temperature gradient of 1023-1123 K. The sample was loaded in the lower temperature zone. The β-ZrClN was transported to the higher temperature zone in a few days as a highly crystalline form. The transport also occurs when the temperature gradient was 100 K along the tube length and the high temperature was varied from 823-1173 K whereas at the temperatures above 1323 K, ZrN was formed. Although optimum transport conditions to get large single crystal have not been determined, pretty large crystals were obtained in a temperature gradient of 1023-1123 K. A typical scanning electron micrograph of the obtained crystal is shown in Fig. 4-6. The transported sample was contaminated with a small amount of oxygen. The analytical data of the sample are shown in Table 4-IV. As shown in section 4.1, as-prepared β-ZrClN contained with about 2% of oxygen. However, the oxygen contamination of the transported sample is reduced to less than 0.3%. Its XRD pattern is shown in Fig. 4-7 in comparison with that of the as-prepared sample. The XRD data for the chemically transported sample are given in Table 4-VII. It should be noted that the reflections for the transported sample can be indexed on the basis of a $\sqrt{3}$ a x 3c super cell, 0.36055(4) nm x 2.7664(4) nm, rather than the

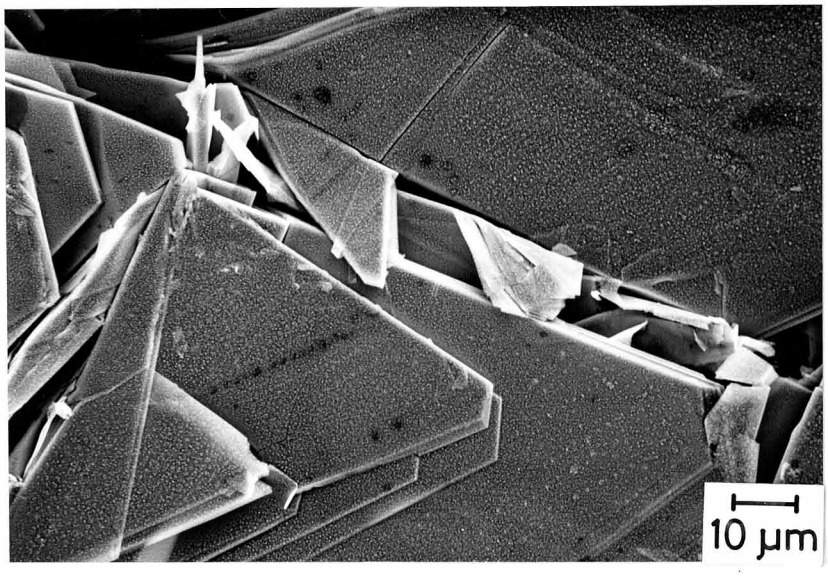


Fig. 4-6 Scanning electron micrograph of crystals β-ZrClN transported in temperature gradient of 1023-1123 K.

Table 4-VI Chemical analysis data of β-ZrClN obtained by chemical transport.

| | Calcd. / % | Found / % | Atomic ratio* |
|---|---|---|---|
| Zr | 64.8 | 65.4 | 1.04 |
| N | 9.96 | 9.68 | 1 |
| Cl | 25.2 | 24.4 | 1.00 |
| O | | 0.30 | 0.03 |
| total | 100.0 | 99.8 | |

* with reference to nitrogen.

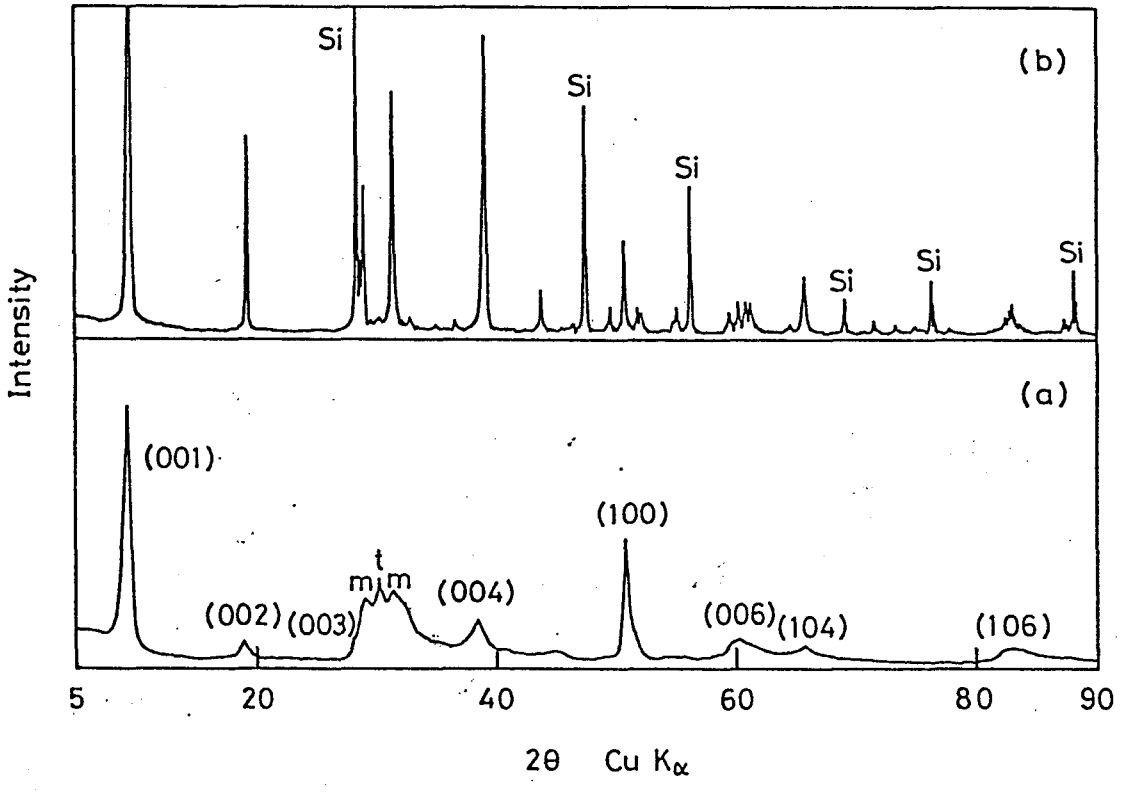


Fig. 4-7 X-ray diffraction pattern of β-ZrClN (a) as-prepared and (b) chemically transported. Peaks for monoclinic and tetragonal $ZrO_2$ are marked by m and t in (a) and peaks for silicon used as an internal standard are marked by Si in (b).

Table 4-VII X-ray diffraction data of β-ZrClN obtained by chemical transport.

| $d_{obs}$ / nm | $I_{obs}$ | h k l* | $d_{calcd}$ / nm |
|---|---|---|---|
| 0.9213 | 100 | 0 0 3 | 0.9221 |
| 0.4604 | 15 | 0 0 6 | 0.4610 |
| 0.3101 | 5 | 1 0 1 | 0.3103 |
| 0.3072 | 10 | 0 0 9 | 0.3074 |
| 0.2844 | 15 | 1 0 4 | 0.2846 |
| 0.2718 | 1 | 0 1 5 | 0.2720 |
| 0.2448 | 1 | 1 0 7 | 0.2450 |
| 0.2317 | 10 | 0 1 8 | 0.2318 |
| 0.2305 | 20 | 0 0 12 | 0.2305 |
| 0.2070 | 5 | 1 0 10 | 0.2071 |
| 0.19589 | 1 | 0 1 11 | 0.19586 |
| 0.18431 | 1 | 0 0 15 | 0.18442 |
| 0.18019 | 10 | 1 1 0 | 0.18029 |
| 0.17696 | 1 | 1 1 3 | 0.17694 |
| 0.17586 | 1 | 1 0 13 | 0.17585 |
| 0.16797 | 1 | 1 1 6 | 0.16791 |
| 0.16706 | 1 | 0 1 14 | 0.16697 |
| 0.15555 | 1 | 1 1 9 | 0.15551 |
| 0.15362 | 5 | 0 0 18 | 0.15368 |
| 0.15221 | 5 | 0 2 4 | 0.15230 |
| 0.15117 | 5 | 1 0 16 | 0.15126 |
| 0.14427 | 1 | 0 1 17 | 0.14431 |
| 0.14194 | 5 | 1 1 12 | 0.14202 |
| 0.13171 | 1 | 0 0 21 | 0.13173 |
| 0.12892 | 1 | 1 1 15 | 0.12892 |
| 0.12642 | 1 | 0 1 20 | 0.12646 |
| 0.12592 | 1 | 0 2 13 | 0.12588 |
| 0.12254 | 1 | 2 0 14 | 0.12251 |
| 0.11797 | 1 | 2 1 1 | 0.11792 |
| 0.11700 | 1 | 1 1 18 | 0.11696 |
| 0.11670 | 1 | 1 0 22 | 0.11664 |
| 0.11630 | 5 | 2 1 4 | 0.11635 |
| 0.11549 | 1 | 1 2 5 | 0.11543 |
| 0.11165 | 1 | 1 2 8 | 0.11170 |

* indexed on the basis of a hexagonal unit cell of a = 0.36005 nm and c = 2.7664 nm.

hexagonal cell used for the as-prepared sample.

Juza and Friedrichsen[39] proposed a random $CdI_2$-$CdCl_2$ structure for β-ZrClN, since the XRD pattern can be indexed on the basis of a fractional hexagonal cell containing only 2/3 ZrClN unit, so that a random stacking sequence of the layers is suggested. On the contrary, the XRD pattern of the highly crystalline sample can be indexed on the basis of the $\sqrt{3}$ a x 3c super cell and only the reflections for which -h+k+l = 3n are present. This indicates that the symmetry is rhombohedral rather than hexagonal. It is reasonable to assume that the structure of the chemically transported sample is $CdCl_2$ type.

The transported crystals were taken out and vacuum sealed again; no transport was observed. If the transported crystals were sealed with a small amount of $NH_4Cl$ (β-ZrClN; 0.5 g, $NH_4Cl$; 30 mg), the crystals could be transported to the higher temperature zone like the as-prepared sample. If the as-prepared sample was sealed after evacuation at 773 K for 3 h, the rate of transport was much reduced even in the temperature gradient of 1023-1123 K. It is very likely that the as-prepared β-ZrClN was contaminated with small amount of $NH_4Cl$ used in the preparation of the β-ZrClN, which can be removed by prolonged evacuation at 773 K. It is apparent that $NH_4Cl$ is a transporting agent for β-ZrClN.

### 4.3.3 Mechanism of the Chemical Vapor Transport

The as-prepared β-ZrClN was mixed with $NH_4Cl$ in a ratio of 1/5 and vacuum-sealed in a Pyrex glass tube, which was placed in a furnace with a temperature gradient of 698-653 K. The mixture was loaded in the higher temperature zone. After 3 d, white crystals of $(NH_4)_2ZrCl_6$ were deposited at the lower temperature end of the sealed glass tube. The reaction can be written by the following equation:

$$\beta\text{-ZrClN(s)} + 5\ NH_4Cl \longrightarrow (NH_4)_2ZrCl_6(s) + 4\ NH_3(g) \quad ...(4.1)$$

where $NH_4Cl$ dissociates into $NH_3(g)$ and HCl(g). In order to understand the gaseous species involved in the sublimation vapors of $(NH_4)_2ZrCl_6$, the vapor pressure was measured as a function of temperature by using a glass Bourdon gauge.

Vapor pressure of $(NH_4)_2ZrCl_6$ $(NH_4)_2ZrCl_6$ is a face-centered cubic crystal with the $K_2PtCl_6$ type structure and easily sublime at elevated temperatures. This is prepared through several reaction routes:

(i) $ZrCl_4 + 2\ NH_4Cl \longrightarrow (NH_4)_2ZrCl_6$

(ii) $Zr + 6\ NH_4Cl \longrightarrow (NH_4)_2ZrCl_6 + 4\ NH_3 + 2\ H_2$

(iii) $ZrH_2 + 6\ NH_4Cl \longrightarrow (NH_4)_2ZrCl_6 + 4\ NH_3 + 3\ H_2$

In the present study, $(NH_4)_2ZrCl_6$ was prepared by the reaction (i), and in order to understand the gaseous species involved in the sublimation vapors, the vapor pressure was measured as a

function of temperature by using a glass Bourdon gauge. The pressure vs. temperature curve is shown in Fig. 4-8. The sublimation vapor pressure increases rapidly from about 600 K. The curve exhibits an inflection point at 730 K, where all the solid was sublimed to vapors. An ideal gas law was assumed, and the total pressures after the inflection point were extrapolated to the origin by a dashed line (Fig. 4-8). The slope of the line indicates that one mole of $(NH_4)_2ZrCl_6$ is sublimed to 4.9 mol of gaseous molecules.

Thermal decomposition of similar series of compound $M_2ZrCl_6$ (M = Na, K and Cs) have been studied by Morozov and In'-Chzhu,[52] and Lister and Flengas.[53] These compounds decompose according to the following equation.

$$M_2ZrCl_6(s) \longrightarrow ZrCl_4(g) + 2\ MCl(s)$$

It is reasonable to assume that $(NH_4)_2ZrCl_6$ decomposes in a similar way.

$$(NH_4)_2ZrCl_6(s) \longrightarrow ZrCl_4(g) + 2\ NH_3(g) + 2\ HCl(g) \quad ...(4.2)$$

where $NH_3$ and HCl come from the decomposition of $NH_4Cl$. This equation shows that one mole of $(NH_4)_2ZrCl_6$ is sublimed to 5 mol of gaseous molecules. The number of gaseous molecules estimated from the vapor pressure measurement of $(NH_4)_2ZrCl_6$ is in good agreement with this value.

When solid $(NH_4)_2ZrCl_6$ co-exists with the vapors, the equilibrium constant($K_p$), for the reaction (4.2) is given by the

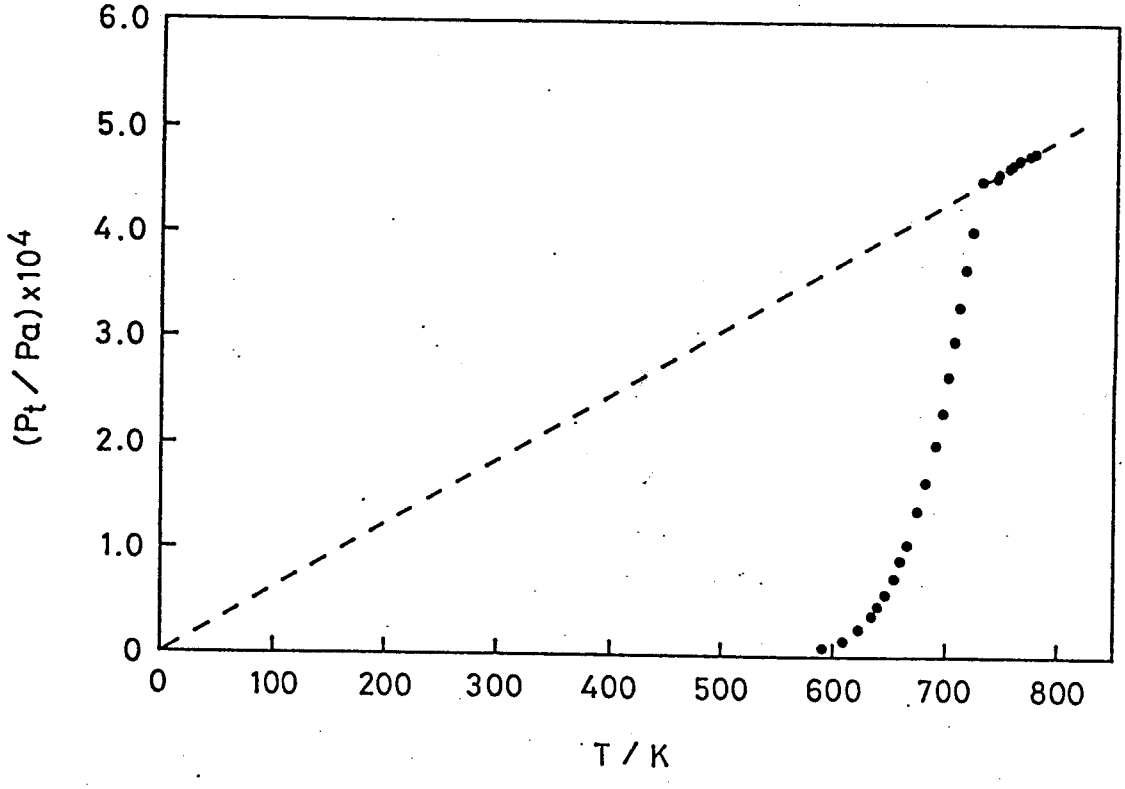


Fig. 4-8 Temperature dependence of vapor pressure of $(NH_4)_2ZrCl_6$.

following equation.

$$K_p = (P_{ZrCl_4}/P_o)(P_{NH_3}/P_o)^2(P_{HCl}/P_o)^2$$

where $P_{ZrCl_4}$, $P_{NH_3}$ and $P_{HCl}$ represent the partial pressures of $ZrCl_4$, $NH_3$ and HCl, respectively, and $P_o$ is the standard pressure. Since all the partial vapor pressures of the components are known, if the total pressure ($P_t$) of the system is measured, $K_p$ is related to $P_t$ by

$$K_p = (P_t/5P_o)(2P_t/5P_o)^2(2P_t/5P_o)^2 = C(P_t/P_o)^5,$$

where C is a constant.

Figure 4-9 shows a plot of $\ln(P_t)$ against 1/T. From the slope of the linear plot and the Gibbs-Helmholtz equation

$$\frac{d(\ln K_p)}{d(1/T)} = -\frac{\Delta H}{R},$$

where R is the gas constant, the enthalpy change for Eq. (4.2), $\Delta H$, is calculated to be 533 kJ/mol.

Since the enthalpy change for the vaporization of $NH_4Cl$,

$$NH_4Cl(s) \longrightarrow NH_3(g) + HCl(g) \qquad ...(4.3)$$

is 161 kJ/mol at 700 K[67] The enthalpy change for the reaction,

$$(NH_4)_2ZrCl_6(s) \longrightarrow ZrCl_4(g) + 2\ NH_4Cl(s) \qquad ...(4.4)$$

is calculated to be 211 kJ/mol. The heat of formation for

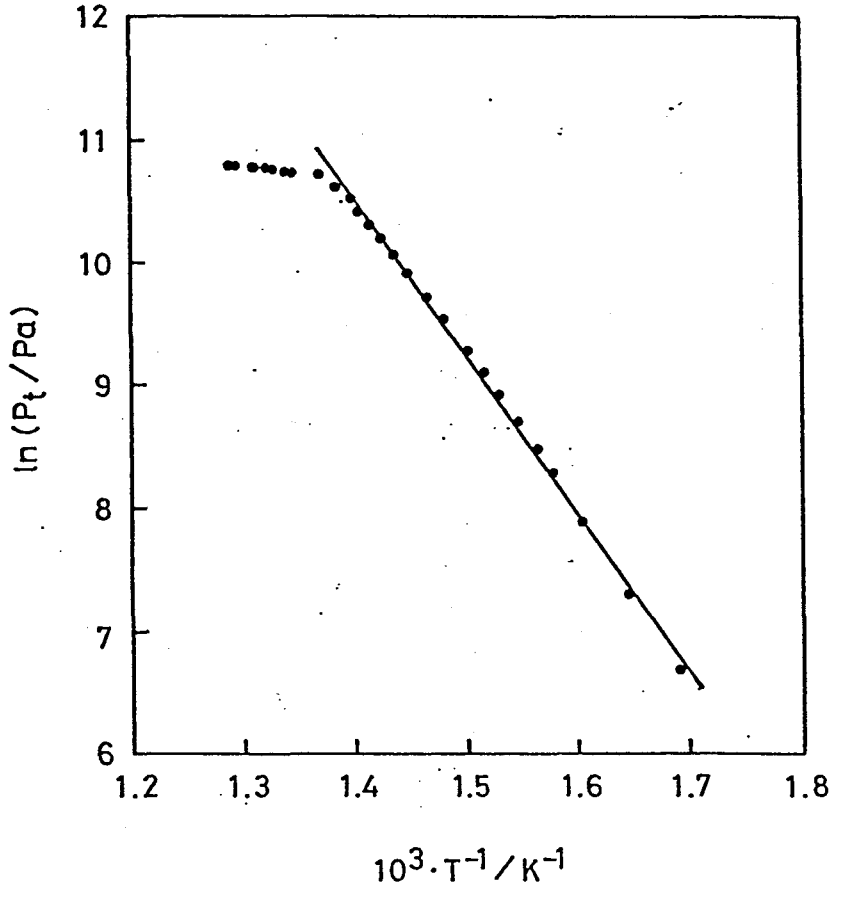


Fig. 4-9 Plots of ln (Pt / Pa) against 1/T.

$(NH_4)_2ZrCl_6$(s) is also calculated to be $\Delta H_{f\ 700}$ = -1693 kJ/mol on the basis of the heats of formations of $ZrCl_4$(g), $NH_3$(g) and HCl(g) at 700 K; -868, -52.6 and -93.6 kJ/mol, respectively.[54] As for $K_2ZrCl_6$ which is isostructural with $(NH_4)_2ZrCl_6$, the enthalpy change for the following decomposition was measured by Morozov and In'-Chzhu,[52] and Lister and Flengas,[53].

$$K_2ZrCl_6(s) \longrightarrow ZrCl_4(g) + 2\ KCl(s)$$

The former group obtained 218 kJ/mol by the transpiration method, whereas the latter group obtained 354 kJ/mol by a Bourdon gauge measurement. Although there is large discrepancy between the values from the two groups, the value (218 kJ/mol) by Morozov and In'-Chzhu is comparable with the value (211 kJ/mol) obtained in this study for the reaction (4.4).

**Mass spectrometry** Figure 4-10 shows a mass spectrum of the volatile components of $(NH_4)_2ZrCl_6$ at 673 K. The amount of volatile components began to increase from about 570 K, and the mass spectra obtained were essentially unchanged in the temperature range 573-823 K. The peak at 232 m/z is attributed to $ZrCl_4^+$. Some fragments of $ZrCl_4^+$ were observed in the m/z range of 90-203. The spectrum also shows intense peaks at m/z = 17 and 36 due to $NH_3^+$ and $HCl^+$, respectively. These findings are in accordance with the conclusion made on the decomposition of $(NH_4)_2ZrCl_6$ from the pressure measurement.

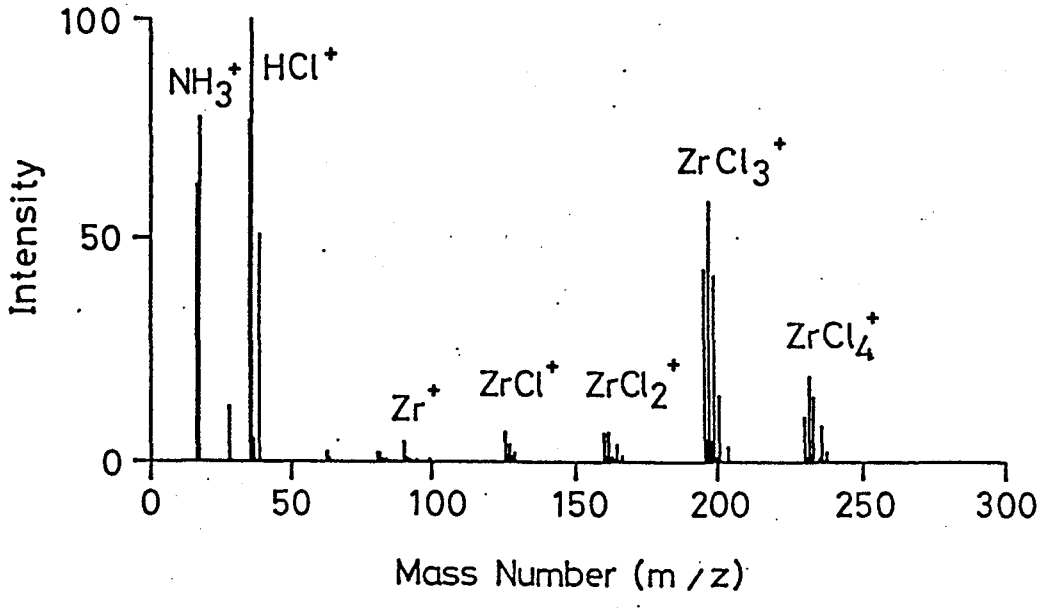


Fig. 4-10 Mass spectrum of $(NH_4)_2ZrCl_6$ vaporized at 673 K.

Mechanism of the transport β-ZrClN reacts with $NH_4Cl$ as a transporting agent and form $(NH_4)_2ZrCl_6$, which is congruently decomposed to $ZrCl_4$, $NH_3$ and HCl at elevated temperatures. The vapor phases are transported to the higher temperature zone and form β-ZrClN. The transport Eq. (4.1) can be simplified into the following equation by using Eq. (4.2) and (4.3).

$$\beta\text{-ZrClN(s)} + 3HCl(g) \rightleftharpoons ZrCl_4(g) + NH_3(g)$$

This equation suggests that HCl gas could also be a transporting agent of β-ZrClN. As a matter of fact, when the transported β-ZrClN was sealed with HCl gas of a pressure of $2.7 \times 10^4$ Pa and placed in a temperature gradient 1023-1123 K, β-ZrClN was transported to the higher temperature zone. The transport reaction must be exothermic because the transport occurs to the higher temperature zone.

In the preparation of β-ZrClN, gaseous $NH_4Cl$ is flowed over $ZrH_2$ or Zr as shown in section 4.1. Since the $NH_4Cl$ acts as the transporting agent as well as the reactant, the $NH_4Cl$ supply must be stopped as soon as the reaction is finished. The prolonged flowing of $NH_4Cl$ vapor would remove the β-ZrClN formed in the form of volatile $(NH_4)_2ZrCl_6$ and result in a low yield of β-ZrClN.

# 5 CHEMICAL LITHIUM INTERCALATION IN β-ZrClN

Owing to the development of the new and simple preparation route, we can now easily obtain β-ZrClN in highly crystalline as well as as-prepared forms. In this chapter, β-ZrClN samples are chemically lithiated by using n-buthyllithium in hexane solution. The lithium intercalate is solvated with a variety of nonaqueous solvent molecules, expanding the basal spacing. The arrangements of the molecules co-intercalated with lithium in the interlayer spaces are discussed.

## 5.1 Experimental

**Materials** β-ZrClN was prepared by the reaction of $ZrH_2$ with ammonium chloride at 923 K in a stream of dry ammonia according to the method described in section 4.1. The as-prepared powder sample was purified by chemical transport in a fused silica tube sealed with trace amount of ammonium chloride as transporting agent in a temperature gradient of 1023-1123 K as described in section 4.3. Crystalline β-ZrClN was obtained at the higher temperature zone. The sample was ground and sieved by a 200 mesh screen. The XRD pattern of the transported sample was indexed on the basis of a hexagonal cell of a = 0.3606 and c = 2.766 nm. Since the unit cell contains three unit layers (3R structure), the basal spacing is 2.766/3 (=0.922) nm. In this

chapter, the two kind of samples, as-prepared and chemically transported, will be called ZrClN(as-prep) and ZrClN(cryst), respectively. For comparison, another β-ZrClN was prepared by the method of Juza and Heners[38], which will be hereafter called ZrClN(J&H). Its XRD pattern was very similar to that of ZrClN(as-prep) shown in Fig. 4-7(a).

Propylene carbonate(PC) was vacuum distilled and then dried with molecular sieve 4A. Anhydrous lithium perchlorate (Mitsuwa Chemical) was dried by evacuation at 423 K for 12 h. Tetrahydrofuran (THF), acetonitrile (AN) and dimethyl sulfoxide (DMSO) were purified by refluxing with calcium hydride, followed by distillation. N,N-dimethylformamide (DMF) and pyridine (Py) were dried with molecular sieves (3A or 4A was used) and then distilled. Formamide (FA) was distilled under reduced pressure after neutralization with sodium hydroxide. The procedure was repeated until neutral distillate was obtained; the final distillation was carried out at temperatures below 353 K under a reduced pressure in the presence of sodium formate. n-Butyllithium (n-BuLi) used was a 15 wt% hexane solution (Katayama Chemical). Naphthyllithium THF solution (0.1 M) was prepared by dissolving a desired amount of lithium metal in 0.1 M naphthalene solution in THF. After 20 h, the solution was filtered through a sintered glass disk in order to separate unsoluble impurities.

Since most of the materials used in these studies are air sensitive, all the manipulations of the samples were performed in

an argon-filled Vacuum Atmosphere glove box.

**Chemical lithiation** β-ZrClN powder was dispersed into the n-BuLi solution. The powder immediately turned black. After being allowed to stand for a few weeks, the colored sample was separated by filtration and rinsed with anhydrous hexane. The separated powder samples were dispersed in several nonaqueous solvents for 24 h and the XRD patterns were recorded to know the changes of the basal spacings by swelling with the solvents. The chemically transported β-ZrClN was also dispersed into 0.1 M naphthyllithium / THF solution. After being allowed to stand for 3 d, the colored sample was separated by filtration and rinsed with THF. For the analysis of the amount of the intercalated lithium, the colored sample was immersed in 0.5 mol $dm^{-3}$ HCl solution. The sample was bleached to the initial yellow green and all the lithium intercalated was released to the water with vigorous evolution of hydrogen. The amount of intercalated lithium was determined on this solution by flame analysis. The XRD patterns of the lithium intercalated samples were measured under an argon atmosphere in a cylindrical cover having thin polyethylene windows using nickel-filtered Cu $K_\alpha$ radiation.

**One-dimensional structural analysis by XRD method** One-dimensional electron-density distributions were determined of the solvated samples on the basis of the observed (00ℓ) reflections. Due to a strong preferred orientation effect, the XRD patterns consisted of only (00ℓ) reflections. The intensities of twelve (00ℓ) reflections were corrected by Lorentz and polarization

factors for a single crystal. The signs of the structure factors were predicted from those of the expanded β-ZrClN layers. They were refined by including the contribution of organic molecules which would lie in the interlayer spaces of the swelled samples.

## 5.2 Results and Discussion

### 5.2.1 Lithium Intercalation and Swelling

Three kinds of β-ZrClN samples, (cryst), (as-prep), and (J&H), were used for the lithiation by n-BuLi. All the β-ZrClN samples turned black immediately when those were dispersed into n-BuLi solution. The basal spacings of the starting and the lithiated β-ZrClN samples, and those after swelling with PC are listed in Table 5-I, together with the amount of lithium intercalated. Although the peaks of the XRD pattern of ZrClN(cryst) were slightly broadened, the spacings are essentially unchanged on intercalation of lithium in n-BuLi solution.

The amount of lithium (x in $Li_xZrClN$) intercalated in the crystalline sample is 0.16 which is much smaller than the amounts for the less crystalline samples, 0.29 and 0.27. This is probably due to the crystallinity of the samples. It is often observed that amorphous samples can react with much larger amount

Table 5-I Basal spacing data of β-ZrClN treated with n-BuLi and propylene carbonate and the amount of lithium intercalated.

| | Basal spacing / nm | | | | x in $Li_xZrClN$ |
|---|---|---|---|---|---|
| | (A) Initial[1] | (B) n-BuLi[2] | (C) +PC[3] | ($\Delta$d)[4] | |
| ZrClN(cryst) | 0.922 | 0.93 | 2.22[5] | (1.29) | 0.16 |
| ZrClN(as-prep) | 0.93 | 0.93 | 2.33 | (1.40) | 0.27 |
| ZrClN(J&H) | 0.93 | 0.93 | 2.33 | (1.40) | 0.29 |

1) Before lithiation

2) After lithiation with n-butyllithium

3) Swelled with PC after the lithiation

4) Increment in basal spacing due to swelling; (C)-(B)

5) Swelled in 1 M $LiClO_4$/PC

of lithium than the crystalline samples.[55,56] Figure 5-1 shows the electric conductivities of the ZrClN(cryst) and the $Li_{0.16}$ZrClN(cryst) as a function of the reciprocal absolute temperature. The temperature dependence of the conductivity becomes slightly negative after the lithium intercalation. These changes are explained in terms of electron transfer from the lithium atoms intercalated to the ZrClN layers. The transfered electrons are delocalized through the crystal, and the lithiated samples behave like metals. The electrical conductivity of the ZrClN(cryst) increased by a factor of 10 on the intercalation of lithium.

The lithium intercalates swelled with PC, expanding the basal spacing remarkably. As shown in the Table 5-I, the interlayer separation after the swelling is as large as 1.3-1.4 nm. Since the uncolored β-ZrClN samples before lithiation did not swell with PC, it is apparent that the PC molecules co-intercalate with lithium, coordinating to the lithium. Whittingham[57] reported that the lithium intercalated compound of $TiS_2$ swelled with PC, forming a co-intercalated complex with an increase of 1.27 nm in the basal spacing. Dahn et al.[58] also reported that $Li_xTiS_2$ in $Li/TiS_2$ cell formed co-intercalated phase with $\Delta d$ = 1.21 nm. Their $\Delta d$ values are approximately coincident with the values obtained for β-ZrClN.

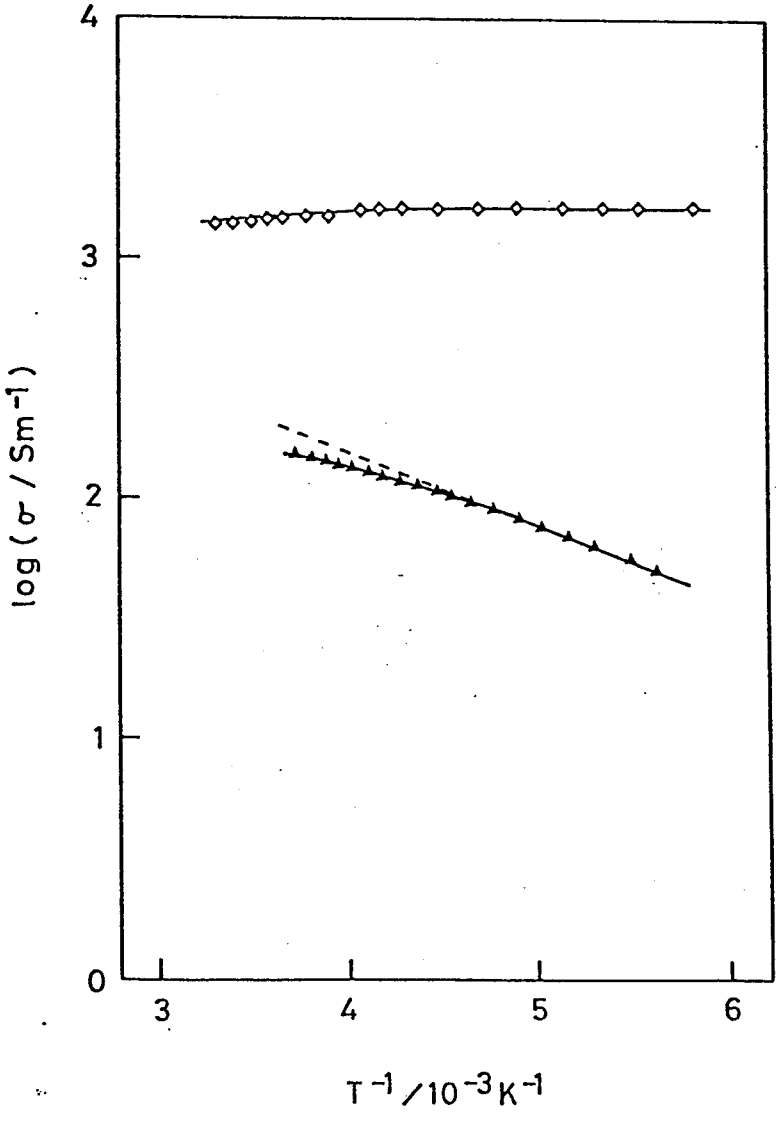


Fig. 5-1 Temperature dependence of the conductivities of ZrClN(cryst) (▲) and $Li_{0.16}ZrClN$(cryst) (◇).

### 5.2.2 Interlayer Molecular Arrangement of Swelled Sample

Figure 5-2 shows the one-dimensional electron-density distribution map projected along the c direction for the lithium and PC co-intercalated ZrClN(cryst) with a basal spacing of 2.22 nm. This map appears to suggest that PC molecules are solvated in double layers. It is known that lithium ions are tetrahedraly coordinated by oxygen atoms of four different $CO_3^{2-}$ ions in the crystal of $Li_2CO_3$. It is assumed that the interlayer $Li^+$ ions were similarly tetrahedraly coordinated by carbonate groups of the PC molecules in the interlayer spaces of ZrClN(cryst). In Table 5-II, the structure factors calculated for the model of $Li_{0.16}(PC)_{0.64}ZrClN$ are compared with those observed. The R factor, $\Sigma \; ||Fo| - |Fc|| \; / \; \Sigma \, |Fo|$, was 0.18. The structural model for the arrangement of the molecules is shown in Fig. 5-2 along with the electron distribution map. The maximum amount of PC molecules is estimated to be 0.50 mol per formula unit of ZrClN on the basis of the increase in the cell volume on swelling and the molecular volume of PC. The maximum number of PC molecules that can be accommodated in the interlayer spaces is smaller than that in the structural model used for calculation. Although it is evident that the PC molecules are solvated in double layers, part of the lithium ions are presumably coordinated by smaller number of PC molecules.

When ZrClN(cryst) was subjected to reaction with 0.1 M naphthyllithium / THF solution. The color of the crystals was

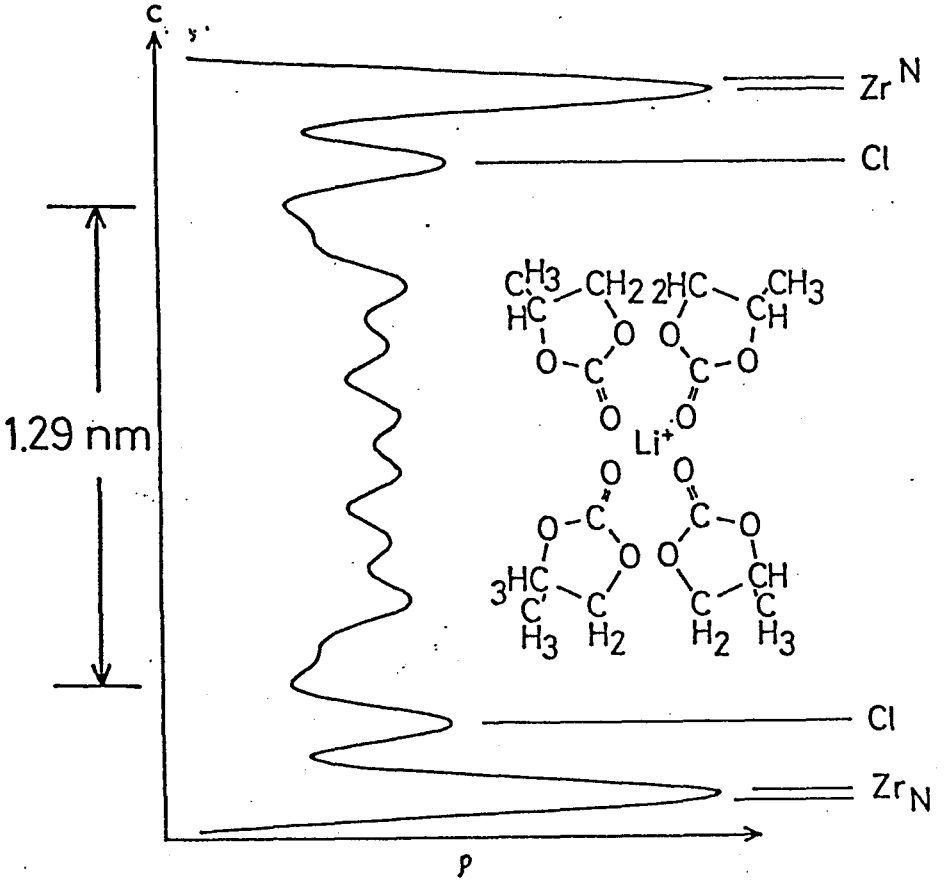


Fig. 5-2 One dimensional electron-density map projected along the c direction and a schematic representation of the orientation of the PC molecules in the interlayer space of the solvated lithium intercalation compound $Li_{0.16}(PC)_{0.64}ZrClN$.

Table 5-II Structural factors observed (Fo) and calculated (Fc) for $Li_{0.16}(PC)_{0.64}ZrClN$.

| (0 0 ℓ) | \|Fo\| | Fc |
|---|---|---|
| 0 0 1 | 17 | 29 |
| 0 0 2 | 25 | 25 |
| 0 0 3 | 14 | 16 |
| 0 0 4 | 6 | - 11 |
| 0 0 5 | 19 | - 14 |
| 0 0 6 | 7 | - 9 |
| 0 0 7 | 12 | - 14 |
| 0 0 8 | 24 | - 21 |
| 0 0 9 | 33 | - 30 |
| 0 0 10 | 32 | - 28 |
| 0 0 11 | 25 | - 25 |
| 0 0 12 | 21 | - 18 |

similarly changed from yellow green to black as found in the reaction with n-BuLi, and a solvated lithium intercalation compound $Li_{0.18}(THF)_yZrClN$ was formed.

$$\beta\text{-ZrClN} + x\ \text{Li-}C_{10}H_8 \xrightarrow[\text{in THF}]{} Li_x(THF)_yZrClN + x\ C_{10}H_8 \qquad (x=0.18)$$

This sample had a basal spacing of 1.49 nm. The thermogravimetric analysis of the sample indicated that about 0.28 mol of THF was solvated per formula unit of ZrClN. The maximum amount of THF molecules in the swelled sample is estimated to be 0.24 mole per a formula unit of ZrClN from a similar manner. This value is in fair agreement with that observed. A one-dimensional electron-density distribution along the c direction was also synthesized(Fig. 5-3). The electron distribution between the ZrClN layers seems to suggest that the THF molecules are oriented with the molecular planes almost perpendicular to the ZrClN layers as shown in the figure. The $Li^+$ ions are located near the center between two ZrClN layers, and coordinated with the THF molecules through the ether groups. In Table 5-III, the structure factors calculated on the basis of this orientation of the THF molecules and the composition $Li_{0.18}(THF)_{0.28}ZrClN$ are compared with those observed. The R factor was 0.23.

The lithium intercalated β-ZrClN also swells in various nonaqueous solvents, increasing the basal spacing. The solvents studied and the basal spacings of the swelled phases are listed

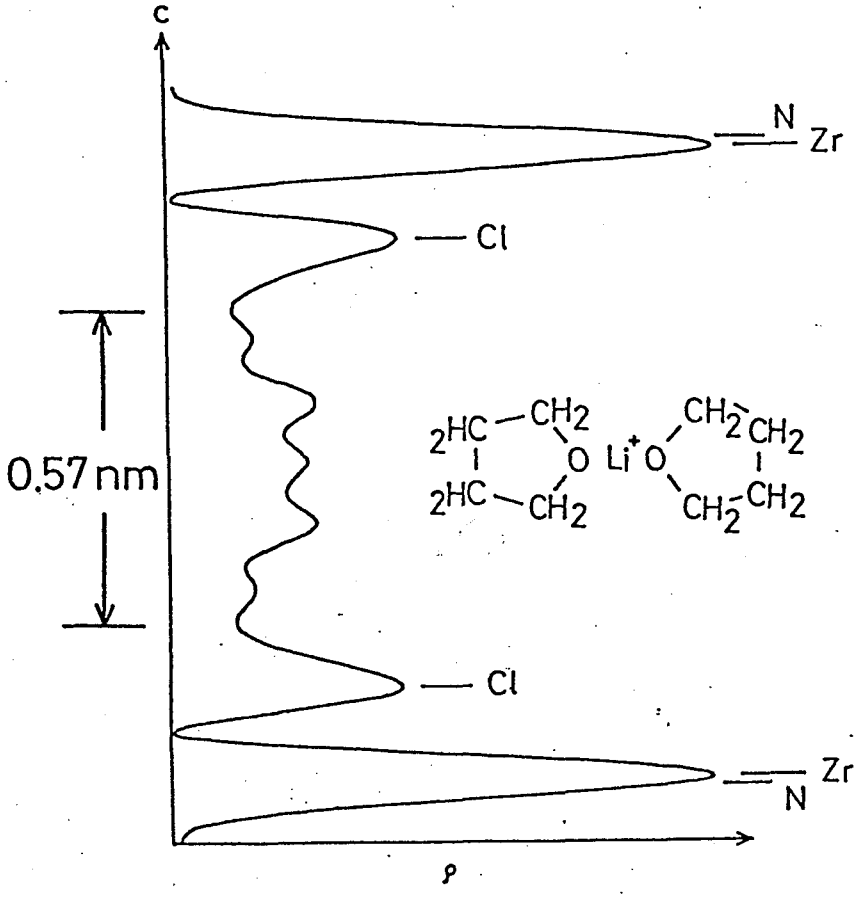


Fig. 5-3 One dimensional electron-density map projected along the c direction and a schematic representation of the orientation of the THF molecules in the interlayer space of the solvated lithium intercalation compound $Li_{0.18}(THF)_{0.28}ZrClN$.

Table 5-III Structure factors observed (Fo) and calculated (Fc) for $Li_{0.18}(THF)_{0.28}ZrClN$.

| (0 0 ℓ) | \|Fo\| | Fc |
|---|---|---|
| 0 0 1 | 27 | 32 |
| 0 0 2 | 13 | 12 |
| 0 0 3 | 15 | - 17 |
| 0 0 4 | 13 | - 14 |
| 0 0 5 | 21 | - 20 |
| 0 0 6 | 41 | - 29 |
| 0 0 7 | 38 | - 29 |
| 0 0 8 | 19 | - 13 |
| 0 0 9 | 7 | - 12 |
| 0 0 10 | 18 | - 25 |
| 0 0 11 | 12 | 20 |
| 0 0 12 | 10 | 11 |

in Table 5-IV. The β-ZrClN sample used for this measurement was $Li_{0.29}ZrClN$(J&H). The lithium intercalate was swelled with all the solvents studied, and as the result, the basal spacing increased from 0.93 to 1.29-2.33 nm. Since all the samples studied did not swell without the presence of the interlayer lithium, those solvent molecules are coordinated to the interlayer lithium ions, presumably, through polar or electronegative functional groups. In the case of the solvation with THF in $Li_{0.29}ZrClN$(J&H), the basal spacing (1.35 nm) was smaller than that of the sample prepared from $Li_{0.16}ZrClN$(cryst). The smaller basal spacing may be due to the different orientation of the THF molecules between the layers. Though it is very difficult to picture the definite arrangements of the molecules only from the data of expansion of the spacings, several tentative structural models are proposed so that the basal spacing values observed can be explained by the values calculated for the models (Fig. 5-4). THF and AN molecules seems to lie with their molecular planes and axis parallel to the ZrClN layers. DMSO and Py molecules seems to be arranged with their molecular planes perpendicular to the ZrClN layers. For the solvated intercalates with very large increments of the spacings, such as FA and PC solvated samples, double layer solvation is very probable as shown in the case of $Li_{0.16}ZrClN$(cryst) solvated with PC.

Table 5-IV Basal spacings of the solvated lithium intercalates of β-ZrClN

| Solvent | Basal spacing / nm | Increase in basal spacing Δd / nm |
|---|---|---|
| Lithium intercalated β-ZrClN | 0.93 | |
| Tetrahydrofuran | 1.35 | 0.42 |
| Acetonitrile | 1.29 | 0.36 |
| Formamide | 2.04 | 1.11 |
| N,N-Dimethylformamide | 1.97 | 1.04 |
| Dimethyl sulfoxide | 1.80 | 0.87 |
| Propylene carbonate | 2.33 | 1.40 |
| Pyridine | 1.57 | 0.64 |

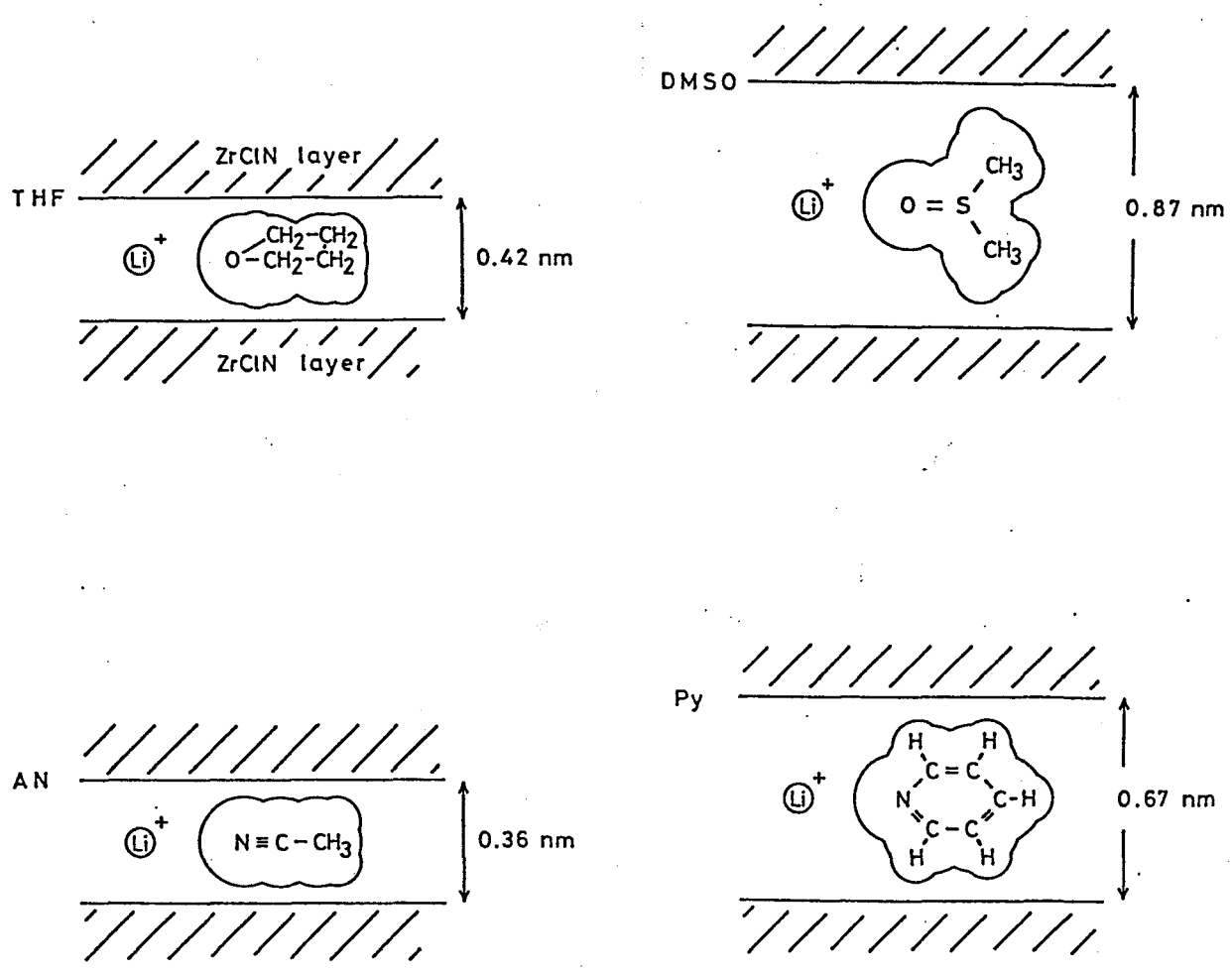


Fig. 5-4 Structural models of solvated lithium intercalates.

# 6 ELECTROCHEMICAL CHARACTERISTICS OF β-ZrClN IN LITHIUM CELLS

In order to examine the capabilities of β-ZrClN to the use for the electrode of secondary lithium batteries and electrochromic displays, electrochemical lithiation of β-ZrClN has been studied. Cyclic voltammograms and charge-discharge properties of the lithium cell are measured.

## 6.1 Experimental

**Materials** β-ZrClN samples used were the same as those prepared in chapter 5. Propylene carbonate (PC) was also similarly purified by vacuum distilled and then dried with molecular sieve 4A.

**Cyclic voltammetry** The working electrode for cyclic voltammetry was prepared as follows: The powder sample of β-ZrClN was dispersed in a 1% polyvinyl alcohol (Katayama Chemical, 1100) aqueous solution. Platinum plate (1.0 x 1.0 $cm^2$) was covered with the dispersion in such a way that a uniform thin film was formed on evaporation of the water. The resulting thin film was heated at 383 K for 15 h. The cyclic voltammogram was measured vs. $Li/Li^+$ by using a platinum counter electrode and 1 M $LiClO_4$/PC as electrolyte.

**Lithium cell** The cathode for galvanostatic measurements

was made by pressing the powder β-ZrClN onto a stainless steel mesh of a diameter of about 8 mm. The effective active area was 0.5 $cm^2$. A schematic structure of the lithium cell is shown in Fig. 6-1. It consists of the β-ZrClN cathode, a lithium foil anode and a glass filter separator soaked with 1 M $LiClO_4$/PC. The electrodes and the separator were put together in a Teflon body by stainless steel bolts and nuts. The cell was galvanostatically discharged and cycled between two preset voltages in an argon-filled glove box.

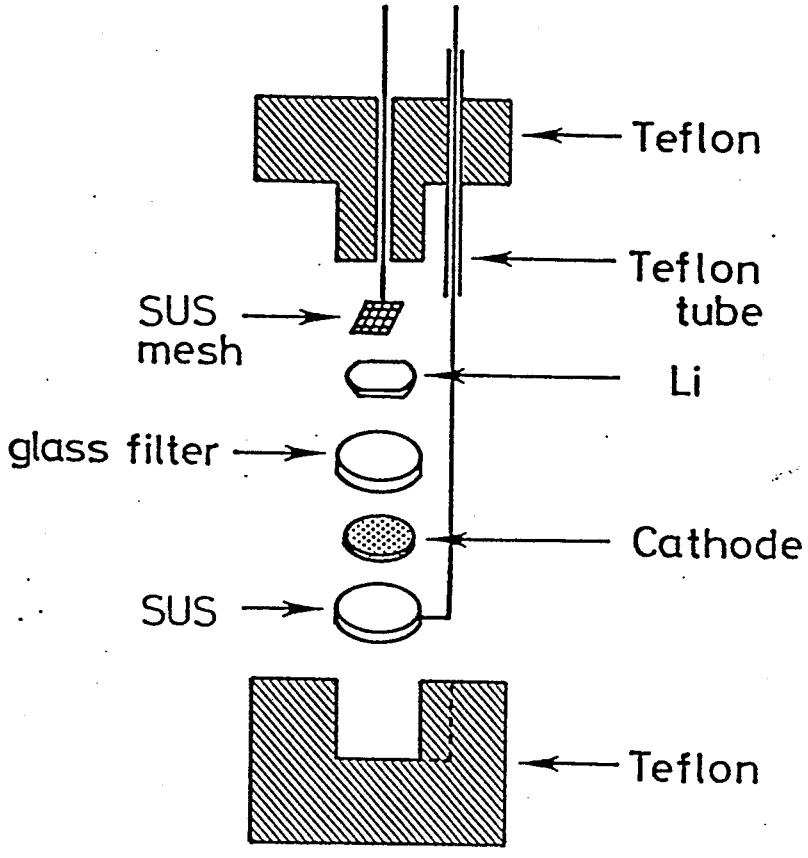


Fig. 6-1 Schematic structure of the lithium cell.

## 6.2 Results and Discussion

**Cyclic Voltammetry** A cyclic voltammetry of a ZrClN(cryst) electrode on platinum (sweep rate: 30 mV $s^{-1}$) is shown in Fig. 6-2. The cyclic voltammogram has two cathodic peaks at 1.85 and 1.0 V. The electrode began to be colored at about 2 V in the cathodic process, and was bleached at about 2 V in the anodic process. A cyclic voltammogram for ZrClN(as-prep) was similarly measured and shown in Fig. 6-3. It should be noted that although the electrode began to be colored at about 2 V in a similar way, the cathodic peak at 1.85 V is very weak, and the intensity of the second cathodic peak at about 1.0 V is increased. The electrode was similarly bleached at about 2 V in the anodic process. The shape of the voltammogram of ZrClN(J&H) was very similar to that of ZrClN(as-prep).

In the course of several dozens of coloring cycles, the current was gradually decreased and part of the electrode remained unbleached. The ZrClN(cryst) electrode showed better cycle performance than the others.

**Electrochemical Properties in Lithium cell** The lithium cell with a ZrClN(cryst) powder pressed cathode was discharged at a constant current density of 0.2 mA $cm^{-2}$. The discharge curve is shown in Fig. 6-4. The curve exhibits the shoulder and the low voltage plateau at 1.85 and 1.0 V, which are correspond to the two cathodic peaks observed in the cyclic voltammogram (Fig. 6-2).

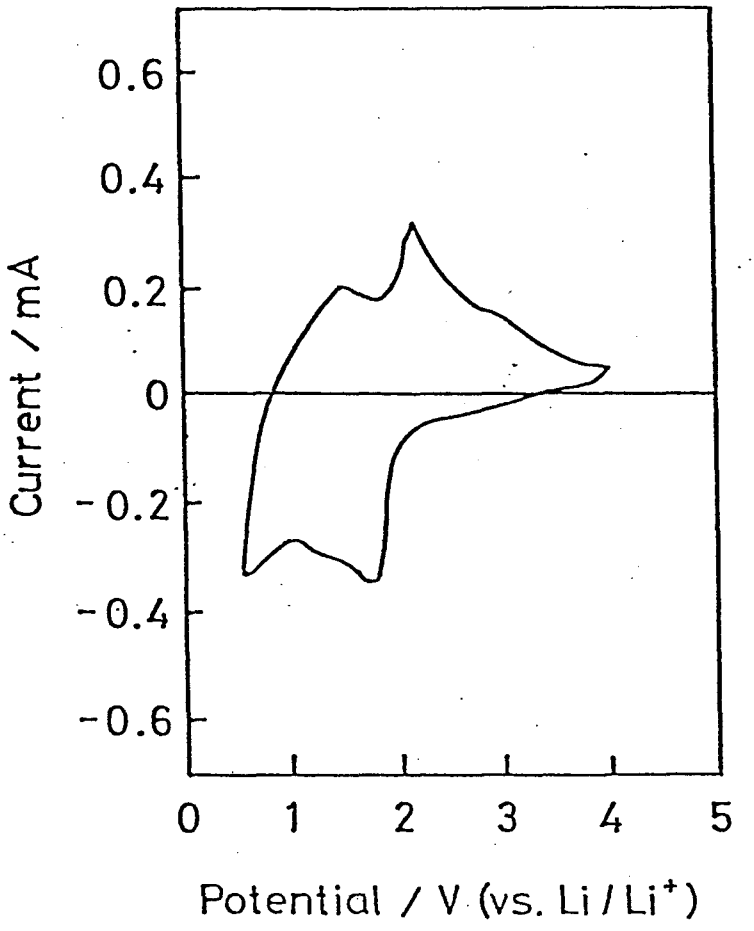


Fig. 6-2 Cyclic voltammogram of ZrClN(cryst) vs. $Li/Li^+$ in 1 M $LiClO_4$/PC at a sweep rate of 30 mV $s^{-1}$.

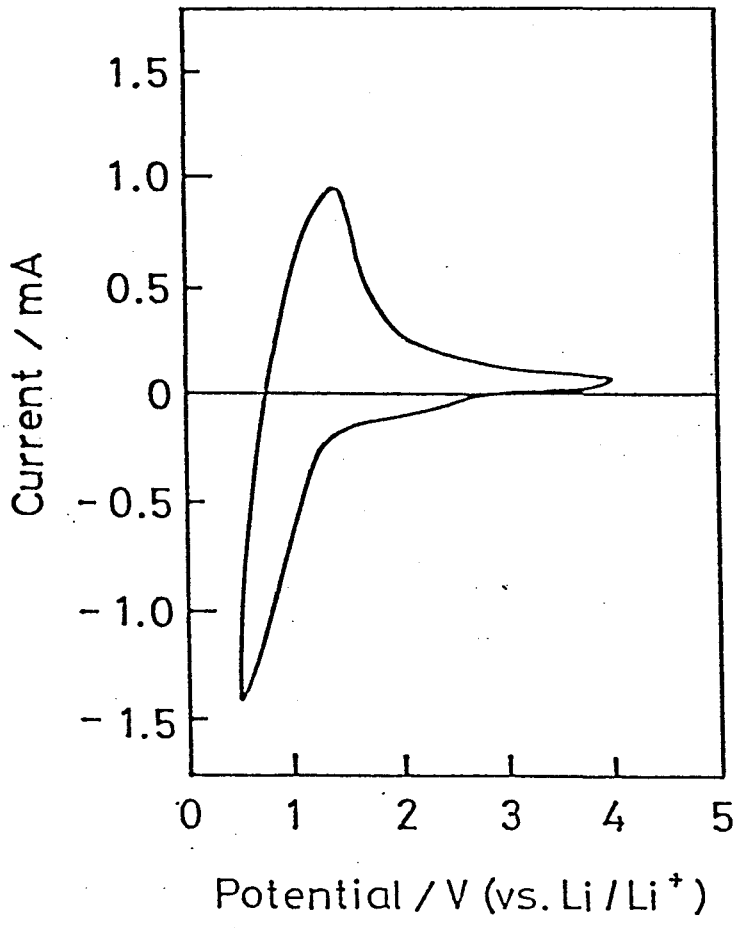


Fig. 6-3 Cyclic voltammogram of ZrClN(as-prep) vs. $Li/Li^+$ in 1 M $LiClO_4$/PC at a sweep rate of 30 mV $s^{-1}$.

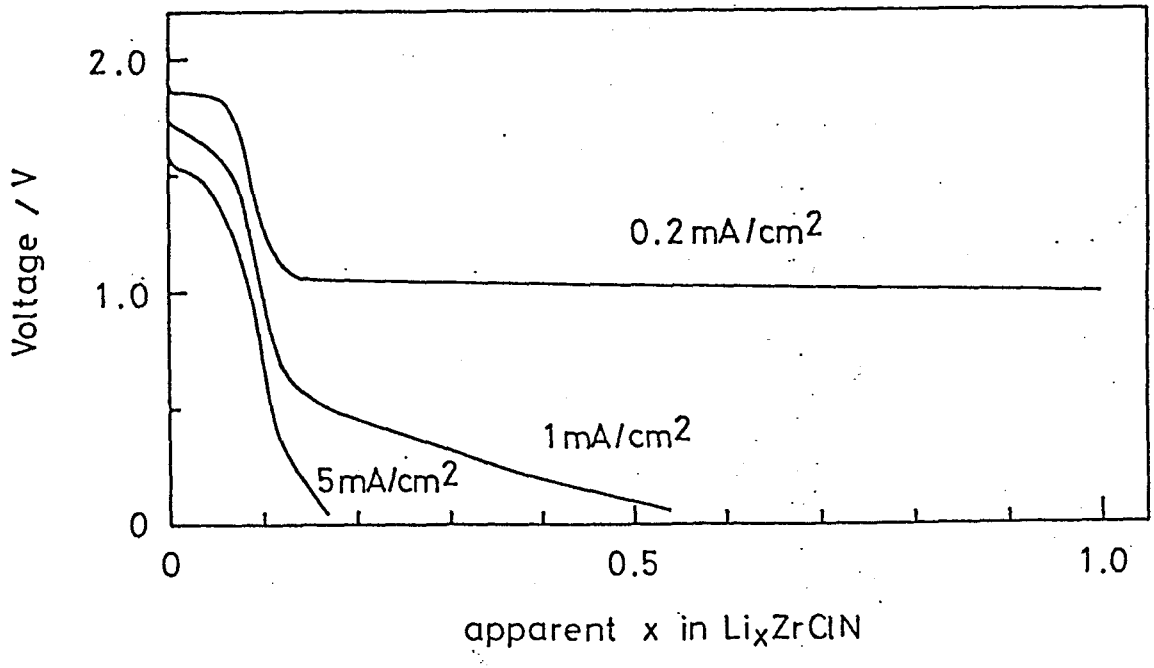


Fig. 6-4 Discharge curves of a Li | 1 M $LiClO_4$/PC | ZrClN(cryst) cell at different current densities.

The shoulder is short and the voltage steeply decreases to the plateau voltage of 1.0 V after a discharge of x = 0.08 for $Li_xZrClN$. The low plateau is very flat and lasts even in the discharge region of x > 2. The cell was discharged at larger current densities up to 5 mA $cm^{-2}$. As shown in Fig. 6-4, the shoulder can be clearly seen even at the current density of 5 mA $cm^{-2}$, while the plateau cannot keep up with the increased current density. In the first discharge to 1.0 V at a current density of 0.2 mA $cm^{-2}$, the current passed is about 0.15 e/ZrClN. This is in good agreement with the amount of lithium intercalated by n-BuLi method. The electrode was taken out after the discharge of 0.15 e/ZrClN and the XRD pattern was measured in an argon atmosphere. As shown in Fig. 6-5, all the reflections can be indexed as integral orders of a reflection of a basal spacing of 2.22 nm. This is identical to the value of β-ZrClN swelled with 1 M $LiClO_4$/PC after the chemical lithiation by n-BuLi method.

The cell was cycled at a current density of 0.2 mA $cm^{-2}$ within the first discharge region between the two preset voltages of 2.5 and 1.6 V. As shown in Fig. 6-6, the rechargeability of the cell was pretty good, more than 70% of the discharged capacity being maintained at the 30th cycle.

The cell was deeply discharged at the same current density to the low plateau region and then cycled between the voltages of 3.5 and 0.95 V. The several discharge-charge curves at different cycles are shown in Fig. 6-7. It is interesting to

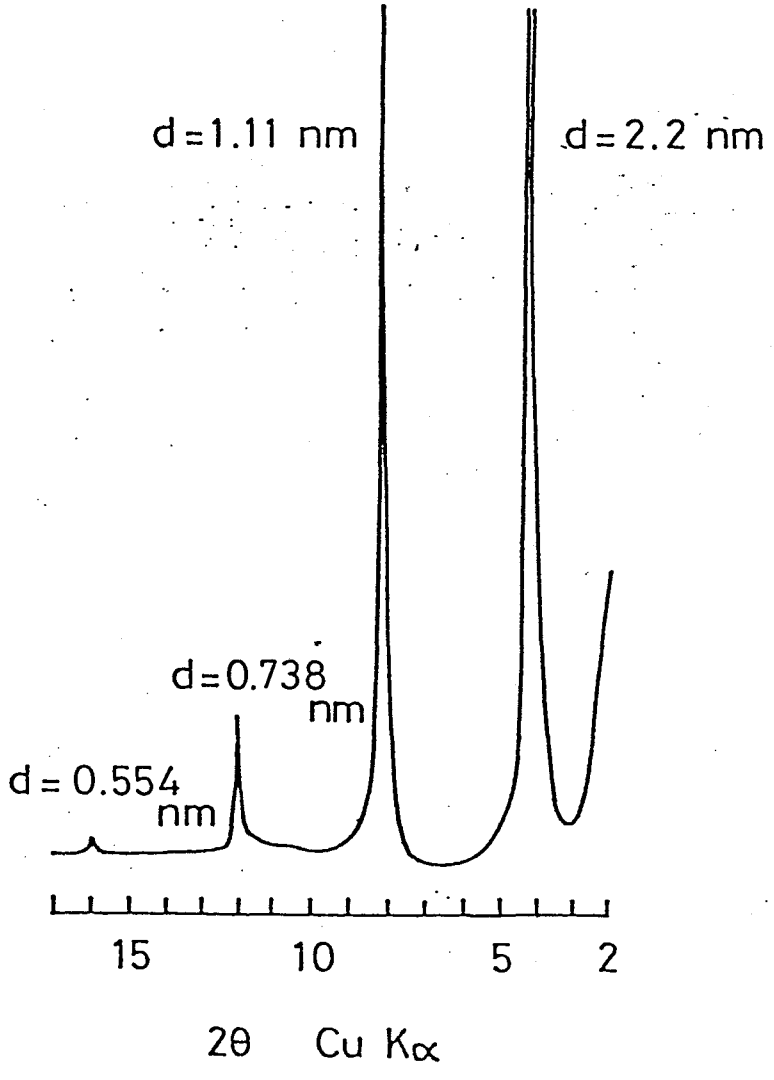


Fig. 6-5 XRD pattern of the cathode product of the ZrClN(cryst) cell after discharge of 0.15e/ZrClN.

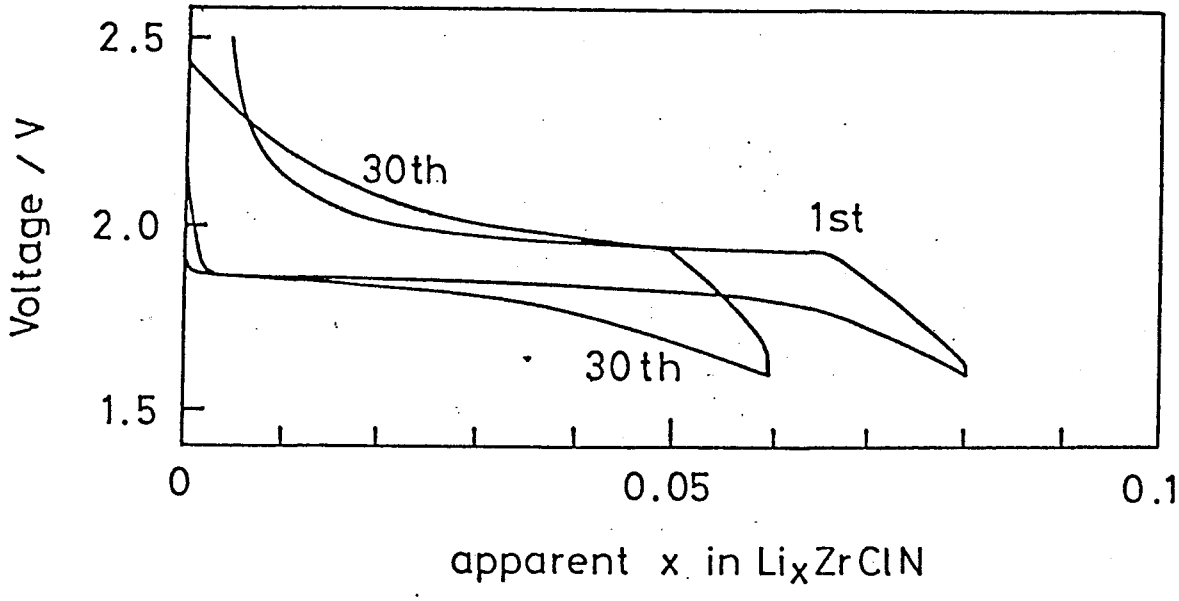


Fig. 6-6 Discharge-charge curves of the ZrClN(cryst) cell for the first and the 30th cycles in the shoulder (current density: 0.2 mA $cm^{-2}$).

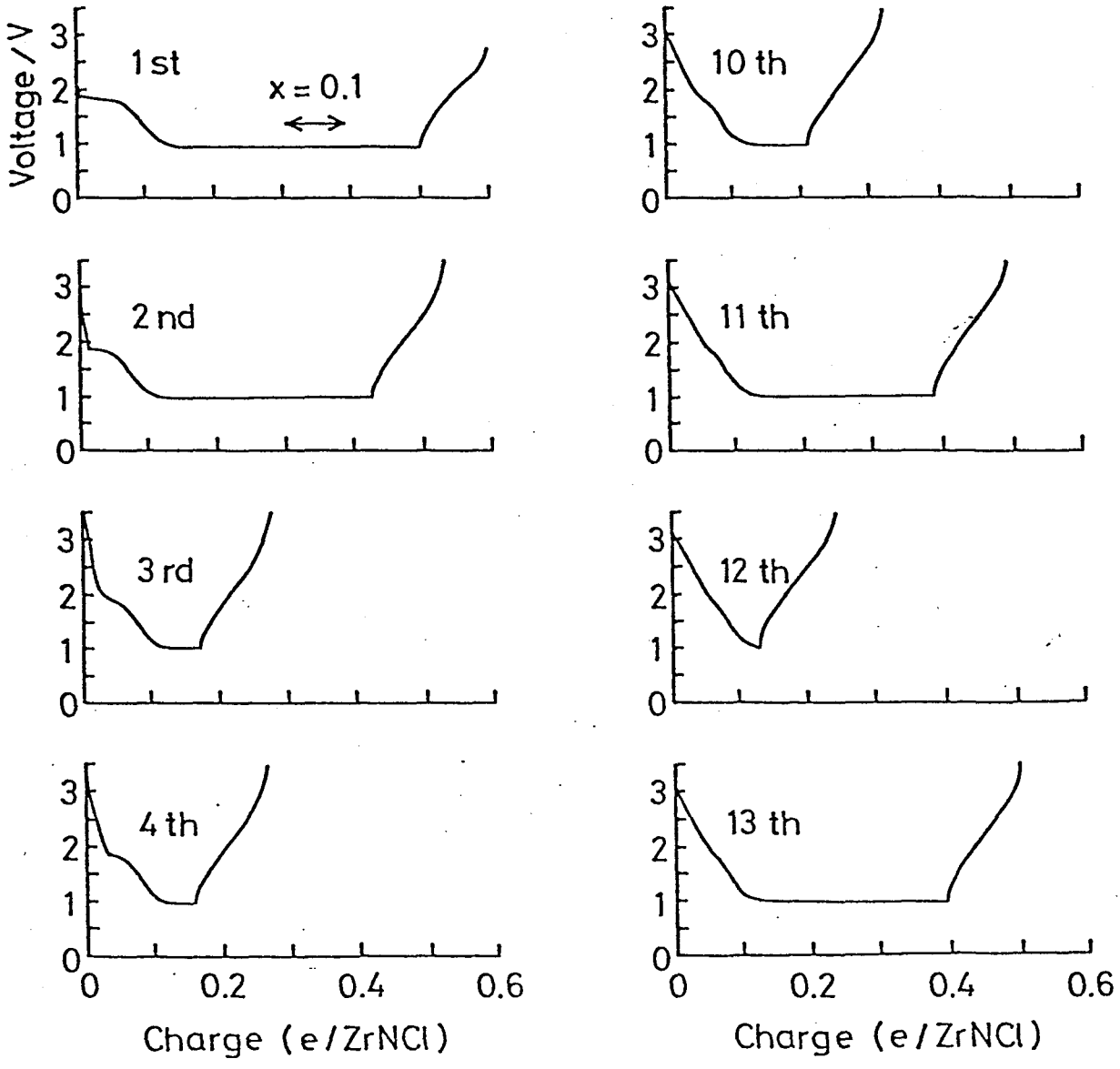


Fig. 6-7 Discharge-charge curves of the ZrClN(cryst) cell for different stage of cycles between 0.95 and 3.5 V (current density: 0.2 mA $cm^{-2}$).

note that the electricity discharged is much larger than that used for recharging, and that the electricity for recharging is about 0.10 e/ZrClN, which is coincident with the electricity discharged in the first process to 1.0 V plateau. In some cycles, for examples 3rd, 4th, 10th and 12th cycles, the low plateaus are greatly short compared with those of the other cycles. This is due to the flatness of the plateau; since the lower preset voltage was placed at 0.95 V, which was slightly lower than the plateau voltage, even very small depression in the voltage automatically switched the cycle mode from discharge to recharge.

It is evident that the low plateau is not reversible process and does not concern the intercalation of lithium. Probably, it can be attributed to the decomposition of the electrolyte on the surfaces of the lithium intercalated β-ZrClN electrode. Dey and Sullivan[59] reported that PC was reduced to carbonate and propene on a graphite electrode in 1 M $LiClO_4$/PC electrolyte at 0.6 V vs. $Li/Li^+$ according to the following equation:

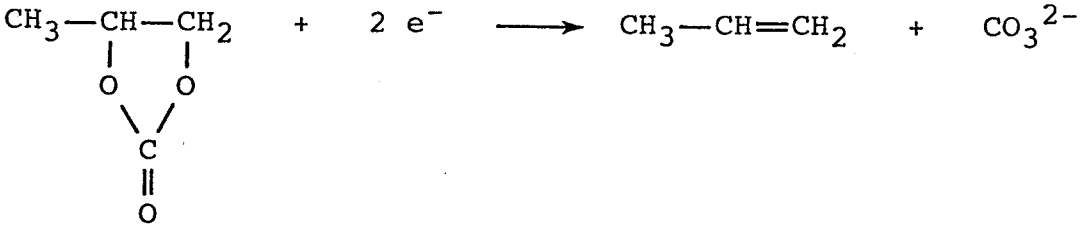

Murphy and Carides[60] also found that an irreversible voltage

plateau at 0.25 V in the discharge of $NbSe_2$/Li cells with 1 M $LiClO_4$/PC electrolyte. After discharging the above β-ZrClN/Li cell at the plateau voltage for 5 h, the electrolyte solution in the separator of the cell was analyzed by a gas chromatograph connected with a mass spectrometer. The analytical results suggested the formation of several kinds of products with the mass numbers larger than propene. Those are probably formed by the electrolysis of the electrolyte solution on the surfaces of the pressed pellet of β-ZrClN with interlayer lithium ions. The identification of the electrolysis products and the deviation of the mechanism for the formation will be the subjects for the future study.

The lithium cells with ZrClN(as-prep) and ZrClN(J&H) cathodes were also discharged and recharged at a constant current density of 0.2 mA $cm^{-2}$ between 3.0 and 0.5 V (Fig. 6-8). In accordance with the respective cyclic voltammogram, which showed a very weak cathodic peak at 2 V, the discharge curves do not have the shoulder, but the voltages decreased monotonically. The electricities used for the recharging are about 0.2 e/ZrClN, which is again much smaller than the electricities discharged. Even though the plateau voltages are lower than 1.0 V observed for the cell of ZrClN(cryst), the irreversible plateau may also be interpreted in terms of the reduction of PC rather than lithium intercalation.

From the view point of application to secondary lithium batteries of high energy densities, β-ZrClN is not a useful

cathode material, because the rechargeable capacity is less than 0.2 e/ZrClN. However, the reversible performance at higher voltages is pretty good. β-ZrClN may still be a promising material as an electrochromic display electrode when operated at shallow cycles. In the foregoing chapter we showed that the lithium intercalate of β-ZrClN swelled with various kinds of nonaqueous solvents such as tetrahydrofuran, acetonitrile, formamide, N,N-dimethylformamide, dimethyl sulfoxide, and pyridine as well as PC. The swelling of the electrode with solvents is not preferable for the reversibility of the cell. This may be solved by developing a non-intercalating solvent or a solid electrolyte.

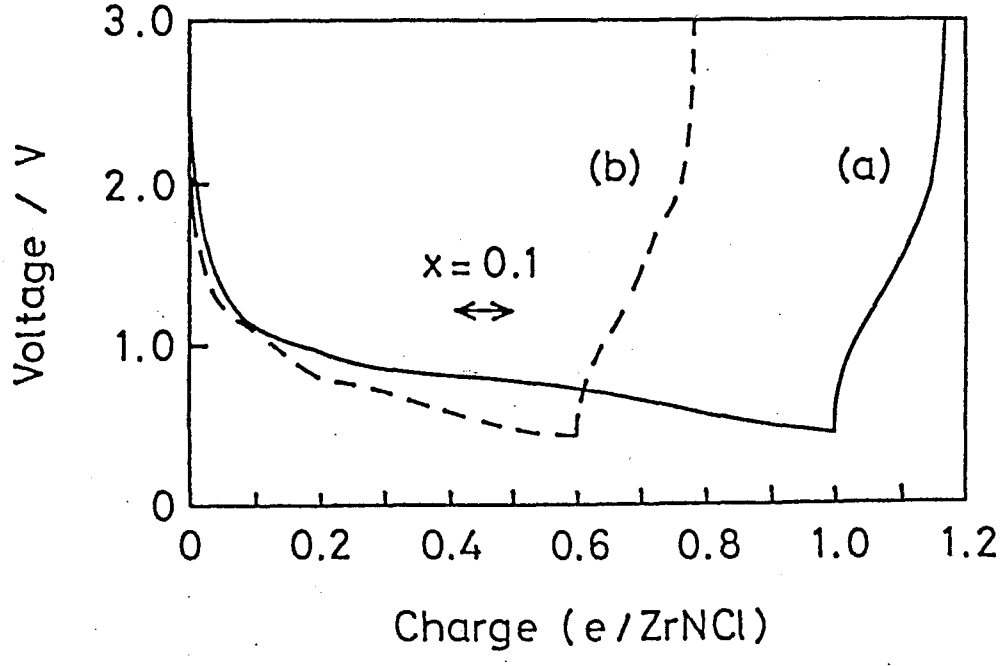


Fig. 6-8 Discharge-charge curves of (a) the ZrClN(as-prep) and (b) the ZrClN(J&H) cells at a current density of 0.2 mA $cm^{-2}$.

# 7 HYDROGEN UPTAKE BY β-ZrClN

Lithium can be intercalated into the interlayer spaces by breaking the weak interactions between the chlorine layers. It was found that not only lithium, but also hydrogen was taken up by β-ZrClN.

When β-ZrClN was decomposed in a vacuum by raising the temperature, $ZrNH_{0.6}$ was partly formed during the process. This finding suggests that hydrogen is included in the β-ZrClN from the beginning. Hydrogenation of β-ZrClN with $NH_4Cl$ and hydrogen gas was studied systematically. Electrochemical dehydrogenations and the measurements of the electrical conductivity of the samples were also studied. A structural model for the hydrogenated sample is proposed.

## 7.1 Experimental

**Materials** β-ZrClN was prepared by the direct reaction of $ZrH_2$ with $NH_4Cl$ vapor at 923 K in a stream of ammonia according to the procedure described in section 4.1. The as-prepared β-ZrClN powder sample was vacuum-sealed with a small amount of $NH_4Cl$ in a fused silica tube, and chemically transported to the higher temperature zone in a temperature gradient of 1023-1123 K as described in section 4.3. In this chapter, this sample will be called as-prepared β-ZrClN.

**Analysis** Hydrogen content in the sample was measured by combustion method. The sample was burned in a stream of oxygen at 1273 K with the aid of CuO, the chlorine being removed by a column filled with silver powder. The resulting water was trapped and determined by gas chromatography. XRD patterns were measured by using graphite monochromatized Cu $K_\alpha$ radiation with Si powder as an internal standard.

**Electrochemical measurements** A compressed β-ZrClN pellet was used as a working electrode (about 50 mg, 13 mm in diameter). Cyclic voltammograms were measured in a 0.1 M tetraethylammonium perchlorate (TEAPC)/ acetonitrile (AN) electrolyte solution with a platinum counter electrode and an A. C. E. reference electrode ($Hg/Hg_2Cl_2$, KCl(satd.), $KClO_4$ (satd.) (AN)).[61] Another electrolyte solution used was 0.1 M $CF_3COOH$/AN, which was coupled with a Ag/0.01 M $AgNO_3$ (AN) reference electrode.

A solid state cell was constructed using NAFION proton conducting membrane, which separated $H_xZrClN$ pellet and Pd metal electrodes. The cell was sealed in epoxy resin to minimize the losses of hydrogen (Fig. 7-1).

**Electric conductivity** The electric conductivity was measured on the powder sample compressed at a pressure of about 100 MPa by the four probe technique in the range of room temperature to 173 K. The copper electrodes were pasted onto the surface of the pellet (10.0 x 2.0 x 0.5 $mm^3$) by a silver paint.

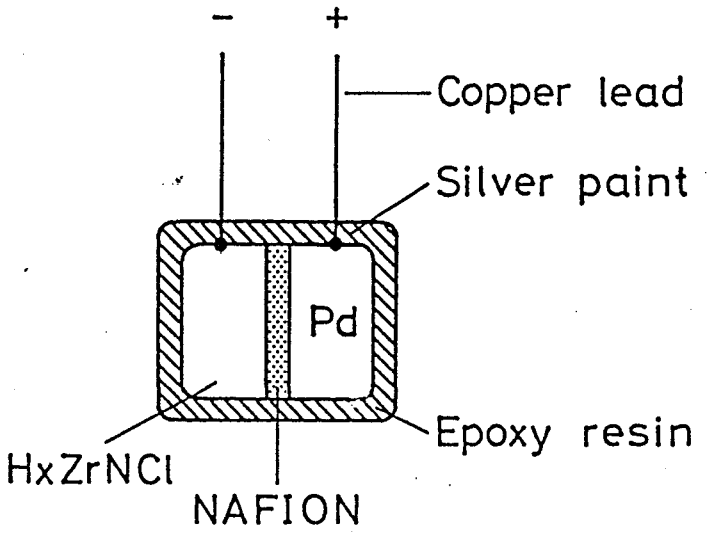


Fig. 7-1 Assembly of a solid state cell with NAFION membrane.

## 7.2 Thermal Decomposition

The β-ZrClN which was chemically transported with the aid of $NH_4Cl$ was decomposed in a vacuum by raising the temperature stepwise up to 1473 K. Being allowed to stand for 1 h at each heating step, the sample was taken out to measure the weight loss and the XRD pattern. The weight loss curve is shown in Fig. 7.2. The sample began to lose the weight gradually from 1120 K. A steep decrease in weight occurred at around 1300 K, and the curve reached a constant weight at 1373 K. The total weight loss is 45.6 %, and the residual was found to be ZrN. The loss observed is in good agreement with the loss (43.9 %) calculated on the basis of the following decomposition:

$$ZrClN \longrightarrow \frac{3}{4}ZrN + \frac{1}{4}ZrCl_4\uparrow + \frac{1}{8}N_2\uparrow$$

where chlorine is removed in the form of $ZrCl_4$.

Fig. 7-3 shows a series of XRD patterns recorded at each heating step. It is seen that β-ZrClN decomposes to ZrN at temperatures above 1320 K. A shaded diffraction peak at $2\theta$ = 30.3 in the figure can be attributed to the (111) reflection of $ZrNH_{0.6}$ reported by Blunck and Juza.[48] The intensity increases with the decomposition of β-ZrClN and disappear above 1323 K. Although the thermal behavior of $ZrNH_{0.6}$ is not well known, it seems reasonable to assume that $ZrNH_{0.6}$ is converted into ZrN, liberating the hydrogen at temperatures above 1323 K.

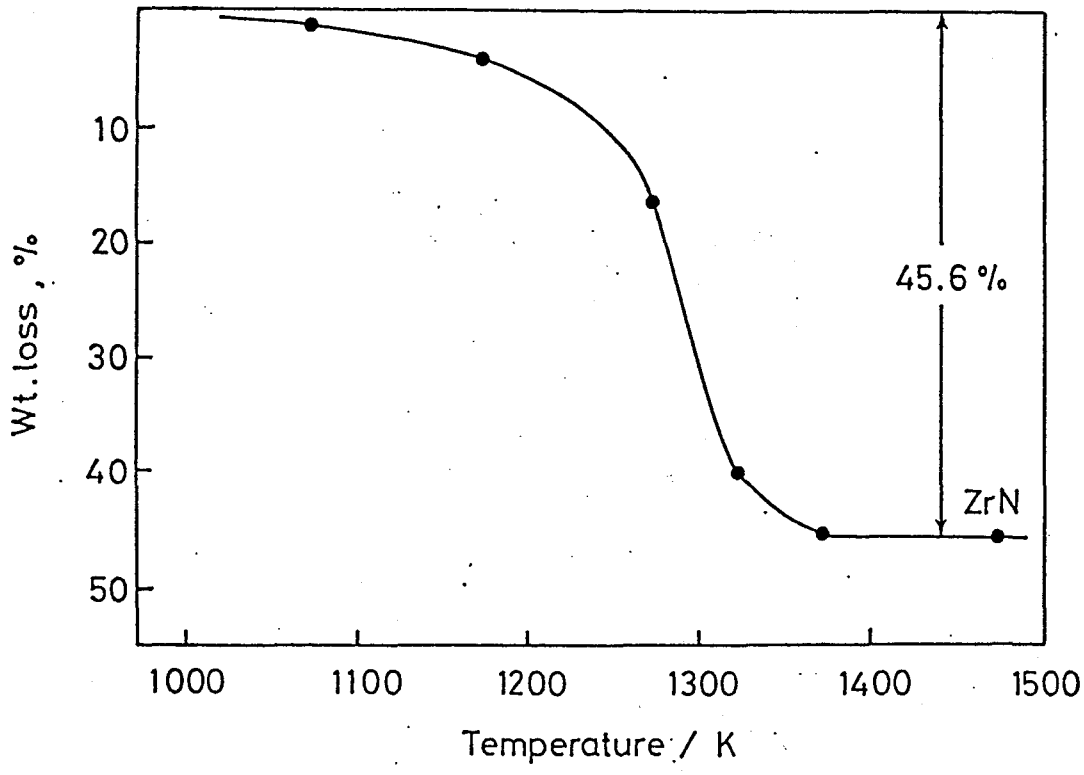


Fig. 7-2 Weight loss curve of β-ZrClN heated stepwise in a vacuum.

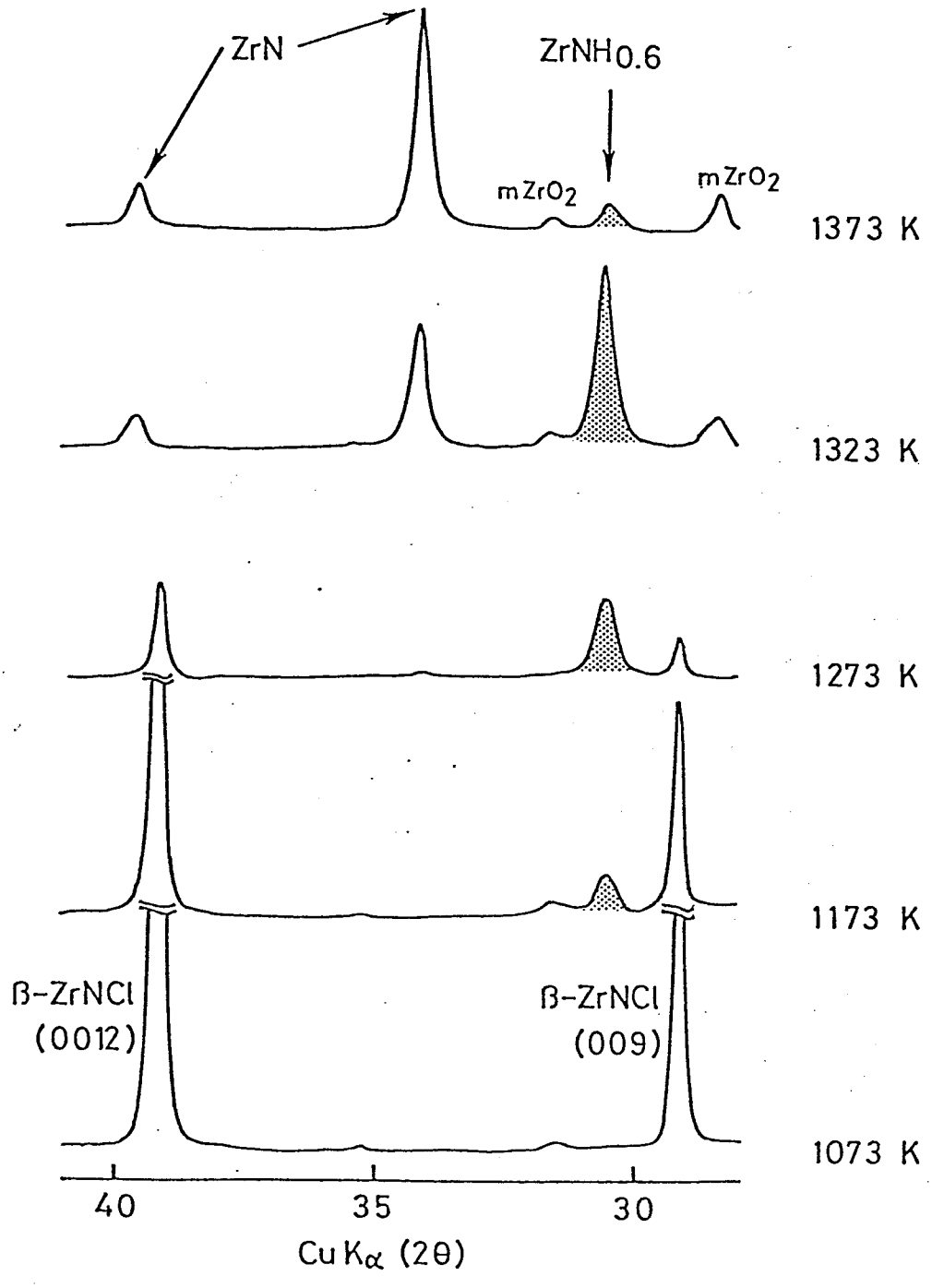


Fig. 7-3 XRD patterns of β-ZrClN at the heating steps shown in Fig. 7-2.

Additional two weak peaks appearing in the XRD patterns measured above 1323 K are due to monoclinic $ZrO_2$, which might be formed by the oxide contamination. The formation of $ZrNH_{0.6}$ during the decomposition suggests that hydrogen must be included in the starting β-ZrClN, because the decomposition was performed under a continuous evacuation at a pressure of $10^{-5}$ Torr, and thus there was no fear of contamination from hydrogen and water. The intensity of the diffraction peaks due to $ZrNH_{0.6}$ varied depending on the samples, and seemed to have some relations with the chemical transport conditions of β-ZrClN, such as the amount of $NH_4Cl$ added as the transporting agent and the treatment temperature. Evidently, the hydrogen in β-ZrClN comes from the $NH_4Cl$ used as the transporting agent. A more systematic study has been made on the uptake of the hydrogen from $NH_4Cl$ by changing the treatment conditions variously.

## 7.3 Hydrogenation

Equimolar mixture of β-ZrClN and $NH_4Cl$ was vacuum-sealed in a fused silica tube, and placed in a furnace with two temperature zones. The end of the glass tube containing the mixture was placed in the higher temperature zone, the temperature of which was controlled in the range of 773 to 1073 K. The other end of the glass tube was kept at 673 K in the lower temperature zone. During this heat-treatment, the tube was filled with $NH_4Cl$ vapor

and excess $NH_4Cl$ was deposited to the lower temperature zone. After the tube was allowed to stand for 24 h, the β-ZrClN was taken out and evacuated at 673 K for 3 h to remove $NH_4Cl$ adsorbed on the surfaces of the sample. The hydrogen contents of the treated samples were determined by the combustion method and are shown in Fig. 7-4 as a function of the treatment temperature. The hydrogen content increases with the temperature until it reaches the maximum amount of $x = 1.2$ for $H_xZrClN$ at 923 K and then decreases with the temperature. The hydrogen content of the as-prepared sample was also analyzed in a similar way. As shown in the figure, even the as-prepared β-ZrClN contains hydrogen of $x = 0.12$. In the above treatment excess amount of $NH_4Cl$ was loaded with β-ZrClN to learn the temperature effect on the uptake amount of hydrogen. If a smaller amount of $NH_4Cl$ is used, β-ZrClN with lower hydrogen content will result. The lattice parameters of the unit cell of the treated samples are shown in Fig. 7-5 as a function of hydrogen content. The parameters were essentially unchanged by hydrogenation, although there is a tendency that the c dimension (c/3 in the figure) decreases very slightly with the increase of hydrogen content. Hydrogenation of β-ZrClN can also be performed under a stream of flowing hydrogen at elevated temperatures. The amount of hydrogen taken up by β-ZrClN is shown in Fig. 7-6 as a function of the temperature. The amounts are smaller than those found for the samples treated with $NH_4Cl$ at the corresponding temperatures.

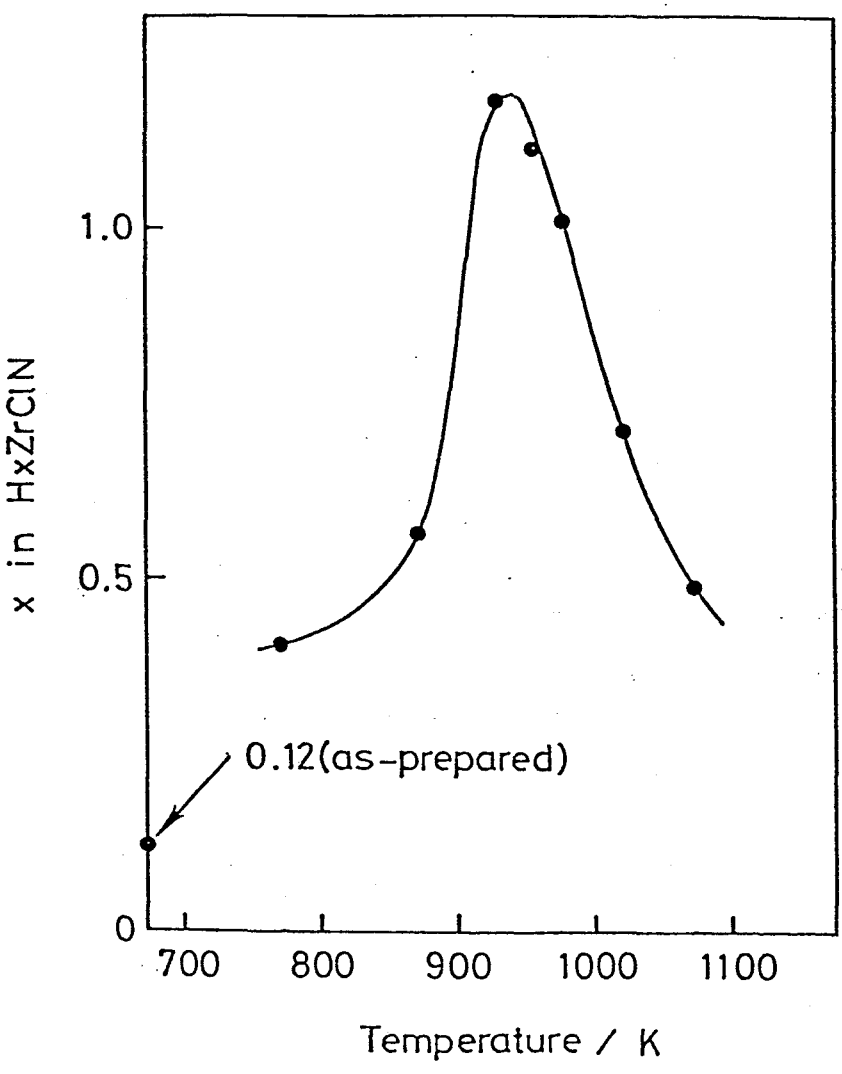


Fig. 7-4 Temperature dependence of the amount of hydrogen taken up by β-ZrClN.

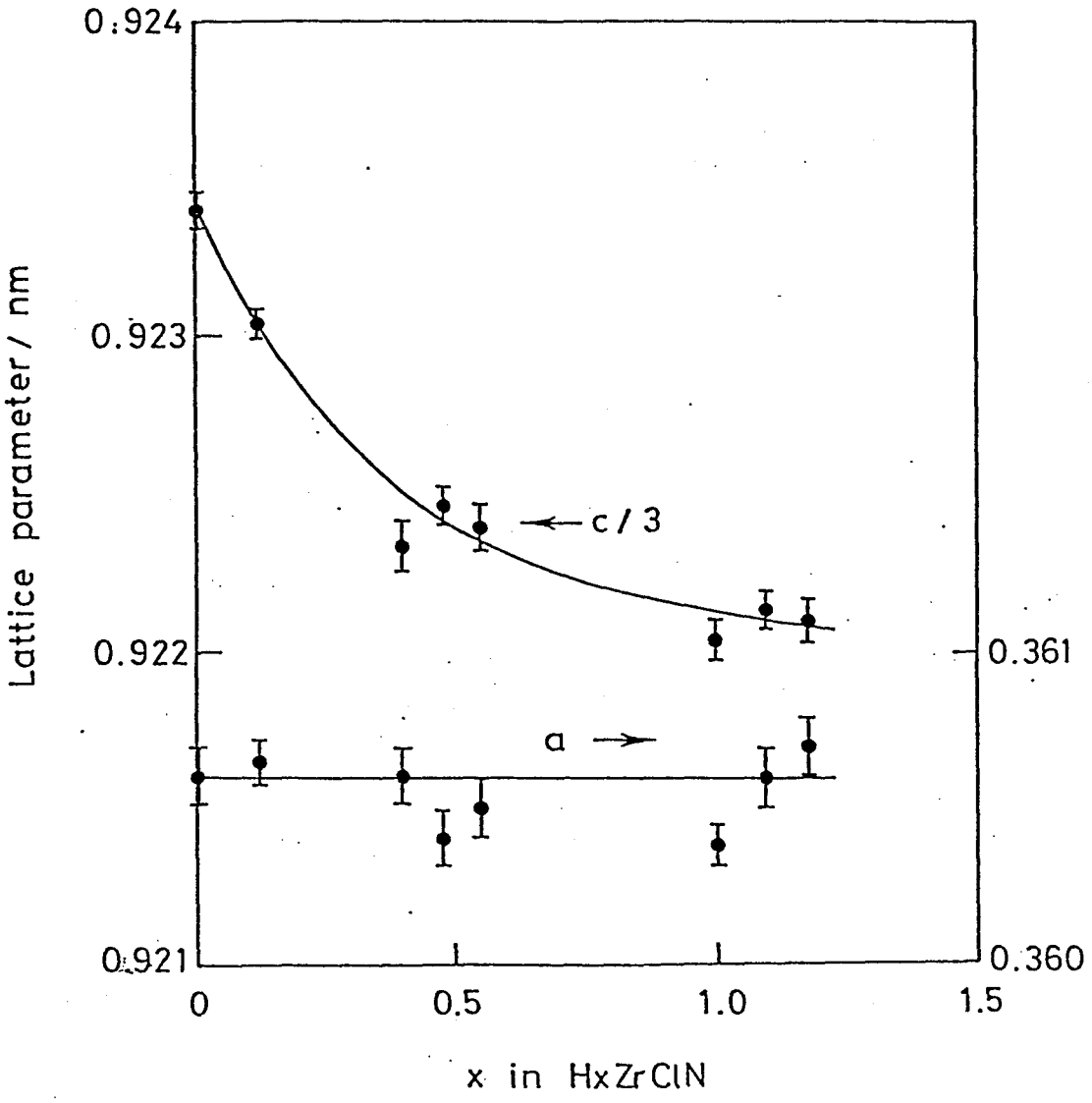


Fig. 7-5 Lattice parameters of $H_xZrClN$ as a function of hydrogen content (x). For the c dimension, c/3 is plotted.

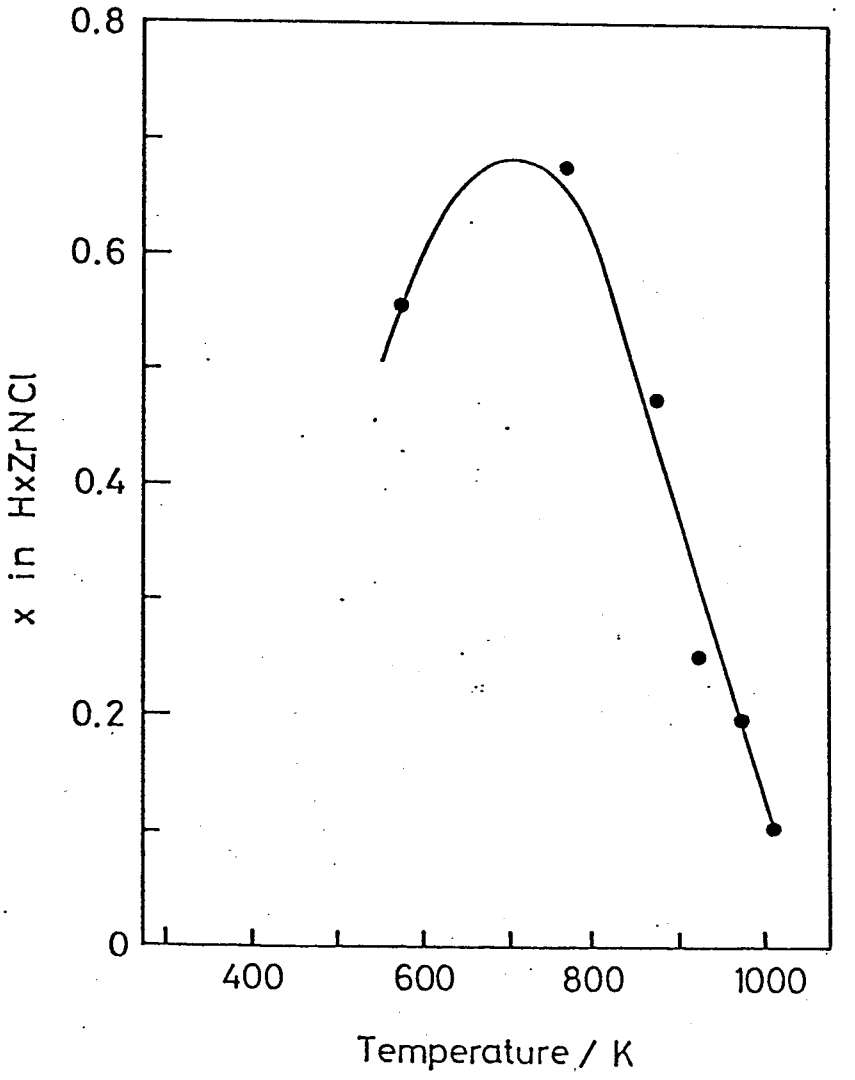


Fig. 7-6 Temperature dependence of the uptake amount of hydrogen by heat treatment in a stream of hydrogen.

## 7.4 Electrochemical Dehydrogenation

Cyclic voltammogram of a pressed $H_{0.70}ZrClN$ electrode (sweep rate: 20 mV $s^{-1}$) was measured in 0.1 M TEAPC/AN with an A.C.E. reference electrode. As shown in Fig. 7-7, an anodic peak was observed at about 0.6 V. This is probably due to the following reaction:

$$H_xZrClN \longrightarrow y\ H^+ + y\ e^- + H_{x-y}ZrClN$$

This procedure was irreversible, and cathodic peak corresponding to the uptake of hydrogen was not observed. Another cyclic voltammogram was recorded by using 0.1 M $CF_3COOH$/AN as an electrolyte solution. A similar anodic peak due to dehydrogenation from $H_xZrClN$ was obtained, but no cathodic peak due to the re-hydrogenation was observed.

In an attempt to remove the hydrogen completely from $H_xZrClN$, an electrochemical cell, $H_xZrClN$/0.1 M $CF_3COOH$ (AN)/Pt was constructed for two samples with x = 0.12 and 0.70, and charged at a constant current of 10 μA. The arrangement of the electrodes in the cell assembly was very similar to that used for the lithium cell of β-ZrClN in section 6.1. The polarization curves obtained are shown in Fig. 7-8. The charging potential is constant at 1.25 V. The polarization occurs after the electricity equivalent to the hydrogen content in $H_xZrClN$ is charged. In the chemical analyses of the samples after charging, hydrogen was hardly detected.

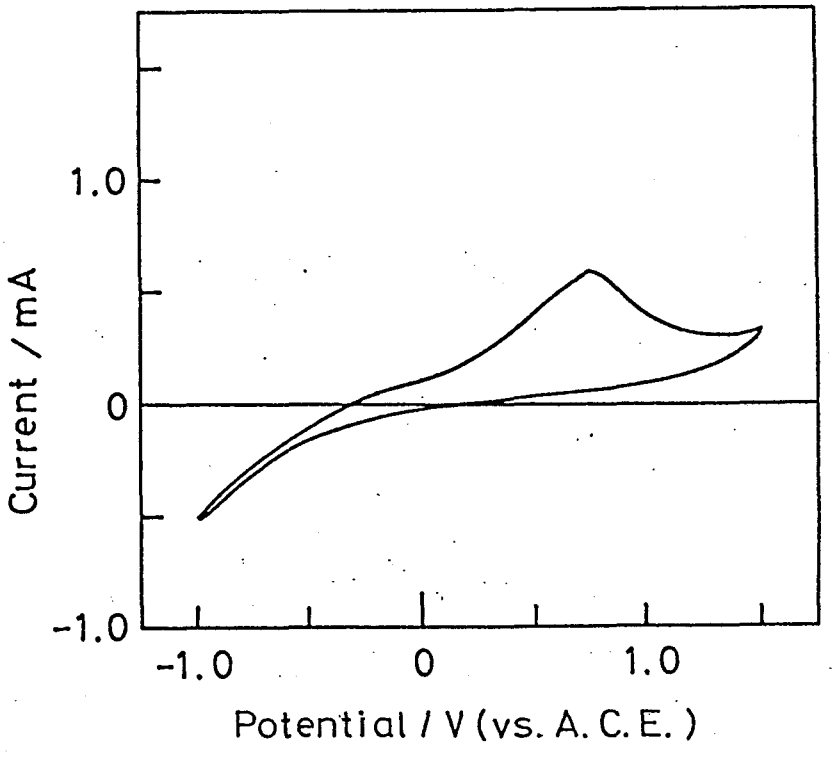


Fig. 7-7 Cyclic voltammogram of $H_xZrClN$

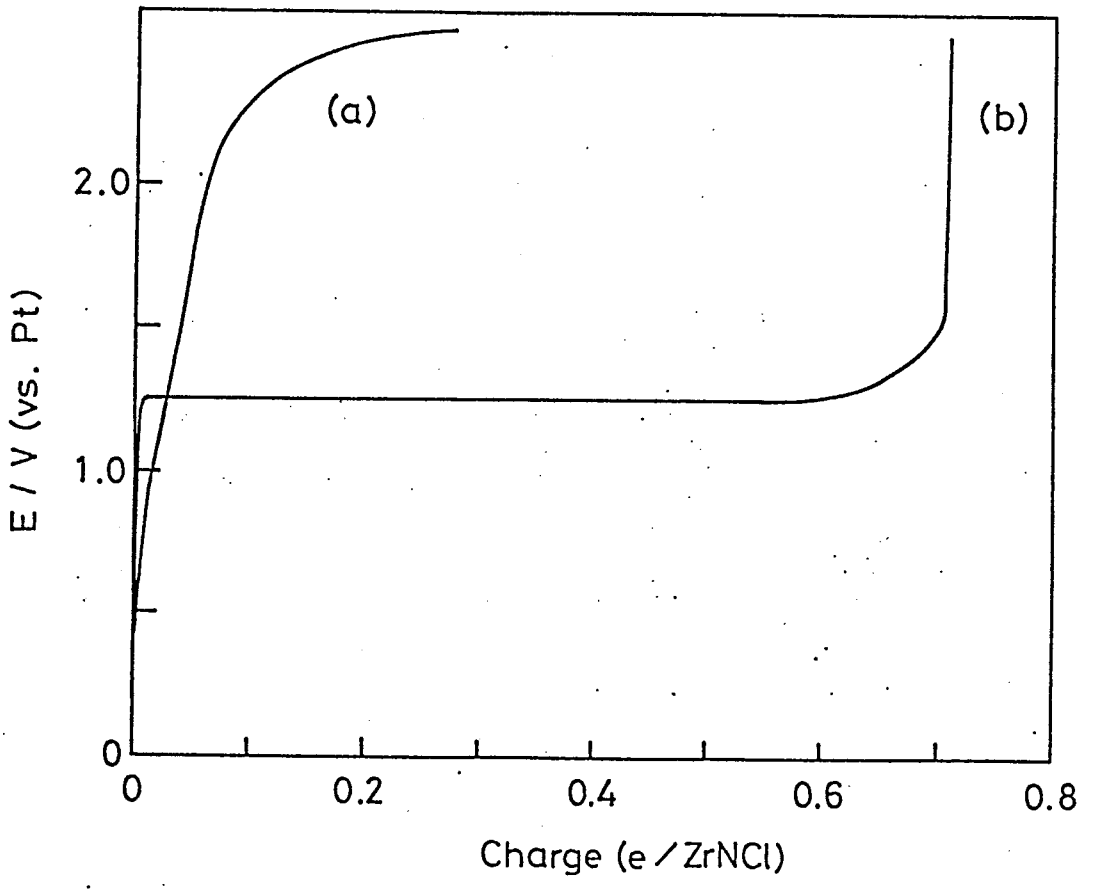


Fig. 7-8 Polarization curves for a cell $H_xZrClN$/0.1 M $CF_3COOH$(AN)/Pt: (a) x = 0.12 and (b) x = 0.70.

Another electrochemical dehydrogenation was performed by using a solid state cell with NAFION proton conducting membrane, $H_xZrClN$/NAFION/Pd. Polarization curves for the cells of $H_xZrClN$ with x = 0.12 and 0.40 are shown in Fig. 7-9. The cell was charged at a constant current of 10 μA until the polarization occurred. It was found that $H_xZrClN$ could be similarly dehydrogenated in the solid state cell, and part of Pd electrode changed into $PdH_2$.

The electrochemical reaction was irreversible, and the re-hydrogenation could not be done successfully in the solid state as well as the liquid electrolyte cells. The lattice parameters of $H_xZrClN$ for x = 0 was measured on the dehydrogenated sample and shown in Fig. 7-5, together with the hydrogenated samples. The c dimension of the dehydrogenated sample is a slightly larger than the other samples.

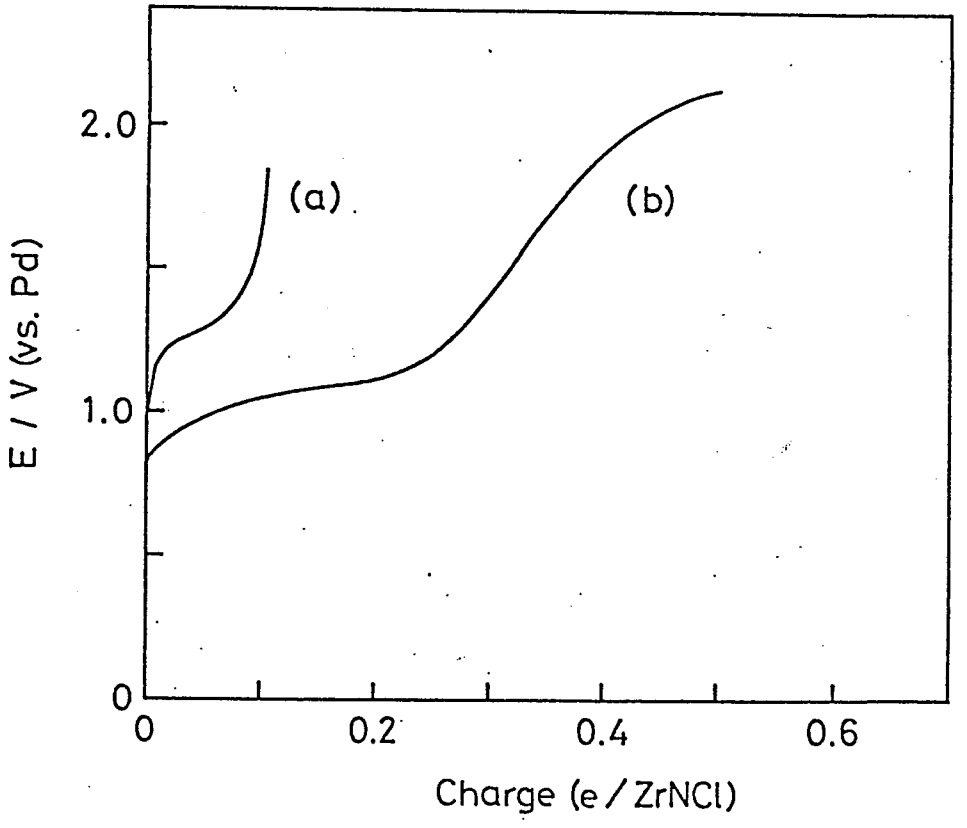


Fig. 7-9 Polarization curves for a solid state cell $H_xZrClN$/NAFION/Pd: (a) x = 0.12 and (b) x = 0.40.

## 7.5 Electric conductivity

The electric conductivities were measured on the pressed $H_xZrClN$ samples with different x values, and are shown in Fig. 7-10 as a function of the reciprocal absolute temperature. The sample with $x \simeq 0$ was prepared from $H_{0.12}ZrClN$ by the electrochemical dehydrogenation in the solid state cell. $H_xZrClN$ is a semiconductor with electrical conductivity of the order of $10^2$ S $m^{-1}$ at room temperature. The activation energy for the conduction at the temperatures around -170 K is as small as 60 meV, which was calculated from the slope of the plots of ln $\sigma$ vs. 1/T (dashed lines in the figure). As the temperature rises, the conductivity moves into a saturation region. The conductivity and the activation energy for the conduction appear to be little affected by the amount of hydrogen, although the dehydrogenated sample showed slightly low conductivity.

In chapter 8, it will be shown that β-ZrClN has an optical band gap of 3.2 eV which is much larger than the activation energy for conduction. The sign of the thermoelectric power was measured, which indicated that $H_xZrClN$ was of n-type. Since the color of the crystals was essentially unchanged by the hydrogenation, the high conductivity of $H_xZrClN$ is due to the ionization of the donor levels formed at 60 meV below the conduction band. The saturation of the conductivity is due to the complete ionization of such shallow donor levels. It seems very likely that the donor levels are formed by the

hydrogen atoms. The low electric conductivity of the dehydrogenated sample can be interpreted in terms of the extremely low concentration of the donors.

The conductivity of the lithium intercalated sample which was already shown in chapter 5 is also shown in Fig. 7-10. The conductivity of as-prepared sample increases by a factor of 10 at room temperature on the intercalation.

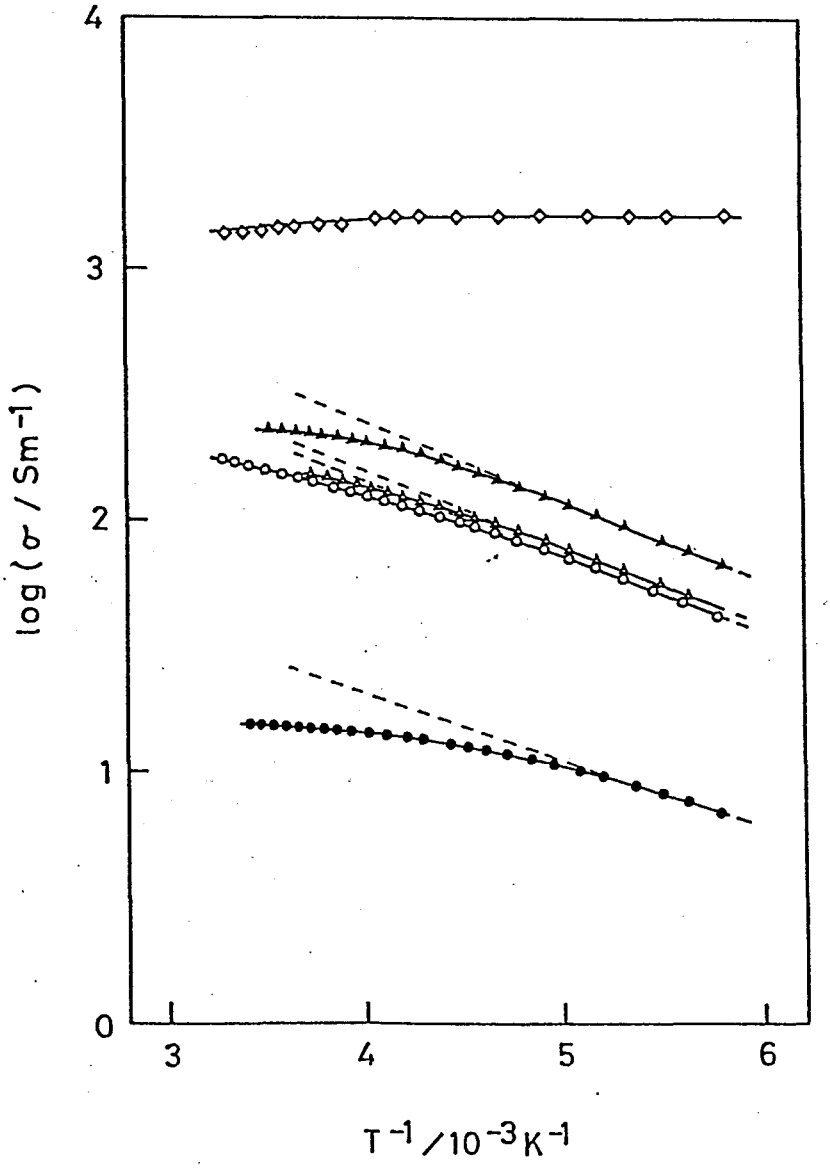


Fig. 7-10 Temperature dependences of the conductivities of $H_xZrClN$ and $Li_{0.16}ZrClN$: x = 0.12 (▲), x = 0.48 (▲), x = 1.0 (○), x ≈ 0 (●), and $Li_{0.16}ZrClN$ (◇).

## 7.6 Electrochemical Lithium Intercalation into Hydrogenated β-ZrClN

Lithium batteries with hydrogenated β-ZrClN cathodes ($H_xZrClN$, x = 0.12, x = 0.48) were constructed with 1 M $LiClO_4$/PC electrolyte, and then the discharge curves at a current density of 200 mA $cm^{-2}$ are shown in Fig. 7-11. The two discharge curves are almost same and indistinguishable with that shown in Fig. 6.4. This finding suggests that the extent of hydrogenation of β-ZrClN does not influence the lithium intercalation properties.

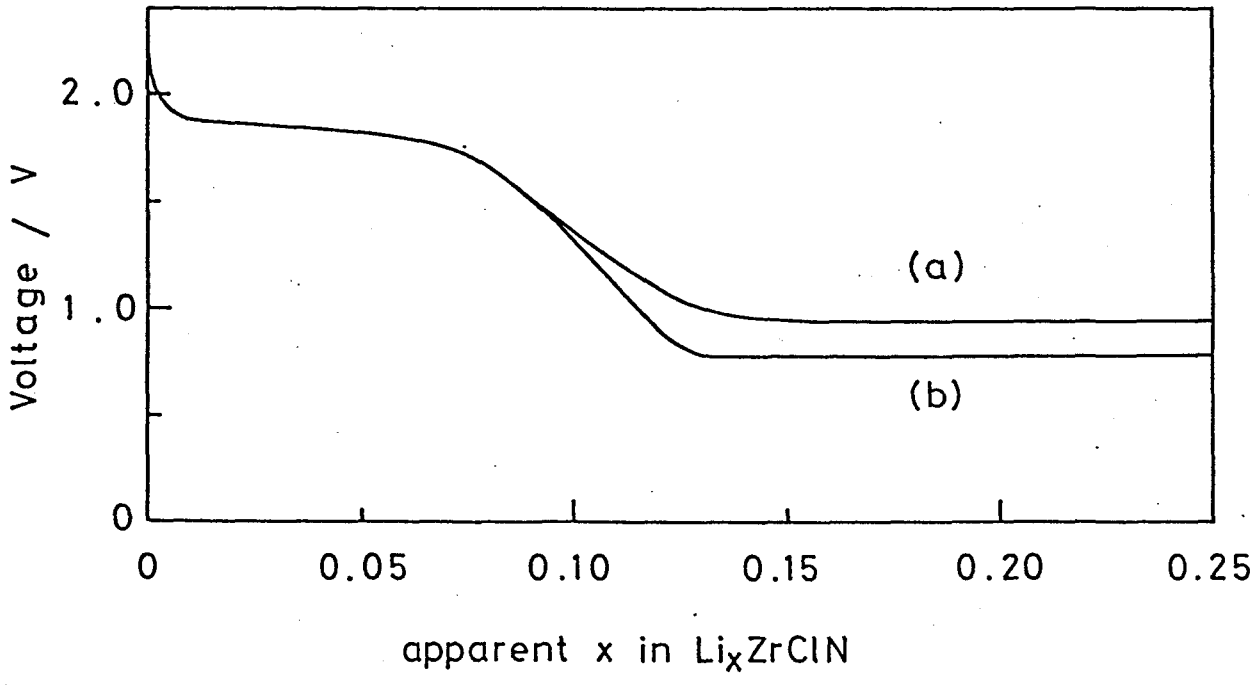


Fig. 7-11 Discharge curves of Li | 1 M $LiClO_4$/PC | $H_xZrClN$ cells: (a) x = 0.12, (b) x = 0.48.

## 7.7 Structural Consideration of Hydrogen Position

It is well known that some transition metal oxides such as $WO_3$ and $MoO_3$ are easily reduced by lithium and hydrogen even at room temperature and form bronzes.[62,63] On the bronze formation, the original crystals are intensely colored and possess metallic properties. Such drastic changes in the optical and the electrical properties are due to the electrons donored from the lithium and the hydrogen inserted or intercalated into the crystals. The electrons are delocalized through the crystals. Usually, the changes in the physical properties of the crystals are independent of the kind of the electron donors.

On intercalation of lithium, the color of β-ZrClN changes from yellow green to black and the electric conductivity increases. These changes are also explained in terms of the electron transfer from the lithium atoms intercalated between the chlorine layers to ZrClN layers. In the present chapter, it has shown that hydrogen as well as lithium is taken up by β-ZrClN. It is interesting to note that although both of the compounds, $Li_xZrClN$ and $H_xZrClN$, retain the original crystal structure of β-ZrClN, the physical properties are greatly different: unlike the lithium intercalated compound described above, the hydrogenated compound retains the yellow green color of β-ZrClN, and its electrical conductivity is little affected by the hydrogen content.

There are a number of layered monohalides MX ( M = Zr, Sc, La, Gd, Er, Lu; X = Cl, Br) which form hydrides MXH.[64,65] All these monohalides have the structures isomorphous to ZrCl[66] or ZrBr[67]. The structure of one unit layer of ZrCl(Br) is shown in Fig. 7-12. The double zirconium metal layers are sandwiched by two close-packed chlorine (or bromine) layers, and such layers sequenced X-Zr-Zr-X (X = Cl, Br) are stacked with each other by van der Waals interactions so as to form 3R structures. The distinction between the ZrCl and ZrBr structures occurs only in the way of stacking the unit layers, e.g., ACB and ABC for ZrCl and ZrBr, respectively.

The positions of the hydrogen have been analyzed by neutron diffraction studies. In the hemihydride $Zr_2Br_2H$,[68] the hydrogen atoms occupy the tetrahedral interstices of the double zirconium metal layers, while in the monohydride ZrBrH[69], hydrogen atoms occupy the octahedral interstices of the double metal layers as shown in Fig. 7-13. The structure of ZrClH is considered to be similar to that of ZrBrH. It is interesting to note that the structure of β-ZrClN is analogous to ZrBrH or ZrClH from a view point that the double zirconium metal layers are sandwiched between two close-packed chlorine layers (Fig. 7-12(b) and (c)). However, there is a marked difference between the two structures; in β-ZrClN, the double zirconium metal layers form trigonal prismatic interstices, whereas in ZrCl or ZrBr, the double metal layers provide trigonal antiprismatic, or octahedral

interstices. The two types of interstices are depicted in Fig. 7-13. According to the neutron diffraction analysis of ZrBrH by Wijeyesekera and Corbett,[69] a pair of hydrogen atoms occupy the octahedral interstices (Fig. 7-13(a)). In β-ZrClN structure, a nitrogen atom occupies the prismatic interstice, being bonded to the three zirconium atoms (Fig. 7-13(b)). As seen from the Fig. 7-13, the sizes of the two interstices are very similar, and it may be possible for a hydrogen atom to occupy the trigonal interstice of β-ZrClN, which is coordinated by three zirconium atoms and a nitrogen atom. The position in β-ZrClN is shown in Fig. 7-14. Certainly, the final position of the hydrogen in $H_x$ZrClN should be carefully determined by the neutron diffraction study.

The electrons from hydrogen are not delocalized through the crystals, instead, donor levels are formed only 60 mV below the conduction band. This suggests that the hydrogen atoms have higher degrees of covalent interactions with β-ZrClN layers than the lithium atoms intercalated between the chloride layers. This difference in the electronic structures also supports the above estimation of the hydrogen position.

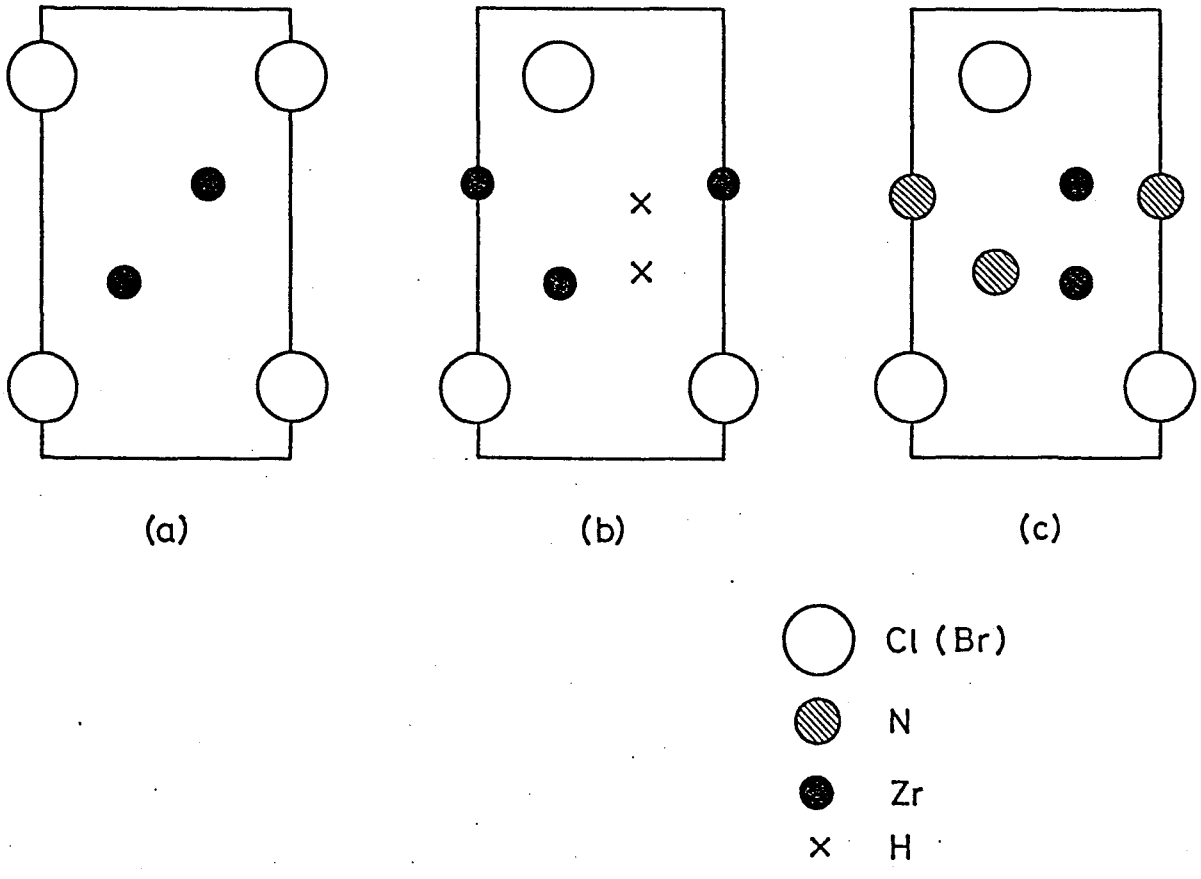


Fig. 7-12 [110] section projections of the structures of the unit layers of (a) ZrBr, (b) ZrBrH and (c) ZrClN.

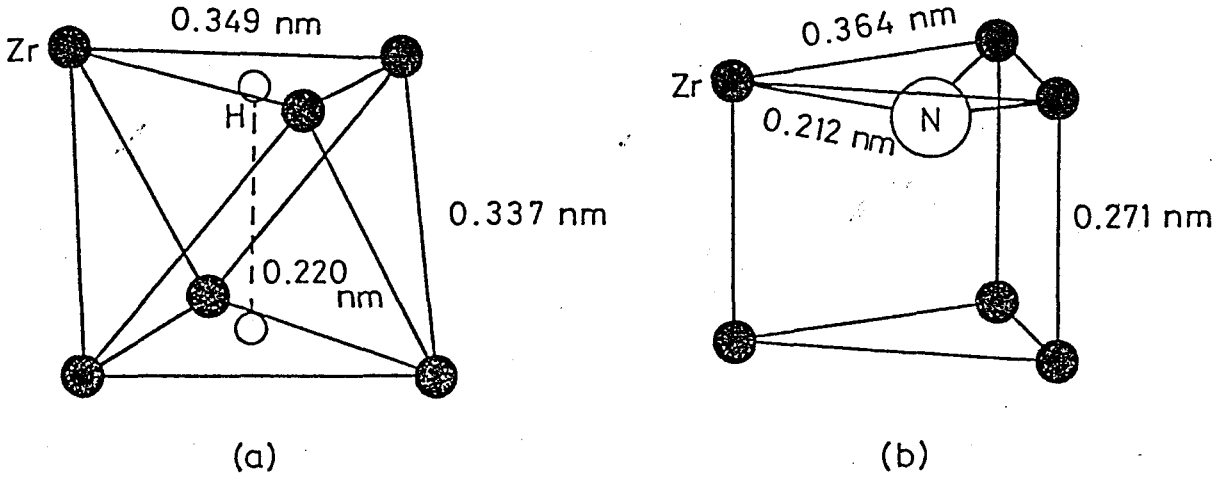


Fig. 7-13 Interstices of the double zirconium metal layers: (a) trigonal antiprism of Zr atoms in the ZrBrH structure and (b) trigonal prism of the ZrClN structure.

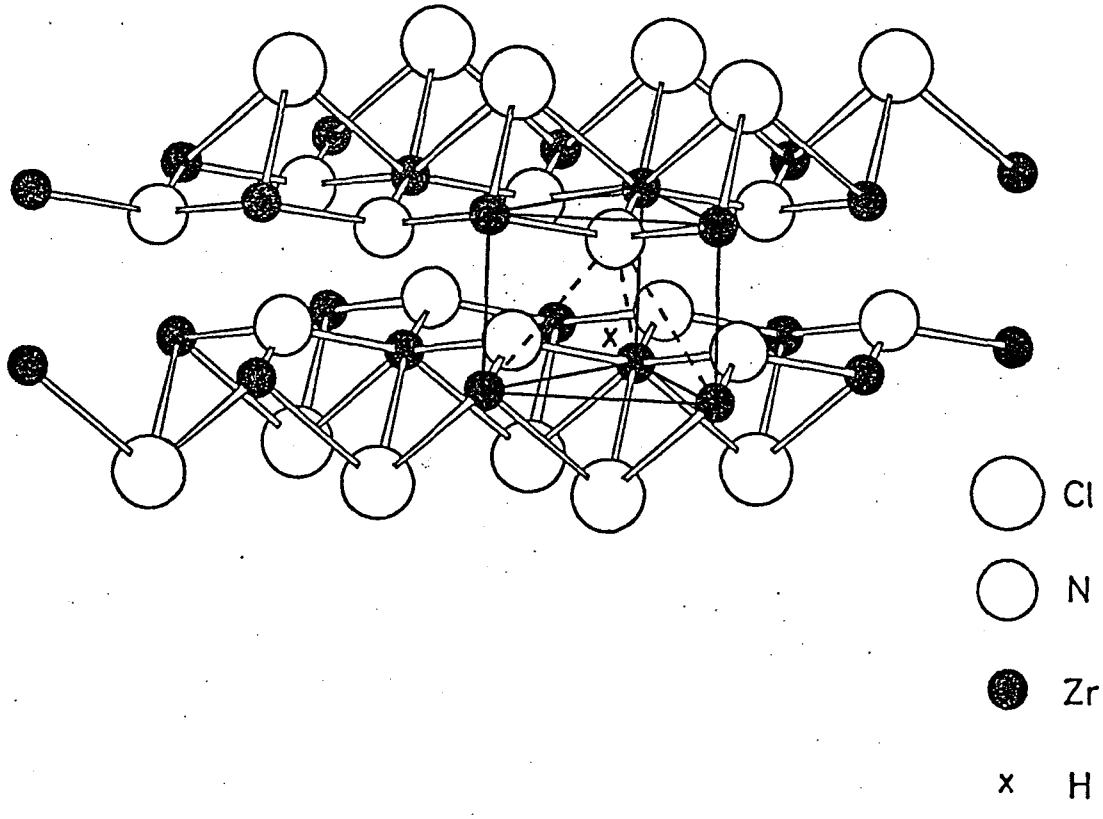


Fig. 7-14 Hydrogen site in β-ZrClN

# 8 PREPARATION AND PROPERTIES OF β-ZrClN FILMS

β-ZrClN can intercalate lithium into the interlayer spaces between the chlorine layers by chemical and electrochemical means. On intercalation of the lithium, the color of β-ZrClN was changed from yellow green to black. Since the color changes occur reversibly on the electrochemical redox intercalation of the lithium, β-ZrClN can be a promising candidate for electrochromic display (ECD) electrode material. Electrochromic electrodes are usually used as thin films deposited on electroconductive transparent substrates. Thin solid films are often prepared by evaporation vacuum and sputtering. These methods were first attempted for β-ZrClN, however, the film could not be formed. In the present chapter, the preparation of β-ZrClN films are attempted from plasma CVD procedures. The electrochemical properties of the films are also studied.

## 8.1 Experimental

Figure 8-1 shows a schematic illustration of the plasma CVD apparatus with a fused silica tube reactor. The dimensions of the tube is 1 m in length and 50 mm in diameter. Stainless steel electrodes (E) were placed outside the tube for the discharge of RF (13.56 MHz) plasma. A Pirani vacuum gauge (G) was used for the pressure measurement in the reactor. After

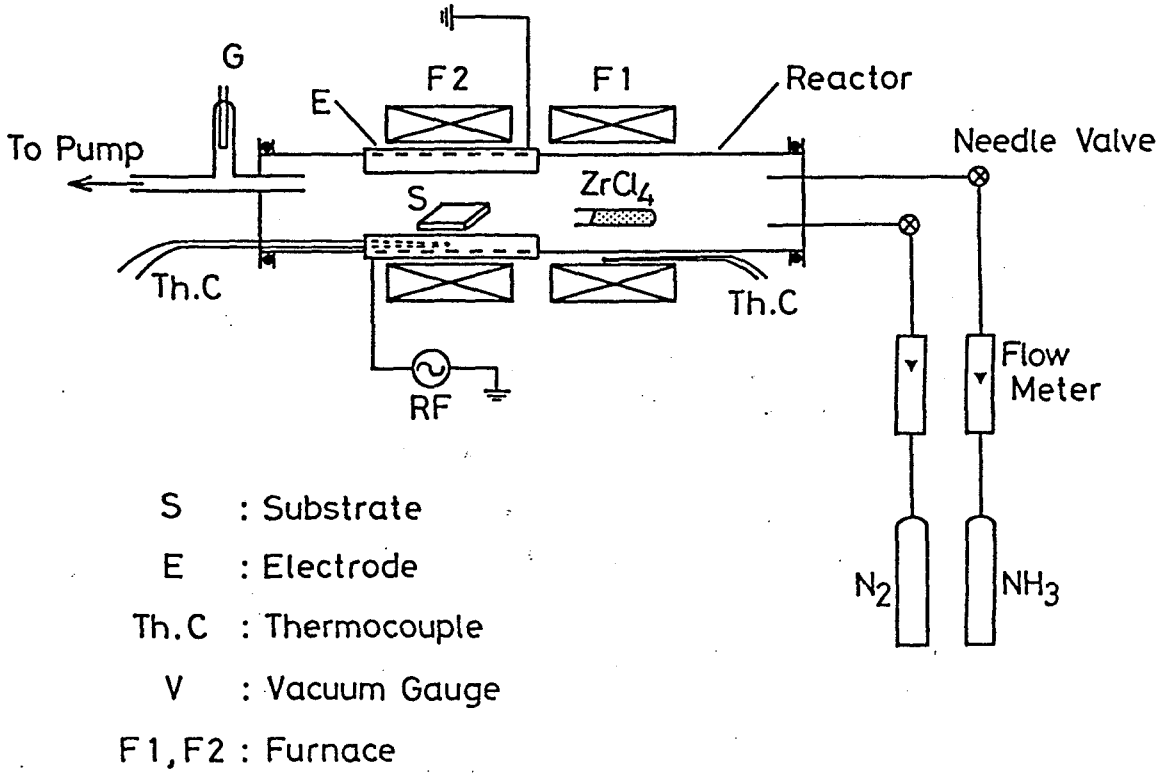


Fig. 8-1 Schematic drawing of plasma CVD apparatus

evacuation at the pressure of $10^{-1}$ Pa, the substrate (S) of barium borosilicate (Cornning 7059) or quartz glass was heated to the temperature range of 673 -973 K by electric heater (F2). Then, the $ZrCl_4$ was vaporized at about 527 K by another heater (F1). The pressure of $ZrCl_4$ was maintained at the range of 10-20 Pa by controlling the vaporization temperature. The gas flow of $N_2$ and/or $NH_3$ was introduced into the reactor. The total pressure in the reactor was maintained at 100 -200 Pa and the reaction was continued for 30 min with the RF discharge of 30 W.

## 8.2 Results and Discussion

The results are summarized in Fig. 8-2. No films were formed from the system of $ZrCl_4$-$N_2$, and zirconium nitride films with zirconium deficit were formed from the system of $ZrCl_4$- $NH_3$. In the system of $ZrCl_4$-$N_2$-$NH_3$, flow rate ratio of $NH_3$ / $N_2$ was varied. At the mixing ratio of $NH_3$ / $N_2 \geq 1$, zirconium nitride films were formed in a similar way to that of the system of $ZrCl_4$-$NH_3$. When the mixing ratio was $NH_3$ / $N_2 \simeq 1$ / 5, yellow transparent α-ZrClN films were deposited at the temperature range of 673-873 K. At higher temperature of 873-973 K, highly crystalline α-ZrClN films were formed. β-ZrClN film was not formed directly from the above plasma CVD systems. The yellow α-ZrClN film was converted into β-ZrClN film of yellow green

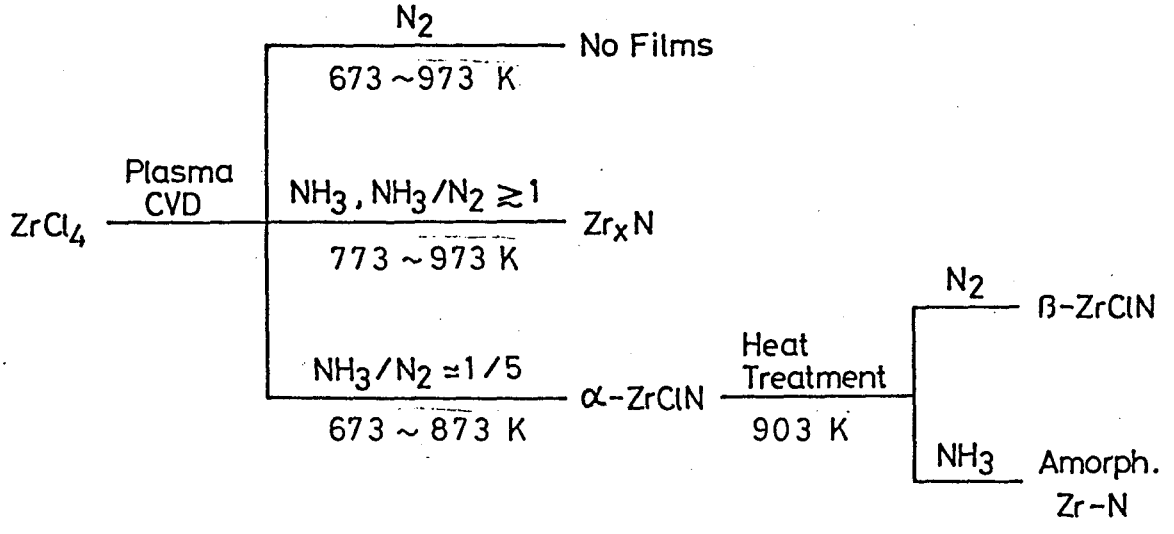


Fig. 8-2 Films obtained by plasma CVD and heat treatment in various gas systems.

after the heat-treatment at 903 K for 30 h in flowing $N_2$. The α-ZrClN film was also treated in flowing $NH_3$ at the same temperature, which resulted in the removal of chlorine from the film, and amorphous Zr-N film was formed.

Konuma et al[70] reported that no films were deposited from the plasma CVD system of $TiCl_4$-$N_2$, however the addition of hydrogen to the plasma system effected the deposition of the titanium nitride. The formation temperature of titanium nitride in plasma is lowered compared with the CVD system of $TiCl_4$-$N_2$-$H_2$ without plasma. They also reported that N-H radicals, especially NH, were identified in the $N_2$-$H_2$ plasma, and concluded that titanium nitride can be formed from the reaction between some titanium species and the N-H radicals. In the plasma CVD system of $ZrCl_4$-$NH_3$, the situation appears very similar. The N-H radicals are also formed and zirconium nitride is formed from the reaction of the zirconium species with the N-H radicals.

From the CVD systems of $ZrCl_4$-$N_2$-$H_2$[71] and $ZrCl_4$-$NH_3$,[44] zirconium nitride was formed above about 1170 K. From the plasma CVD system of $ZrCl_4$-$NH_3$, zirconium nitride films were formed at the lower temperature range of 873-973 K compared with the CVD systems. This result must be attributed to the effect of plasma discharge. Transparent α-ZrClN film was formed from the plasma CVD system. This transparent α-ZrClN can be converted to the transparent β-ZrClN film. The plasma CVD process is usefull for the preparation of transparent β-ZrClN films.

Figure 8-3(a) shows the scanning electron micrograph (SEM) of the β-ZrClN film obtained by the heat treatment of α-ZrClN film at 903 K in $N_2$. The film consists of the platelets of β-ZrClN crystals with the planes growing perpendicular to the substrate. The platelets are about 0.1 μm in thickness and 5 μm in size. Figure 8-3(b) shows the SEM photograph of the β-ZrClN film obtained by the heat treatment of α-ZrClN film at the higher temperature of 973 K in evacuated tube for 30 min. The crystal size is larger than that shown in Fig. 8-3 (a), and the film was turbid. Although there was no information about the phase transition of α-ZrClN to β-ZrClN, it does not seem to be a simple structural transition. The possibility of the formation of intermediate vapor phase is present, because the reaction is slow and the crystal size changes according to the temperature of the heat treatment. Figure 8-4 shows the current response curves of the β-ZrClN film deposited on gold coating substrate. It was measured by using the square wave of 0.5 Hz and ± 2.5 V vs. platinum counter electrode in 1 M $LiClO_4$/PC electrolyte. Reversible color changes were clearly observed up to 500 cycles, though unbleached area of the electrode increased in the course of the cycles. After more the 10000 cycles, the whole film remained unbleached. The current response curves for the unbleached films are still similar to the initial curves. This suggest that lithium intercalation-deintercalation reactions occur on the lithium intercalated unbleached β-ZrClN.

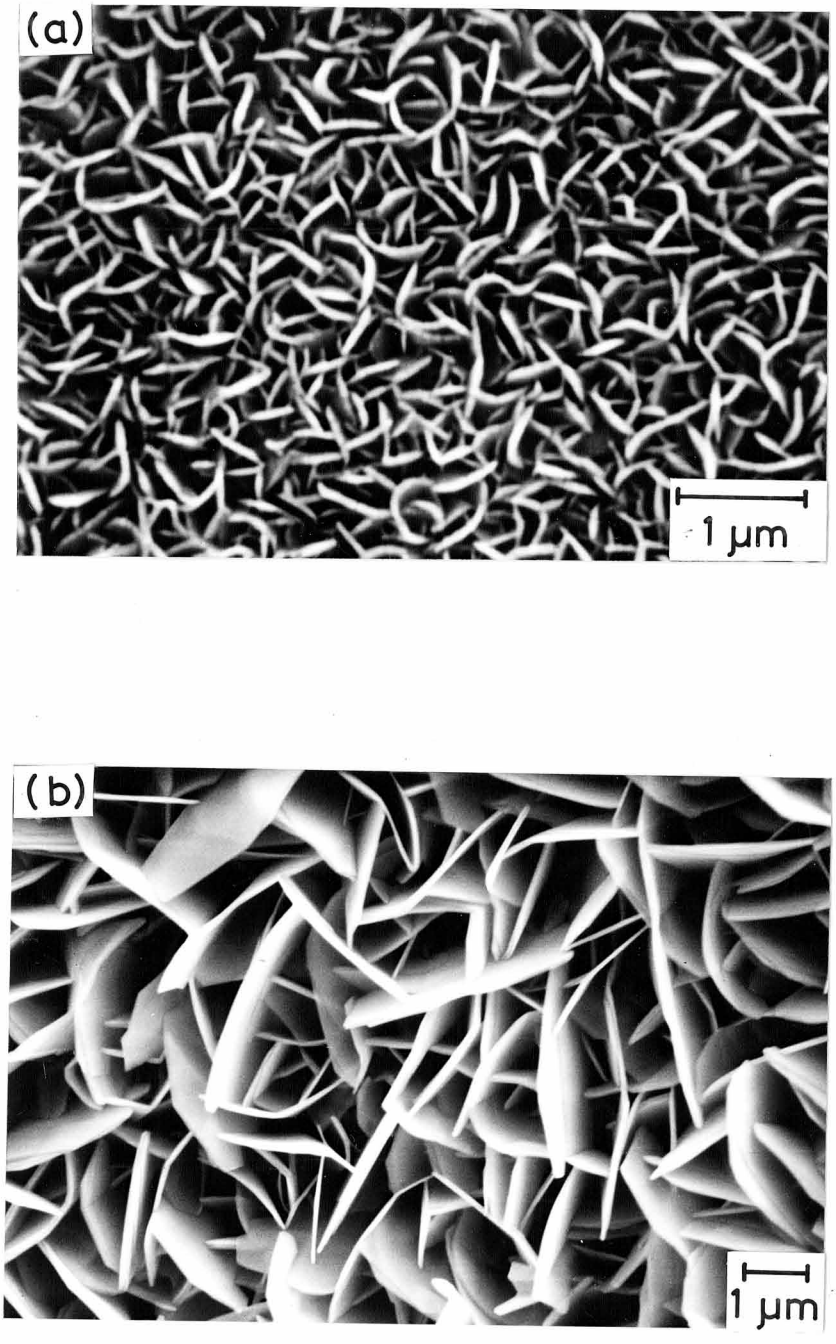


Fig. 8-3 SEM photographs of the β-ZrClN films obtained by the heat treatment of α-ZrClN film at 903 K in $N_2$(a), and at 973 K in a vacuum(b).

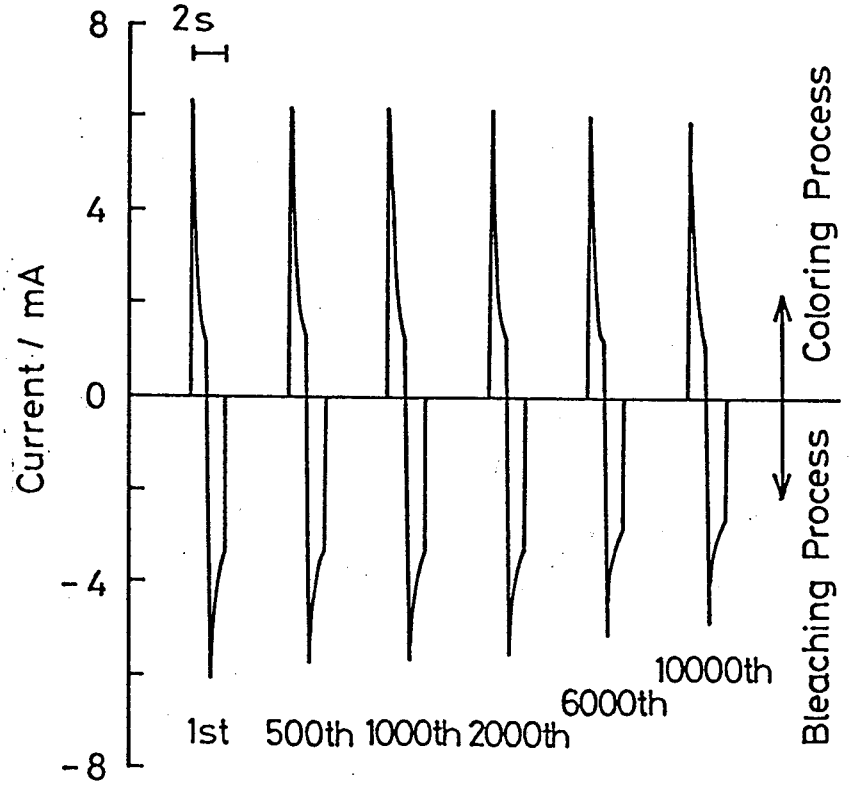


Fig. 8-4 Current response curves of the electrochromic β-ZrClN electrode during the cycles.

Optical absorption spectrum in ultraviolet and visual region was measured for the β-ZrClN film formed on the quartz substrate. Figure 8-5 shows the plot of the square of the optical density vs. photon energy. If the optical absorption due to a direct excitation process across the energy band gap, the optical density (O.D.) holds the following equation.

$$O.D. = B ( h\nu - E_o )^{1/2}$$

Where $E_o$ is band gap (optical band edge) and B is a proportional constant.[72] The band gap ($E_o$) can be determined to be 3.2 eV from the extrapolation of the linear part in Fig. 8-5.

In conclusion transparent β-ZrClN thin film could be obtained from the plasma CVD process followed by the annealing in $N_2$ atmosphere. The film exhibited electrochromic behavior, but the properties for ECD electrode seemed to be not satisfactory.

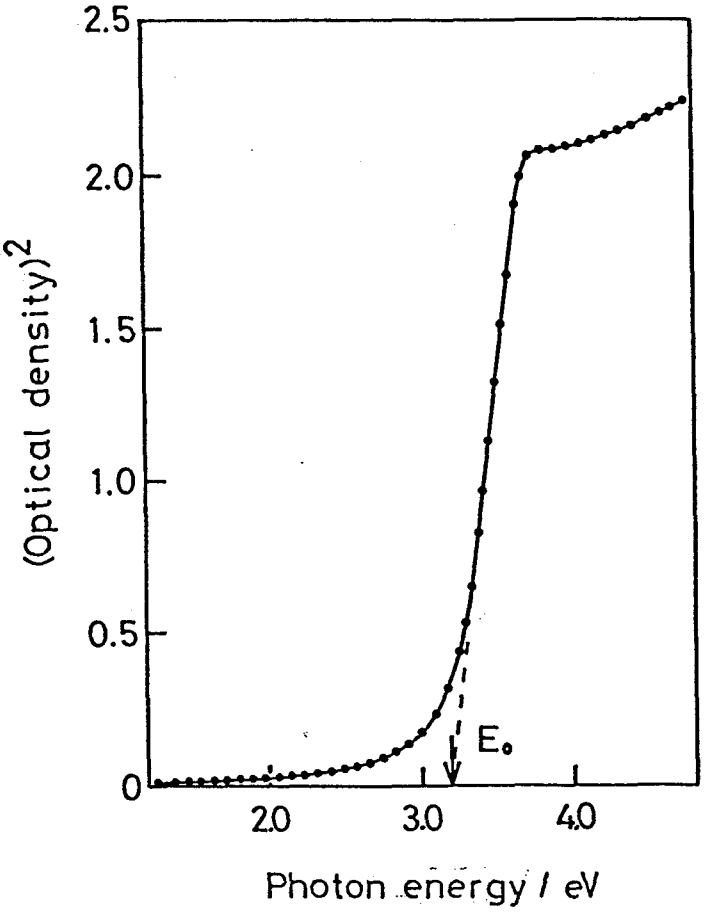


Fig. 8-5 The plot of (optical density)$^2$ vs. photon energy for the β-ZrClN film. The band gap ($E_0$) is determined to be 3.2 eV from the extrapolation of the linear part.

# 9 SUMMARY

A new type of intercalation host crystal, β-ZrClN was developed. β-ZrClN had been prepared by the reaction of $ZrCl_4$ and ammonia at elevated temperatures. This preparation method had the problem of very low yield. In order to improve the yield, the formation process of β-ZrClN was re-examined, and it was found that the formation and the thermal behavior of $(NH_4)_2ZrCl_6$ are the keys to understand the low yield, i. e. $(NH_4)_2ZrCl_6$ was easily formed in the course of the reaction of $ZrCl_4$ with $NH_3$, and transported as vapors to the outside of the reaction system. To avoid the formation of $(NH_4)_2ZrCl_6$, zirconium amide trichloride $ZrCl_3(NH_2)\cdot xNH_3$ was prepared, and thermally decomposed to β-ZrClN in ammonia.

A new preparation method of β-ZrClN was developed. β-ZrClN could be synthesized in high yield by the direct reaction of zirconium metal or zirconium hydride with the vapor of ammonium chloride. This method has the advantages of being able to use non-hydrolyzable starting materials, high yield, and simple procedure. The as-prepared β-ZrClN can be purified into a highly crystalline form by a chemical vapor transport with the aid of $NH_4Cl$. The transport mechanism was clarified from the vapor pressure measurement by a Bourdon gauge. The fundamental transport reaction derived is the following:

$$\beta\text{-ZrClN(s)} + 3\ HCl(g) \rightleftharpoons ZrCl_4(g) + NH_3(g)$$

The transported β-ZrClN had a 3R type stacking structure although it was previously reported that the β-ZrClN had a random stacking structure.

Lithium can be intercalated in β-ZrClN by chemical and electrochemical methods. The chemically transported β-ZrClN formed a lithium intercalate with a composition of $Li_{0.16}ZrClN$ by the reaction with n-butyllithium. On the intercalation, the color of the crystal changes from yellow green to black. Some non-aqueous solvent molecules such as PC, THF, AN, FA, DMF, DMSO, and Py are co-intercalated with the lithium ions, expanding the basal spacings of the lithiated β-ZrClN. Structural models for the interlayer arrangements of the molecules are proposed. Electrochemical properties of β-ZrClN in a lithium cell with 1 M $LiClO_4$/PC electrolyte solution has been studied. The discharge curve exhibited a shoulder and a low voltage plateau at 1.85 and 1.0 V (vs. $Li/Li^+$), respectively. The shallow upper voltage discharge was reversible. The lower voltage discharge was irreversible and attributed to the decomposition of PC on the surface of the electrode. The electrode was also swelled with PC during the discharge process.

Not only lithium, but also hydrogen were taken up by β-ZrClN. In the case of the lithium intercalation, a bronze was formed, being accompanied by the color change from yellow green to black. In contrast, on the hydrogen uptake, the color of β-ZrClN was not changed. All $H_xZrClN$ samples were semiconductors with the activation energy of 60 meV for

conduction and electric conductivities of the order of $10^2$ S $m^{-1}$ at room temperature. The sample could be dehydrogenated electrochemically. The highly dehydrogenated sample had a lower conductivity although the activation energy for conduction was not changed at 60 meV. The electrical conductivity of β-ZrClN increased by a factor of 10 on lithium intercalation. The temperature dependence was slightly negative. The hydrogen positions in $H_x$ZrClN were estimated from the analogous layer structures of zirconium monohalides. It is very likely that hydrogen atoms occupy the trigonal interstices between zirconium atom layers.

The uniform and transparent films of β-ZrClN could be prepared by a plasma CVD process, and the films were characterized as an electrochromic electrode.

## References


1) B. K. G. Theng, "The Chemistry of Clay-Organic Reactions", Adam Hilger, London, (1974).

2) F. Hulliger, "Structural Chemistry of Layer-Type Phases", D. Reidel Publishing Co., Dordrecht, (1976).

3) M. S. Whittingham, Prog. Solid State Chem., 12, 41(1978).

4) F. Levy Ed., "Intercalated Layered Materials", D. Reidel Publishing Co., Dordrecht, (1979).

5) C. F. van Bruggen, C. Haas, and H. W. Myrow Eds., "Proceedings of the International Conference on Layered Materials and Intercalates", Physica, B99, (1980).

6) R. Schöllhorn, Angew. Chem. Int. Ed. Engl., 19, 983(1980).

7) M. S. Whittingham and A. J. Jacobson Eds., "Intercalation Chemistry", Academic Press, Inc., New York, (1982).

8) J. A. Wilson and A. D. Yoffe, Advance in Phys. 18, 193(1969).

9) L. B. Ebert, Ann. Rev. Mat. Sci., 6, 181(1967).

10) M. S. Dresselhaus and G. Dresselhaus, Adv. Phys., 30, 139(1981).

11) R. Schöllhorn, R. Kuhlmann, and J. O. Besenhard, Mat. Res. Bull., 11, 83(1976).

12) S. Son, F. Kanamaru, and M. Koizumi, Inorg. Chem., 18, 400(1979).

13) M. S. Whittingham, J. Electrochem. Soc., 123, 315(1976).

14) K. Mizushima, P. C. Jones, P. J. Wiseman, and J. B. Goodenough, Mat. Res. Bull., 15, 783(1980).

15) S. Yamanaka, H. Kobayashi, and M. Tanaka, Chem. Lett., 329(1976).

16) R. Brec, D. M. Schleich, G. Ouvrard, A. Louisy, and J. Rouxel, Inorg. Chem., 18, 1814(1979).

17) S. Otani, M. Shimada, F. Kanamaru, and M. Koizumi, Inorg. Chem., 19, 1249(1980).

18) R. Clement and M. L. H. Green, J. Chem. Soc. Dalton, 1566(1979)

19) R. Brec, J. Ritsma, G. Ouvrard, and J. Rouxel, Inorg. Chem., 16, 660(1977).

20) R. Schöllhorn and A. Weiss, Z. Naturforsch., 28B, 716(1973).

21) S. Yamanaka, T. Nagashima, and M. Tanaka, Thermochim. Acta, 19, 236(1977).

22) S. Kikkawa, F. Kanamaru, and M. Koizumi, Bull. Chem. Soc. Jpn., 52, 963(1979).

23) J. J. Banewicz and J. A. Maguire, Mat. Res. Bull., 21, 93(1986).

24) J. F. Ackerman, Mat. Res. Bull., 23, 165(1988).

25) Jin-Ho Choy, Dong-Youn Noh, and Jung-Chul Park, Mat. Res. Bull., 23, 73(1988).

26) S. Yamanaka, Y. Horibe, and M. Tanaka, J. Inorg. Nucl. Chem., 38, 323(1976).

27) S. Yamanaka, Inorg. Chem., 15, 2811(1976).

28) J. W. Johnson, Chem. Comm., 263(1980).

29) G. Lagaly and K. Beneke, J. Inorg. Nucl. Chem., 38, 1513(1976).

30) S. Kikkawa and M. Koizumi, Mat. Res. Bull., 15, 533(1980).

31) E. T. Blues and D. Bryce-Smith, Chem. Comm., 699(1970).

32) G. F. Walker and D. G. Hawthorne, Trans. Faraday Soc., 63, 166(1967).

33) T. Ohno, K. Nakao, and H. Kamimura, J. Phys. Soc. Jpn., 47, 1125(1979).

34) G. Dresselhaus and S. Y. Leung, Solid State Comm., 35, 819(1980).

35) T. J. Pinnavaia, Science, 220, 365(1983).

36) S. Yamanaka, T. Nishihara, and M. Hattori, Materials Chemistry and Physics, 17, 87(1987).

37) R. B. Somoano, V. Hadek, and A. Rembaum, J. Chem. Phys., 58, 697(1973).

38) R. Juza and J. Heners, Z. Anorg. Allg. Chem., 332, 159(1964).

39) R. Juza and H. Friedrichsen, Z. Anorg. Allg. Chem., 332, 173(1964).

40) R. L. Rister and S. N. Flengas, Can. J. Chem., 42, 1102 (1964).

41) G. Engel, Z. Krist., 90, 341(1935).

42) G. M. Toptygina and I. B. Barskaya, Russ. J. Inorg. Chem., 10, 1226(1965).

43) J. E. Drake and G. W. A. Fowles, J. Less-Common Metals, 3, 149 (1961).

44) A. Yajima, Y. Segawa, R. Matsuzaki, and Y. Saeki, Bull. Chem. Soc. Jpn., 56, 2638(1983).

45) M. Allbutt and G. W. A. Fowles, J. Inorg. Nucl. Chem., 25, 67 (1963).

46) G. W. A. Fowles and F. H. Pollard, J. Chem. Soc. 1953, 4128.

47) J. E. Drake and G. W. A. Fowles, J. Less-Common Metals, 2, 401 (1960).

48) H. Blunck and R. Juza, Z. Anorg. allg. Chem., 406, 145(1974).

49) V. V. Savranskii, K. P. Burdina, A. N. Tsvigunov, and E. V. Zubova, Vestn. Mosk. Univ. Khim., 246(1975).

50) R. Juza, A. Rabenau, and I. Nitschke, Z. Anorg. Allg. Chem., 332, 1(1964).

51) M. Saeki, J. Crystal Growth, 36, 77(1976).

52) I. S. Morozov and Sun In'-Chzhu, Russ. J. Inorg. Chem., 4, 1176(1959).

53) R. L. Lister and S. N. Flengas, Can. J. Chem., 43, 2947(1965).

54) JANAF thermochemical tables, National Standard Reference Data Series, 2nd ed., U. S. National Bureau of Standards, Washington, DC. (1971).

55) M. S. Whittingham, J. Electroanal. Chem., 118, 229(1981).

56) Y. Sakurai and J. Yamaki, J. Electrochem. Soc., 132, 512(1985).

57) M. S. Whittingham, in ref. 3), p. 69.

58) J. R. Dahn, M.A. Py, and R. R. Haering, Can. J. Phys., 60, 307(1982).

59) A. N. Dey and B. P. Sullivan, J. Electrochem. Soc., 117, 222(1970).

60) D. W. Murphy and J. N. Carides, J. Electrochem. Soc., 126, 349(1979).

61) O. Bravo and R. T. Iwamoto, Electoanal. Interface Electrochem., 23, 419(1969).

62) P. G. Dickens and M. F. Pye, in ref. 7), p. 539.

63) M. Greenblatt, Chem. Rev., 88, 31(1988).

64) A. W. Struss and J. D. Corbett, Inorg. Chem., 16, 360(1977).

65) G. Meyer, S.-J. Hwu, S. Wijeyesekera, and J. D. Corbett, Inorg. Chem., 25, 4811(1986).

66) D. G. Adolphson and J. D. Corbett, Inorg. Chem., 15, 1820(1976).

67) R. L. Daake and J. D. Corbett, Inorg. Chem., 16, 2029(1977).

68) S. D. Wijeyesekera and J. D. Corbett, Inorg. Chem., 25, 4709(1986).

69) S. D. Wijeyesekera and J. D. Corbett, Solid State Commun., 54, 657(1985).

70) M. Konuma, Y. Kanzaki, and O. Matsumoto, J. Less-Common Met., 75, 1(1980).

71) T. Takahashi, H. Itoh, and S. Noguchi, Nippon Kagakukaishi, 627(1975).

72) R. H. Bube, "Electronic Properties of Crystalline Solids", Academic Press, Inc., (1984), p. 440.

**Acknowledgment**

I would like to thank Professor Makoto Hattori and Associate Professor Shoji Yamanaka of Hiroshima University for encouragement and support during the course of this work. I would also like to express my gratitude to Professor Fumikazu Kanamaru and Associate Professor Shinich Kikkawa of Osaka University for useful advice and discussions. I am indebted to Professor Mitsue Koizumi of Ryukoku University and Professor Masahiko Shimada of Tohoku University for encouragement in this work. I am also indebted to Professor Shichio Kawai, Professor Keiji Kuwata and Professor Sumio Kaizaki of Osaka University for useful discussions. Finally, I wish to express my thanks to all the members of the research group of Professor Makoto Hattori.

## List of Publications

1. Lithium Intercalation and Electrochromism in β-ZrNCl Layered Crystal;
   S. Yamanaka, M. Ohashi, M. Sumihara and M. Hattori,
   Chemistry Letters, 1984, 1403-1406.

2. Lithium Intercalation in Layer Structured Compound β-ZrNCl;
   M. Ohashi, S. Yamanaka, M. Sumihara and M. Hattori,
   J. Inclusion Phenomena 2, 289-295(1984).

3. Synthesis of β-ZrClN by Thermal Decomposition of Zirconium(IV) Amide Trichloride;
   M. Ohashi, S. Yamanaka, and M. Hattori,
   Bull. Chem. Soc. Jpn., 59, 2627-2628(1986).

4. Preparation and Properties of Ammonium Hexachlorozirconate(IV) and Its Reaction with Gaseous Ammonia;
   M. Ohashi, S. Yamanaka, Y. Morimoto and M. Hattori,
   Bull. Chem. Soc. Jpn., 60, 2387-2390(1987).

5. Preparation of β-ZrClN Films by Plasma CVD;
   M .Ohashi, S. Mizoguchi, S, Yamanaka, and M. Hattori,
   Nippon-kagakukaishi, 1987, 1924-1927.

6. Novel Synthesis of the Layer Structured β-ZrNCl by the Direct Reactions of Zirconium Metal or Zirconium Hydride with Ammonium Chloride;
M. Ohashi, S. Yamanaka, M. Sumihara and M. Hattori,
J. Solid State Chem., 75, 99-104(1988).

7. Chemical Vapor Transport of Layer Structured Crystal β-ZrNCl;
M. Ohashi, S. Yamanaka and M. Hattori,
J. Solid State Chem., 77, 342-347(1988).

8. Electrochemical Characteristics of Layer Structured β-ZrNCl in Lithium Cells;
M. Ohashi, T. Shigeta, S. Yamanaka and M. Hattori,
J. Electrochem. Soc., in press.

9. Hydrogen Uptake by Layer Structured β-ZrNCl;
M. Ohashi, H. Nakano, S. Yamanaka and M. Hattori,
Proceedings of the 11th International Symposium on the Reactivity of Solid, in press.